MAGNETIC PROPERTIES OF TRANSITION ION PYROPHOSPHATES

MAGNETIC PROPERTIES OF TRANSITION ION PYROPHOSPHATES

by

DAVID COLIN FOWLIS, B.Sc.

A Thesis
Submitted to the School of Graduate Studies
in Partial Fulfilment of the Requirements
for the Degree
Doctor of Philosophy

McMaster University
December 1970

DOCTOR OF PHILOSOPHY (1971)
(Physics)

McMASTER UNIVERSITY
Hamilton, Ontario.

TITLE: Magnetic Properties of Transition Ion Pyrophosphates

AUTHOR: David Colin Fowlis, B.Sc. (Glasgow University, Scotland)

SUPERVISOR: Professor C. V. Stager

NUMBER OF PAGES: ix, 114

SCOPE AND CONTENTS:

The magnetic properties of $Mn_2P_2O_7$, $Cu_2P_2O_7$, $Co_2P_2O_7$ and $Ni_2P_2O_7$ were studied. They were investigated using magnetic susceptibility and magnetic resonance techniques. They were all found to become magnetically ordered between 10°K and 30°K. In all the predominant exchange interaction was antiferromagnetic. $Ni_2P_2O_7$ however did show a resultant moment at low temperatures which was attributed to weak ferromagnetism. The experimental results were analysed in the molecular field approximation which accounted for their behaviour except in the case of $Cu_2P_2O_7$ where the High Temperature Series Expansion method was necessary to explain the temperature dependence of its paramagnetic susceptibility.

ACKNOWLEDGEMENTS

I would like to thank my supervisor Dr. C. V. Stager for his assistance and guidance throughout this work.

My appreciation also goes to Dr. C. Calvo for his assistance in the crystallography and alignment of the crystal, to Dr. R. J. Atkinson and D. Twiney for their contributions to the growing of the crystals and to Dr. S.H. Choh and J. Stiles for their help in some of the experimental work.

Dr. W. R. Datars and Dr. T. Timusk are acknowledged for the use of their equipment.

Last but not least I would like to thank the Government of Ontario and the National Research Council of Canada for financial support in the form of scholarships.

TABLE OF CONTENTS

LIST OF FIGURES

LIST OF TABLES

CHAPTER I

INTRODUCTION

The purpose of this work is to examine the magnetic properties of a series of transition metal ion pyrophosphates $M_2P_2O_7$ where M is one of Mn, Cu, Co or Ni. They were investigated using magnetic susceptibility and magnetic resonance measurements.

The thesis is subdivided into chapters. In Chapter II the theory necessary to understand the experimental measurements is presented. The crystallography and preparation of the crystals is given in Chapter III. The experimental method is described in Chapter IV. Chapter V is subdivided into four sections. In each section the experimental results are presented for one compound as well as a discussion and interpretation of these measurements. Chapter VI gives a comparison of the magnetic properties of the four pyrophosphates studied. The remainder of the introduction is concerned with the response of magnetic materials to an applied magnetic field and the type of magnetic ordering encountered in the pyrophosphates. Also included is a summary of other relevant measurements on these compounds.

The most natural way to examine the magnetic properties of a material is by its response to an applied magnetic field. This response is characterised by its magnetic susceptibility χ defined by the following relation

$$\vec{M} = \overline{\overline{\chi}}\cdot\vec{H} \ ,$$

where M is the induced magnetization and H is the applied magnetic field. In the determination of χ one must include the effects of the local environment of the magnetic ion, the effect of temperature and the effects of exchange and dipole interactions between the magnetic ions.

Magnetism in the "iron group" transition ions is due to the 3d electrons. Their free ion ground state may be determined by "Hund's" rule, which is just a consequence of the coulomb interaction between 3d electrons and the Pauli exclusion principle. When these ions form insulating compounds the 3d electrons may be considered to be localised on their respective ions. However the ion experiences strong electric fields, due to its non-magnetic neighbours, which produce a Stark effect and thus split the free ion ground state. Knowing the local symmetry of the ion one may use group theory, to determine how the free ion degeneracy is changed by the interaction with the neighbouring non-magnetic ions.

The applied magnetic field tends to align the individual magnet moments whereas thermal agitation tends to preserve a random orientation of the magnetic moments. Since in a sample these are approximately 10^{23} ions this effect must be treated by statistical mechanics. The statistical treatment involves the calculation of the average value of the magnetic moment. On the microscopic level the Zeeman interaction is the perturbation and the summation is taken over all the energy levels of the magnetic ion. It is the thermal effects which produce the characteristic 1/T dependence of the susceptibility.

The exchange interaction between magnetic ions tends in general to align the magnetic moments parallel or anti-parallel. The interaction is the inter-atomic equivalent of the intra-atomic exchange between electrons which is responsible for "Hund's" rule. When the magnetic ions are separated by a non-magnetic ion which mediates the exchange, the exchange is called superexchange. This is thought to be the type of exchange which predominates in the pyrophosphates.

The exchange interaction in insulators is well represented by the Heisenberg Hamiltonian

$$\mathcal{H} = \sum_{i<j} J_{ij} \vec{S}_i \cdot \vec{S}_j$$

where S_i and S_j are the spins of the i^{th} and j^{th} ion. A most convenient and simplifying approximation is that the individual magnetic ions experience an effective field due to the rest of the crystal. This is the so called Weiss molecular field. In this approximation a single ion Hamiltonian may be written

$$\mathcal{H}_i = -g\beta \vec{S}_i \cdot \vec{H}_{ex}$$

where H_{ex} is the effective field and is called the exchange field.

The magnetic dipole interaction is the classical interaction between magnetic moments one gets from electromagnetic theory. The energy of interaction E_{ij} between magnetic moments m_i and m_j is

$$E_{ij} = \frac{\vec{m}_i \cdot \vec{m}_j}{r_{ij}^3} - \frac{3(\vec{m}_i \cdot \vec{r}_{ij})(\vec{m}_j \cdot \vec{r}_{ij})}{r_{ij}^5}$$

where r_{ij} is the distance between the i^{th} and j^{th} moments. The total energy of the i^{th} ion is then the sum of the interactions over all the other ions in the crystal

$$E_i = \sum_j \left[\frac{\vec{m}_i \cdot \vec{m}_j}{r_{ij}^3} - \frac{3(\vec{m}_i \cdot \vec{r}_{ij})(\vec{m}_j \cdot \vec{r}_{ij})}{r_{ij}^5}\right]$$

For purposes of evaluation the sum is divided into two parts. The first part is the sum over a sphere of large radius centered on the i^{th} ion. In the second part the sum is replaced by an integral for ions outside the sphere. It is this second part which gives rise to the Lorentz and demagnetizing fields, the latter being shape dependent. However if the sample is spherical the Lorentz and demagnetizing fields make equal and opposite contributions to the sum.

In the temperature range in which the thermal effect is much larger than the exchange effect the material is paramagnetic. However when the exchange effect predominates then the material becomes magnetically ordered. The type of ordering depends on the details of the exchange interaction. The transition to the ordered state is marked by the onset of long range magnetic order. The transition is a second order phase transition with the specific heat showing a λ type behaviour. The transition temperature is called the Néel temperature when the predominant exchange interaction is antiferromagnetic. This temperature is best determined by specific heat measurements, but it may also be determined from magnetic susceptibility measurements and where possible by detecting the disappearance of the electron spin resonance of the magnetic ion.

The antiferromagnetically ordered state is now considered. A general reference to the discussion of this state is the review article by Nagamiya et al. (1955). The antiferromagnetically ordered state is characterised by a series of interpenetrating sublattices. On each sublattice all of the individual magnetic moments point in the same direction. When there are only two sublattices they are aligned antiparallel in zero field. It is the exchange interaction which is responsible for this antiparallel alignment. In the molecular field approximation the exchange interaction is represented by a magnetic field H_{ex} such that the field on each sublattice has the following form

$$\vec{H}_{ex}^{(i)} = \sum_{j=1}^{n} \overset{=}{\Gamma}^{ij} \vec{M}^{j}$$

where n is the number of sublattices and M_j is the magnetization of the j^{th} sublattice. For two sublattices this reduces to

$$\vec{H}^{\pm}_{ex} = -\bar{\bar{A}}\vec{M}^{\mp} - \bar{\bar{\Gamma}}\vec{M}^{\pm}$$

where M^{+} and M^{-} denote the magnetization of the two sublattices. The exchange interaction is in general isotropic so that it does not determine the direction of the spins with respect to the crystallographic axes. The energy which determines the spin direction is called the anisotropy energy. In the spirit of the molecular field approximation this energy E_A has the following form for a two sublattice model (Date 1961).

$$E_A = \vec{M}^{+}\bar{\bar{A}}'\vec{M}^{-} + \frac{1}{2}[\vec{M}^{+}\bar{\bar{\Gamma}}'\vec{M}^{+} + \vec{M}^{-}\bar{\bar{\Gamma}}'\vec{M}^{-}]$$

where A' and Γ' are tensors. The energy E_A is a function of the orientation of M^{+} and M^{-} with respect to the crystallographic axes. The orientation which minimizes E_A corresponds to the zero field spin direction. The anisotropy field $H^{\pm}_A$ is defined by the relation $\delta E_A = -\vec{H}^{+}_A \cdot \delta\vec{M}^{+} - \vec{H}^{-}_A \cdot \delta\vec{M}^{-}$ therefore

$$\vec{H}^{\pm}_A = -\bar{\bar{A}}'\vec{M}^{\mp} - \bar{\bar{\Gamma}}'\vec{M}^{\pm} .$$

The exact nature of the field depends on the symmetry of A' and Γ'. When the symmetry is orthorhombic then there are two anisotropy fields. The anisotropy energy comes from various sources e.g. crystal field effects and magnetic dipole interactions.

In the antiferromagnetic state the perpendicular susceptibility $\chi_\perp$, when the field is very much greater than the anisotropy field(s), measures the exchange field. By equating the torques on each sublattice to zero when the field is applied perpendicular to the spin direction, one obtains the result $A = 1/\chi_\perp$. However, when the anisotropy field is not negligible compared with the exchange field the perpendicular susceptibility is modified by the anisotropy field and in orthorhombic symmetry the perpendicular susceptibility is dependent on the direction of the applied magnetic field in the plane perpendicular to the spin direction.

Antiferromagnetic resonance (AFMR) measures the product of the exchange and anisotropy fields. In the case of uniaxial anisotropy and when H_{ex} is very much greater than H_A the resonance frequency is given by the following relation

$$\left(\frac{\omega}{\gamma}\right) = (2\ H_{ex}\ H_A)^{\frac{1}{2}}$$

where ω is the angular frequency and γ is the magnetomechanical ratio. If the resonance falls in the microwave region where continuously variable frequency sources are not available the resonance can be observed by the application of a magnetic field. At low temperatures when the magnetic field, H, is along the spin direction the resonance condition is

$$\left(\frac{\omega}{\gamma}\right) = (2\ H_{ex}\ H_A)^{\frac{1}{2}} \pm H.$$

In the case of orthorhombic anisotropy there are two zero field resonance frequencies. If H_{ex} is much greater than both H_{A1}

and H_{A2} then

$$(\frac{\omega_1}{\gamma}) = (2\ H_{ex}\ H_{A1})^{\frac{1}{2}} \text{ and } (\frac{\omega_2}{\gamma}) = (2\ H_{ex}\ H_{A2})^{\frac{1}{2}}.$$

H_{A1} and H_{A2} are the two values of the anisotropy field. As in the uniaxial case these resonances can be tuned by an applied magnetic field.

The spin direction in antiferromagnets can be determined from both magnetic susceptibility and AFMR. Thus from the combination of magnetic susceptibility and AFMR measurements it is possible to determine the exchange field, the anisotropy field(s) and the antiferromagnetic spin direction. A characteristic of antiferromagnets is the phenomenon of "spin flop". For a small anisotropy field and low temperatures this occurs when the applied magnetic field is along the spin direction and has the following value

$$H_c = (2\ H_{ex} H_{A1})^{\frac{1}{2}}.$$

The result being that the spins "flop" from being parallel to perpendicular to the applied magnetic field. In this state there is a resonance mode called the Spin Flop Mode (SFM) which has the following frequency dependence when the applied magnetic field is parallel to the zero field spin direction.

$$(\frac{\omega}{\gamma})^2 = H^2 - (2\ H_{ex}\ H_{A1})^{\frac{1}{2}} \qquad H > H_c\ .$$

Up until this point the antiferromagnetic state has been described in terms of sublattices with no mention as to which sublattice the individual magnetic ions belong. This is described by the spin configuration. Experimentally the spin configuration can be determined by neutron diffraction. Neutrons are scattered by nuclei and magnetic moments. Thus by measuring the sample in the paramagnetic and ordered regions it is possible from the difference in the scattering to determine the spin configuration.

A first principle calculation of exchange energy even in the simplest antiferromagnet is at present an impossible task so that the exchange energy has to be taken from a physical measurement. The anisotropy energy may be calculated in a phenomenological way. Two sources of the anisotropy energy are crystal field energy and magnetic dipole energy. The former may be taken from Electron Spin Resonance (ESR) of the magnetic ion in an isomorphic host. The magnetic dipole energy is calculated by a lattice sum. However for the summation the spin configuration must be known.

There are many deviations from the antiferromagnetic state. One such deviation is when there is small resultant magnetic moment which is of order 10^{-2} of the sublattice magnetization and when the behaviour of the paramagnetic susceptibility shows that the predominant exchange interaction is antiferromagnetic. This magnetic state is called weak ferromagnetism (Moriya (1963). There are two main causes for weak ferromagnetism. The first one is when there are two inequivalent magnetic ions such that the anisotropy energies of the two ions favour different spin directions. This has been shown to be the cause of weak ferromagnetism in NiF_2 (Moriya 1960a), where the anisotropy energy minimum of the two ions are at right angles to each other. The second one results from the anisotropic exchange interaction which is a combined effect of spin orbit coupling and the exchange interaction. The energy due to such an interaction may be written

$$\vec{d}\cdot(\vec{S}_i \times \vec{S}_j)$$

where S_i and S_j are the spins of the respective ions. Dzialoshinski (1958) has shown that under certain symmetries such a term can exist in the energy. This is the case of weak ferromagnetism in Fe_2O_3 (Dzialoshinski 1958).

Normally when magnetic systems order the ordering takes place at one temperature, however magnetic systems have been observed which show ordering in two dimensions and do not show ordering in the third dimension until much lower temperatures. The classical example of a two dimensional antiferromagnet is K_2NiF_4. Lines (1967) had discussed this case and he concludes that the ordering in the third dimension is stabilized by the anisotropy energy. One would expect such systems to behave like regular three dimensional antiferromagnets at low temperatures. This is the case of K_2NiF_4 and it is found that the ratio of anisotropy energy to exchange energy is very small in K_2NiF_4. Birgeneau et al (1970) report a ratio of 1:500.

There have been a number of previous measurements on the pyrophosphates. Atkinson and Stager (1969), Atkinson et al. (1970) and Atkinson (1969) have measured the shift of the ^{31}P nuclear magnetic resonance (NMR) in the four magnetic pyrophosphates in the paramagnetic region. Choh and Stager (1970) have measured the shift of the ^{31}P NMR in $Mn_2P_2O_7$ in the ordered state and have suggested possible spin configurations consistent with their results. Recently neutron diffraction measurements have been made on $Mn_2P_2O_7$ powder and the spin configuration determined (Gill et al 1970). Stiles (1970) has observed highly anisotropic shifts of the ^{31}P NMR in $Cu_2P_2O_7$ at 4.2°K. There have been electron spin resonance (E.S.R.) measurements of Mn^{++}, Cu^{++} and Co^{++} in a non-magnetic pyrophosphate host. Chambers et al (1964); Calvo et al (1967); Atkinson et al (1970).

CHAPTER II

THEORY

This section is divided into three parts. The first part is concerned with the ground state of the magnetic ions in the solid. The second part gives the theory of the magnetic properties of a solid when the exchange interaction between the ions is small compared to thermal energies. This is the paramagnetic region. The third part is concerned with the temperature range in which the exchange interaction predominates over the thermal energy. This is the magnetically ordered state. The transition between the two states is characterized by a temperature called the Néel temperature when the predominant exchange interaction is antiferromagnetic.

1. GROUND STATE OF MAGNETIC IONS

In studying the magnetic properties of solids it is important to know the state of the magnetic ion in the solid. Knowledge of the crystal structure tells us the environment of the magnetic ion. It is well known that the magnetic properties of compounds of the "iron group" transition series are inconsistent with the magnetic ion having its free ion ground state. The reason for this being that in the crystal the magnetic ion experiences strong electric fields due to its diamagnetic neighbours. The theory of how the free magnetic ion degeneracy is partially lifted in crystals is called Crystal Field Theory. It is customary in discussing the ground state of a magnetic ion to describe the state by a fictitious spin. The fictitious spin of a level is determined by how the level splits in the presence of an applied magnetic field. Its value being chosen such that twice the value of the fictitious spin plus one is equal to the degeneracy of the level. The amount of splitting of the level is determined by a g value. g is in general a tensor since it depends on the direction of the applied magnetic field. Thus a spin Hamiltonian for a level can be written as

$$\mathcal{H} = \beta\ \vec{H}\cdot\bar{\bar{g}}\cdot\vec{S}'$$

where S' is the fictitious spin. In a similar manner all other levels can be described by a fictitious spin and a g tensor.

Mn^{++} ion

The Mn^{++} ion has five 3d electrons which gives rise to a free ion ground state $^6S_{5/2}$ ($^{2S+1}L_J$). The next excited state is of the order of 15,000 cm^{-1} above the ground state. Due to spin-orbit coupling and a low symmetry crystal field the ground state is split in zero field into three Kramer's doublets with $S_z = \pm 5/2, \pm 3/2, \pm 1/2$. This splitting of the ground state is very small as it is the result of high order perturbation theory so that the fictitious spin is set equal to the true spin of $S = 5/2$. The spin Hamiltonian for Mn^{++} may be written in the following way

$$H = \beta\vec{H}\cdot\overline{\overline{g}}\cdot\vec{S} + DS_x^2 + E(S_x^2 - S_x^2) + \vec{I}\cdot\overline{\overline{A}}\cdot\vec{S}$$

where the first term is the electron Zeeman term, the second and third are the zero field splittings for rhombic symmetry and the fourth term the nuclear hyperfine interaction. Since the last term is small it may be neglected.

Cu^{++} ion

The Cu^{++} ion has nine 3d electrons and the free ion ground state is a $^2D_{5/2}$. Here the crystal field effects are quite pronounced. A cubic crystal field splits the free ion ground state into an orbital triplet and an orbital doublet. A tetragonal field partially lifts the orbital degeneracy while the combined action of a rhombic field and spin orbit coupling completely remove the orbital degeneracy leaving five Kramer's doublets. The appropriate spin Hamiltonian to describe the lowest doublet would be

$$H = \beta\vec{H}\cdot\overline{\overline{g}}\cdot\vec{S}$$

where S = 1/2. In this case the fictitious spin equals the true spin. The principal axes of the g tensor would coincide with those of the crystal field.

Co^{++} ion

The Co^{++} ion has seven 3d electrons which gives a free ion ground state $^4F_{9/2}$. Like the Cu^{++} ion the effects of the crystal field on the Co^{++} ion are very significant. Under a cubic crystal field the ^4F level is split into two triplets (Γ_4 and Γ_5) and one singlet (Γ_2). One of the triplets

Γ_4 lies lowest in energy. The next level Γ_5 is typically 10^4 cm^{-1} above the ground state, so that only the lowest level Γ_4 need be considered. The total degeneracy of this Γ_4 level is twelve, three fold orbital and four fold spin. Under the combined action of spin-orbit coupling and crystalline fields of tetragonal and rhombic symmetry the Γ_4 level splits into six Kramer's doublets. Each of the Kramer's doublets may be described by a spin Hamiltonian

$$H = \beta\vec{H}\cdot\overline{\overline{g}}\cdot\vec{S}'$$

where S' is the fictitious spin with the value 1/2. The true spin of a Co^{++} ion is 3/2.

Ni^{++} ion

The Ni^{++} ion has eight 3d electrons giving a free ion ground state $^3F_4$. A cubic crystal field splits the ^3F state into two triplets and a singlet, the singlet lying lowest in energy. Distortions from cubic symmetry split the first triplet only slightly. Again the lowest level can be described by the following spin Hamiltonian

$$H = \beta\vec{H}\cdot\overline{\overline{g}}\cdot\vec{S}' .$$

2. THE PARAMAGNETIC STATE

The magnetic properties of a solid in the paramagnetic state are usually described by its susceptibility χ which is its response to an applied magnetic field. This is given by the following expression

$$\vec{M} = \overline{\overline{\chi}} \cdot \vec{H} \qquad (1)$$

where M is the induced magnetization and H is the applied magnetic field. χ is a second rank tensor and from thermodynamical considerations the tensor is symmetric. Since χ represents a physical property of a crystal it must be related to the crystal symmetry. Neumann's Principle (Nye 1957) tells us that the symmetry elements of any physical property must include the symmetry elements of the point group of the crystal. Applying this to a crystal with the point group 2/m, which is the point group of the crystals studied here, the suscepbitility tensor is reduced as shown below.

$$\begin{pmatrix} \chi_{11} & \chi_{12} & \chi_{13} \\ \chi_{12} & \chi_{22} & \chi_{23} \\ \chi_{13} & \chi_{23} & \chi_{33} \end{pmatrix} \qquad 2/m \qquad \begin{pmatrix} \chi_{11} & 0 & \chi_{13} \\ 0 & \chi_{22} & 0 \\ \chi_{13} & 0 & \chi_{33} \end{pmatrix}$$

where the reference frame $(\hat{x}_1, \hat{x}_2, \hat{x}_3)$ is such that $\hat{x}_2$ is along thw two-fold axis. Thus the two-fold axis is a principal axis of the susceptibility tensor. The other principal axes lie in the plane perpendicular to the two fold axis but their directions in this plane are not specified by symmetry.

An expression for the magnetic susceptibility may be derived from a microscopic point of view. The method used is due to Van Vleck (1932). The susceptibility is derived for the case with no exchange interactions between the magnetic ions and the result given when exchange is included.

In general a magnetic ion in a crystal has a series of energy levels with energy E_n. Each level has associated with it a magnetic quantum number m. The application of a magnetic field splits these levels. The Hamiltonian $\mathcal{H}$ for the perturbation due to such a magnetic field in the z direction may be written

$$\mathcal{H} = \beta(L_z + 2S_z)H_z \tag{2a}$$

where L_z and S_z are the z components of the orbital and spin momentum respectively of the magnetic ion, β is the Bohr magneton and H_z the magnetic field applied along the z-direction. In terms of the z-component of the magnetic moment μ_z the Hamiltonian is

$$\mathcal{H} =-\mu_z H_z \tag{2b}$$

where $\mu_z = -\beta(L_z+2S_z)$.

The energy of the nth level may be expanded in a series in the applied magnetic field

$$E_n = E_n^o + H_z\, E_{n,m}^{(1)} + H_z^2\, E_{n,m}^{(2)} + \ldots$$

where E_n^o is the energy of the nth level in zero applied field and $E_{n,m}^{(1)}$ and $E_{n,m}^{(2)}$ are the following

$$E_{n,m}^{(1)} = (-1)\langle n,m|\mu_z|n,m\rangle$$

and $$E_{n,m}^{(2)} = \sum_{n',m'} \frac{|\langle n,m|\mu_z|n'm'\rangle|^2}{E_n - E_{n'}} .$$

The z-component of the magnetic moment of the n^{th} level m^{th} state is given by

$$\mu_z^{n,m} = - \frac{\partial E_{n,m}}{\partial H_z} \quad .$$

The total magnetic moment in the z-direction μ_z^T of N ions is the statistical mean over all states using a Boltzman distribution.

$$\mu_z^T = \frac{N \sum\limits_{n,m} \mu_z^{n,m} e^{-E_n/kT}}{\sum\limits_n e^{-E_n/kT}}$$

The exponential may be expanded in the following way

$$e^{-E_n/kT} = \exp\left[- \frac{E_n^o + H_z E_{n,m}^{(1)} + \ldots}{kT}\right]$$

$$\simeq e^{-E_n^o/kT} \left[1 - \frac{H_z E_{n,m}^{(1)}}{kT} \right]$$

Substituting this into the expression for the total magnetic moment one gets

$$\mu_z^T = \frac{N \sum\limits_{n,m} (-E_{n,m}^{(1)} - 2H_z E_{n,m}^{(2)}) (1 - \frac{H_z E_{n,m}^{(1)}}{kT}) e^{-E_n^o/kT}}{\sum\limits_n e^{-E_n^o/kT}}$$

If there is assumed to be no permanent magnetic moment and if only terms linear in H are retained then

$$\mu_z^T = NH_z \frac{\sum\limits_{n,m} (\frac{|E_{n,m}^{(1)}|^2}{kT} - 2 E_{n,m}^{(2)}) e^{-E_n^o/kT}}{\sum\limits_n e^{-E_n^o/kT}}$$

The susceptibility in the z direction $\chi_z = \mu_z^T/H_z$ is

$$\chi_z = \frac{N \sum\limits_{n,m} \left(\frac{|E^{(1)}_{n,m}|^2}{kT} - 2E^{(2)}_{n,m} \right) e^{-E^o_n/kT}}{\sum\limits_{n} e^{-E^o_n/kT}} \qquad (3)$$

When the splitting of the ground state is small compared to kT and the energy of the first excited state is large compared to kT, Van Vleck (1932) has shown that the susceptibility reduces to

$$\chi_z = N \sum_m \left[\frac{|E^{(1)}_{om}|^2}{j_m kT} - 2 \frac{E^{(2)}_{om}}{j_m} \right] \qquad (4)$$

where

$$E^{(1)}_{om} = (-1) \langle o,m|\mu_z|o,m\rangle$$

and

$$E^{(2)}_{om} = \sum_{nm} \frac{|\langle o,m|\mu_z|n,m\rangle|^2}{E_o - E_n}$$

and j_m is the multiplicity of the ground state. The first term of equation (4) is temperature dependent. The second term is temperature independent and gives a positive contribution to the susceptibility. It is called the Van Vleck term. The temperature dependent term can be further reduced to

$$\chi_z = \frac{N g_z^2 \beta^2 S'(S'+1)}{3kT} \qquad (5)$$

where for μ_z we have used the fictitious spin S' and the g_z component of the g tensor such that $\mu_z = -g_z \beta S'_z$. This is just the Curie law for the magnetic susceptibility.

Atkinson et al (1970) have derived an expression for the magnetic susceptibility with the following Hamiltonian for the i^{th} ion

$$H_i = -\vec{\mu}_i \cdot \vec{H} + \sum_{j=1}^{z} J_{ij}\, \vec{S}_i \cdot \vec{S}_j \qquad (6a)$$

The summation is over the z nearest neighbours. The molecular field approximation was used so that the Hamiltonian becomes the following

$$H_i = -\vec{\mu}_i \cdot \vec{H} + J\langle\vec{S}\rangle \cdot \vec{S}_i \qquad (6b)$$

where $\langle S \rangle$ is the thermal average of the spin and $J = zJ_{ij}$. The expression for the susceptibility in the z direction is given by the following.

$$\chi_z = N \sum_{n,m} \left[\frac{|E^{(1)}_{n,m}|^2}{kT} - 2 \sum_{n'm'} \frac{|E^{(2')}|^2}{E_n - E_{n'}} \right] e^{-E^o_n/kT} \Big/ \sum_n e^{-E^o_n/kT}$$

$$+ \frac{\frac{N}{H_z} \sum_{n,m} \left[\frac{E^{(1)}_{n,m} E^{(3)}_{nm} \langle S_z \rangle}{kT} - 2 \sum_{n'm'} \frac{E^{(2')}_{nm} E^{(4)}_{nm}}{E_n - E_{n'}} \langle S_z \rangle \right] e^{-E^o_n/kT}}{\sum_n e^{-E^o_n/kT}} \qquad (7)$$

where

$E^{(2')}_{n,m} = (-1)\langle n,m|\mu_z|n',m'\rangle$, $E^{(3)}_{n,m} = J\langle n,m|S_z|n,m\rangle$,

$E^{(4)}_{n,m} = J\langle n,m|S_z|n'm'\rangle$

and

$$\langle S_z \rangle = H_z \sum_{n,m} \frac{\left[\frac{(-1)E^{(1)}_{n,m} E^{(3)}_{nm}}{JkT} + \frac{2}{J} \sum_{n'm'} \frac{E^{(2')}_{n,m} E^{(4)}_{nm}}{E_n - E_{n'}} \right] e^{-E^o_n/kT}}{\sum_n e^{-E^o_n/kT}}$$

$$+ \langle S_z \rangle \frac{\sum_{n,m} \left[\frac{(-1)|E^{(3)}_{n,m}|^2}{JkT} + \frac{2}{J} \sum_{n'm'} \frac{|E^{(4)}_{nm}|^2}{E_n - E_{n'}} \right] e^{-E^o_n/kT}}{\sum_n e^{-E^o_n/kT}}$$

If the energy of the first excited state is large compared to kT, the exchange J is small compared to kT and the fictitious spin equals the true spin then the temperature dependent part of equation (7) reduces to

$$\chi_z = \frac{Ng_z^2\ \beta^2\ S(S+1)}{3k} / (T + \Theta) \qquad (8)$$

where $\Theta = \frac{J\ S(S+1)}{3k}$.

In the antiferromagnetic state J is positive. The effect of antiferromagnetic exchange tends to reduce the susceptibility. Equation (8) is just the Curie Weiss law.

The Weiss molecular field approximation gives good agreement with experiment at high temperatures. In fact the agreement improves with increasing temperature. However it has a few serious deficiencies. It gives a transition temperature which is too high and it does not predict short range order. A better approximation which corrects these deficiencies and approaches the molecular field approximation in the high temperature limit is the High Temperature Series Expansion (H.T.S.E.). The method involves expanding the magnetic susceptibility in a series in inverse powers of the temperature. Using the following Hamiltonian

$$\mathcal{H} = J \sum_{<ij>} \vec{S}^i \cdot \vec{S}^j + g\beta H_z \sum_i S_z^i$$

where <ij> indicates the sum is only over nearest neighbours Rushbrooke and Wood (1958) give the series as

$$\frac{2Ng^2\beta^2}{J\theta\chi_T} = \frac{3}{S(S+1)} \sum_{n=0}^{\infty} \frac{b_n}{\theta}$$

where $\theta = \frac{kT}{J}$, $b_o = 1$ and there are 2N ions in the crystal. χ_T is the temperature dependent susceptibility. The coefficients b_n in the expansion have only been evaluated for a few simple lattices in two and three dimensions (Rushbrooke and Wood 1958).

The series has been calculated for two of the two dimension lattices, the quadratic layer lattice and the honeycomb layer lattice for a spin S = 1/2. The quadratic layer lattice is a two dimension square net such that each lattice point has four nearest neighbours. The series for this lattice is the following for S = 1/2.

$$\frac{2Ng^2\beta^2}{\chi_T J} = 4\theta[1 + \frac{1.0}{\theta} + \frac{0.5}{\theta^2} + \frac{0.167}{\theta^3} + \frac{0.156}{\theta^4} + \frac{0.0151}{\theta^5} + \frac{0.00002}{\theta^6} + \ldots] \qquad (9)$$

The honeycomb layer lattice is a two dimensional hexagonal net such that each lattice point has three nearest neighbours. The series for this lattice is the following for S = 1/2.

$$\frac{2Ng^2\beta^2}{\chi_T J} = 4\theta[1 + \frac{0.75}{\theta} \quad \frac{0.275}{\theta^2} \quad \frac{0.125}{\theta^3} \quad \frac{0.0078}{\theta^4} \quad \frac{0.0296}{\theta^5} + \frac{0.0046}{\theta^6} + \ldots] \qquad (10)$$

Both series are plotted in figure 1. The minimum of the inverse susceptibility for the quadratic case occurs at θ = 0.92. In the honeycomb case no minimum was observed,

Figure 1. The calculated temperature-dependent contribution to the paramagnetic susceptibility χ as a function of temperature for a quadratic layer antiferromagnet, dashed line and a honeycomb layer antiferromagnetic, solid line. The calculations were done using a High Temperature Series Expansion with nearest neighbour exchange J, spin S = 1/2 and for 2N ions.

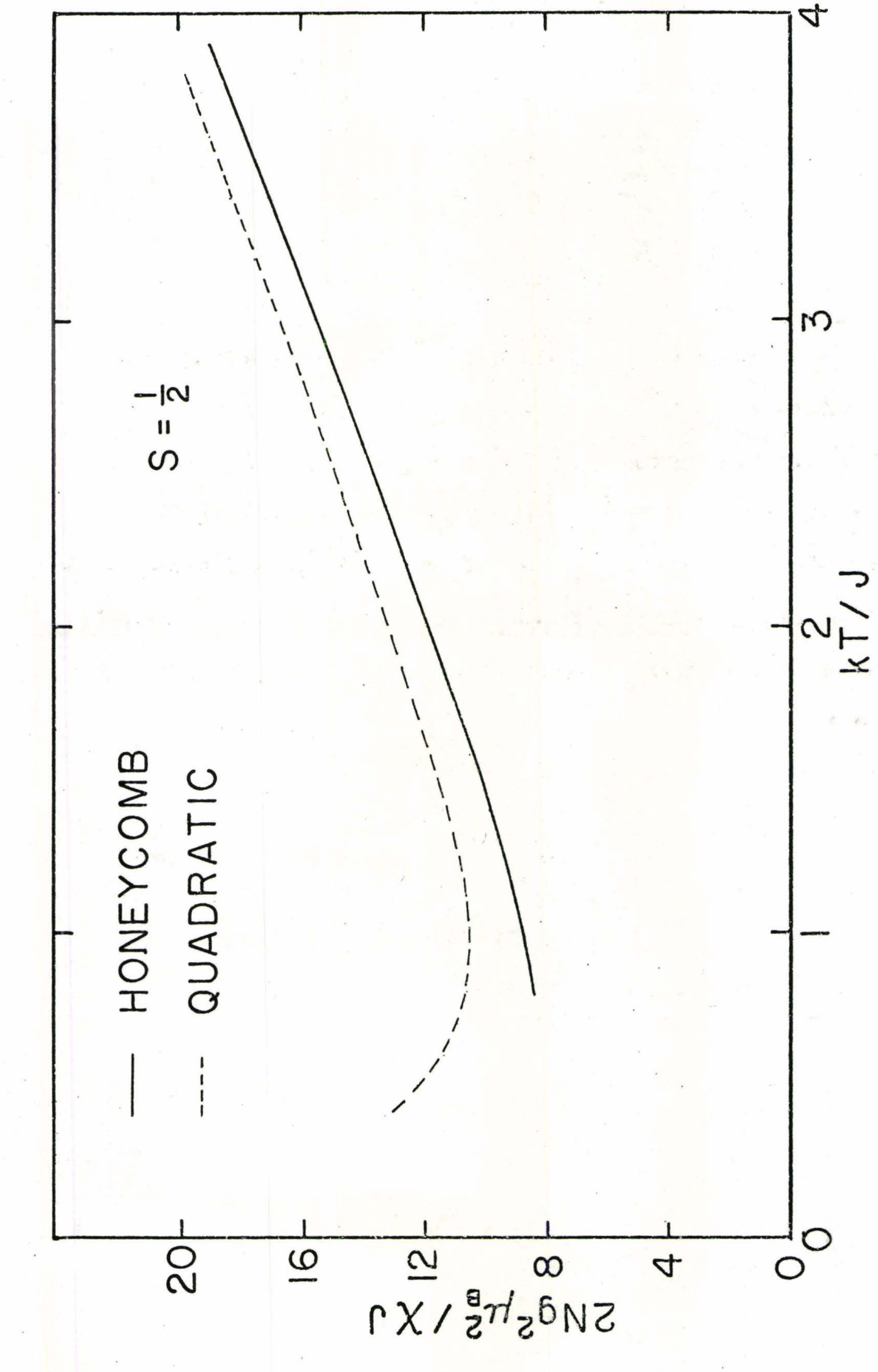
— HONEYCOMB
--- QUADRATIC
S = 1/2
0
1
2
3
4
kT/J
0
4
8
12
16
20
2Ng²μ_B²/χJ

however, the series could not be plotted beyond $\theta = 0.80$ due to insufficient terms in the expansion. Both of these series, equations (9) and (10) reduce to the molecular field approximation in the high temperature limit. The molecular field gives

$$\chi = \frac{2Ng^2\beta^2\ S(S+1)}{3k} / (T + \Theta)$$

where $\Theta = zJ\ S(S+1)/3k$.

For the quadratic case, $z = 4$ $\quad \Theta = \frac{4J\ S(S+1)}{3k}$

and for the honeycomb case $z = 3$ $\quad \Theta = \frac{3J\ S(S+1)}{3k}$.

3. MAGNETICALLY ORDERED STATE

In the antiferromagnetic state the system is regarded as being divided into sublattices. In what follows we consider only two sublattices. Using the molecular field approximation the most general expression for the energy of E of a two sublattices system may be written in the following way (Date 1961)

$$E = \vec{M}^{+}\cdot\bar{\bar{A}}\cdot\vec{M}^{-} = \frac{1}{2}[\vec{M}\cdot\bar{\bar{\Gamma}}\cdot\vec{M}^{+} + \vec{M}^{-}\cdot\bar{\bar{\Gamma}}\cdot\vec{M}^{-}] + \vec{M}^{+}\cdot\bar{\bar{A}}'\cdot\vec{M}^{-}$$

$$+\frac{1}{2}[\vec{M}^{+}\cdot\bar{\bar{\Gamma}}'\cdot\vec{M}^{+} + \vec{M}^{-}\cdot\bar{\bar{\Gamma}}'\cdot\vec{M}^{-}] \qquad (11)$$

where A and Γ are isotropic tensors and A' and Γ' are anisotropic traceless tensors. M^{+} and M^{-} represent the magnetization of the two sublattices. In equation (11) the first and second terms represent isotropic exchange interaction energy, the third and fourth represent the anisotropy energy which would include any anisotropic exchange. The resultant effective field H_{eff} at each sublattice is obtained in the following way

$$\delta E = -H^{+}_{eff}\, \delta M^{+} - H^{-}_{eff}\, \delta M^{-}$$

thus

$$\vec{H}^{\pm}_{eff} = -\bar{\bar{A}}\vec{M}^{\mp} - \bar{\bar{\Gamma}}\vec{M}^{\pm} - \bar{\bar{A}}'\vec{M}^{\mp} - \bar{\bar{\Gamma}}'\vec{M}^{\pm} . \qquad (12)$$

At low applied magnetic fields, ie when the applied field is very much less than the critical field for "spin flop", the susceptibility of an antiferromagnet may be represented by a tensor. Its principal values are $\chi_{\parallel}$ the susceptibility when the applied field is parallel to the zero field spin direction and $\chi_{\perp}$(s) the susceptibility when the applied field is perpendicular to the zero field spin direction.

When the symmetry of the anisotropy energy has the orthorhombic form it is customary to choose the following orthogonal coordinate system. The x-axis is chosen as the spin direction in zero field. The direction in the plane perpendicular to the spin direction in which the spins flop to when the applied field along the spin direction exceeds the critical field is called the y-axis. The y-axis is then thought of as being the intermediate axis. The z-axis is thus in the plane perpendicular to the zero field spin direction and at right angles to the y-axis. The z-axis is referred to as the hard axis.

When the exchange field is very much larger than the anisotropy field(s) it is a good approximation to equate $\chi_\perp$ to 1/A. However when the anisotropy field(s) are not negligible with respect to the exchange field then the perpendicular susceptibility is modified. Using equation (12) and balancing torques one obtains the following results

$$\underset{(H||y\text{-axis})}{\chi_\perp^y} = 1/[A + \tfrac{1}{2}(P_y+Q_x)] \qquad (13a)$$

and

$$\underset{(H||z\text{-axis})}{\chi_\perp^z} = 1/[A + \tfrac{1}{2}(P_z+Q_x)] \qquad (14a)$$

where P = A' + Γ' and Q = A' - Γ'. P and Q like A' and Γ' are traceless tensors. The above coordinate system is assumed to diagonalize both A' and Γ'. When the A' tensor is zero the perpendicular susceptibilities reduce to

$$\chi_\perp^y = 1/[A + \tfrac{1}{2}(\Gamma_y' - \Gamma_x')] \qquad (13b)$$

and

$$\chi_\perp^z = 1/[A + \tfrac{1}{2}(\Gamma_z' - \Gamma_x')] \ . \qquad (14b)$$

The parallel susceptibility measures the imbalance of the sublattices due to the applied magnetic field. Date and Mitokawa (1967) give the following expression when the temperature is very much less than the Néel temperature

$$\chi_{||} = \frac{Ng^2\mu_B^2}{kT} \exp\left(\frac{-3}{S+1} \cdot \frac{T_N}{T}\right). \qquad (15)$$

where N is the number of ions in the crystal and T_N is the Néel temperature.

The elementary excitations of an ordered magnetic system are called magnons. Here the reversal of a single spin is shared by the whole system. In an isotropic Heisenberg antiferromagnet the magnon excitation system would extend continuously to zero energy. However, in the presence of anisotropy energy there is an energy gap at zero wavevector. Antiferromagnetic resonance is just the excitation of zero wavevector magnons and thus gives a measure of the zero wavelength energy gap in the magnon spectrum. In low Néel temperature antiferromagnets it is expected that the AFMR frequency would be in the microwave region of the electromagnetic spectrum. In this region continuous frequency sources are not available so that the resonance has to be observed with the aid of an applied magnetic field. It is found that the resonance then depends on the direction of the applied magnetic field with respect to the crystal.

The theory of AFMR in the presence of an applied magnetic field has been treated by Kittel (1952), Keffer and Kittel (1952), Nagamiya et al (1955), Date (1961) and others. The first step is to set up the equations of motion of the system. The equations of motion are just an extension of Kittel's used in the ferromagnetic resonance problem. In the two sublattice antiferromagnetic case the torque of each sublattice is equal to the rate of change of angular momentum of each sublattice. Thus

$$\frac{1}{\gamma}\frac{dM^{\pm}}{dt} = M^{\pm} \times H^{\pm}_{eff} \qquad (16)$$

where γ is the magnetomechanical ratio which relates the magnetic moment to the angular momentum. $M^{\pm}$ are the sublattice magnetizations and $H^{\pm}_{eff}$ is the effective field acting on the respective sublattice. γ is assumed to be equal for each sublattice since we are dealing with an antiferromagnet. The effective field H_{eff} can be written as a sum of magnetic fields

$$\vec{H}^{\pm}_{eff} = \vec{H}^{\pm}_{ex} + \vec{H}^{\pm}_{A} + \vec{H}^{\pm}_{mf} + \vec{H}^{\pm}$$

where the fields on the right hand side of the equation are the exchange field, the anisotropy field, the microwave field and the applied static field respectively. Using equations (12) and (16) Date (1961) has developed the resonance equations for the applied magnetic field in different directions in the crystal. As before we define $P = A' + \Gamma'$ and $Q = A'-\Gamma'$

The resonance equations are given by the following:

(i) The applied magnetic field is parallel to the zero field spin direction (x-axis) but is less than the critical field for spin flop. Since the equation is involved it is shown in determinental form

$$\left|\begin{array}{cccc} -\frac{i\omega}{\gamma}, & H[1+\frac{1}{2}(P_z-P_x)\chi_{||}], & 0 & (Q_x-Q_z)M_o \\ -H[1-\frac{1}{2}(P_y-P_x)\chi_{||}] & -\frac{i\omega}{\gamma}, & (Q_y-Q_x)M_o & 0 \\ 0 & 2[A+\frac{1}{2}(P_z+Q_x)]M_o, & -\frac{i\omega}{\gamma} & H[1-(A+\frac{1}{2}(P_x-Q_z))\chi \\ -2[A+\frac{1}{2}(P_y+Q_x)]M_o & 0 & H[1-(A+\frac{1}{2}(P_x+Q_y)\chi_{||}], & -\frac{i\omega}{\gamma} \end{array}\right.$$

$$= 0 \qquad (17)$$

Equation (17) can be simplified when $H = 0$ and $\frac{\omega}{\gamma} = 0$. If $H = 0$ then,

$$(\frac{\omega}{\gamma})^2 = 2(Q_x-Q_y)[A + \frac{1}{2}(P_z+Q_x)]M_o^2. \tag{17a}$$

If $(\frac{\omega}{\gamma}) = 0$ then,

$$H^2[1 - \frac{1}{2}(P_y-P_x)\chi_{||}][1 - \{A + \frac{1}{2}(P_x+Q_z)\}\chi_{||}] = 2(Q_x-Q_y)[A + \frac{1}{2}(P_y+Q_x)]M_o^2 . \tag{17b}$$

(ii) The applied field parallel to the x-axis and greater than the spin flop field.

$$(\frac{\omega}{\gamma})^2 = H^2\{1 + \frac{1}{2}(P_z-P_x)\chi_\perp^x\}\{1 + \frac{1}{2}(P_y-P_x)\chi_\perp^x\} -2(Q_x-Q_y)\{A + \frac{1}{2}(P_z+Q_y)\}M_o^2 \tag{18}$$

and

$$(\frac{\omega}{\gamma})^2 = 2(Q_y-Q_z)\{A + \frac{1}{2}(P_x+Q_y)\}M_o^2 - H^2\{1-[A + \frac{1}{2}(P_x+Q_y)\ \chi_\perp^x\} \times \{1 - [A + \frac{1}{2}(P_x + Q_z)]\chi_\perp^x\} \tag{19}$$

(iii) The applied field parallel to the y-axis then,

$$(\frac{\omega}{\gamma})^2 = H^2\{1 + \frac{1}{2}(P_x-P_y)\chi_\perp^y\}\{1 + \frac{1}{2}(P_z-P_y)\chi_\perp^y + 2(Q_x-Q_y)\{A + \frac{1}{2}(P_z+Q_x)\}M_o^2 \tag{20}$$

In these equations M_o is the zero field sublattice magnetization. In equations (18) and (19) $\chi_\perp^x$ is the perpendicular susceptibility when the field is parallel to the x-axis but greater than the critical-field and has the value

$$\chi_\perp^x = 1/[A + \frac{1}{2}(P_x+Q_y)] \tag{21}$$

Equations (18) and (20) can be simplified when terms in P^2 can be neglected.

Equation (18) then becomes

$$\left(\frac{\omega}{\gamma}\right)^2 = \left(1 - \frac{3}{2} P_x \chi_\perp^x\right) H^2 - 2(Q_x - Q_y)\left[A + \frac{1}{2}(P_z + Q_y)\right] M_o^2 \quad (18a)$$

and equation (20) becomes

$$\left(\frac{\omega}{\gamma}\right)^2 = \left(1 - \frac{3}{2} P_y \chi_\perp^y\right) H^2 + 2(Q_x - Q_y)\left[A + \frac{1}{2}(P_z + Q_x)\right] M_o^2 \ . \quad (20a)$$

A simplified theory of AFMR can be given when the A' tensor is zero. This is the more familiar theory of Nagamiya and Yosida (Nagamiya et al 1955). In this case the energy of a two sublattice system has the following form

$$\begin{aligned} E = {} & \vec{M}^+ \cdot \bar{\bar{A}} \cdot \vec{M}^- + \frac{1}{2}[\vec{M}^+ \cdot \bar{\bar{\Gamma}} \cdot \vec{M} + \vec{M}^- \cdot \bar{\bar{\Gamma}} \cdot \vec{M}^-] \\ & + \frac{1}{2} k_1 (\beta_+^2 + \beta_-^2) + \frac{1}{2} k_2 (\gamma_+^2 + \gamma_-^2) \end{aligned} \quad (22)$$

where A and Γ are isotropic tensors, k_1 and k_2 $(k_2 > k_1 > 0)$ are the anisotropy constants, $\beta_\pm$ and $\gamma_\pm$ are the direction cosines of the sublattice $M^\pm$ with respect to the y and z axes. The anisotropy fields H_a on the two sublattices are

$$H_{ax}^\pm = 0 \ , \quad H_{ay}^\pm = -\frac{k_1}{M_o} \beta_2 \ , \quad H_{az}^\pm = -\frac{k_2}{M_o} \gamma_\pm .$$

From equations (16) and (22) the resonance equations of the Nagamiya Yosida theory are developed. The equations are given for the case that the exchange field is very much larger than the anisotropy fields.

(i) Applied field parallel to x-axis, but less than spin flop field.

$$(\frac{\omega}{\gamma})^2 = \frac{1}{2}\{(1+\alpha^2)H^2 + A(k_1+k_2) \pm [(1-\alpha^2)H^4 + 2(1+\alpha^2)H^2A(k_1+k_2) + A^2(k_1-k_2)^2]^{\frac{1}{2}}]\} \quad (23)$$

where $\alpha = 1 - \chi_{\parallel}/\chi_{\perp}$.

(ii) Applied field parallel to x-axis but greater than spin flop field

$$(\frac{\omega}{\gamma})^2 = H^2 - 2Ak_1 \quad (24)$$

(iii) Applied field parallel to y-axis

$$(\frac{\omega}{\gamma})^2 = H^2 + 2Ak_1 \quad (25)$$

The spin flop field H_c is given by the following

$$H_c = (2Ak_1/\alpha)^{\frac{1}{2}} \quad (26)$$

It can be shown that the resonance equations of Date (1961) reduce to those of the Nagamiya Yosida theory in the limit of $A' = 0$. When the exchange field is very much larger than the anisotropy field then $k_1 = (\Gamma_y' - \Gamma_x')M_o^2$ and $k_2 = (\Gamma_z' - \Gamma_x')M_o^2$.

CHAPTER III

CRYSTALLOGRAPHY AND CRYSTAL PREPARATION

CRYSTALLOGRAPHY

The crystal structures of many of the pyrophosphates have been determined. The space groups of the compounds relevant to this thesis are shown in Table 1. The first four compounds are magnetic while the last two are diamagnetic. The diamagnetic ones have been included since they are isomorphic to some of the magnetic ones and have been used to investigate the local environment of the magnetic ions by electron spin resonance techniques.

All the pyrophosphates listed in Table 1 have the same crystal structure at high temperatures, the so-called β-phase, and all except $Mn_2P_2O_7$ show a phase transition to a lower symmetry structure at a lower temperature, the α-phase. The basic change in structure between the two phases is not the same for all the compounds. Some of the changes in structure and the phase transition temperature are listed in Table I for each compound. $Mn_2P_2O_7$ shows no change in structure down to 100°K (Calvo 1968). Table 2 lists the lattice parameters of the magnetic pyrophosphates. When the Bravais lattice is monoclinic it is customary to choose the β angle as the angle not equal to 90 degrees.

In the high temperature form, β phase, when all the

Table 1

Space groups of the pyrophosphates and some structural changes between the phases

	Low Temp α-phase	High Temp β-phase	Transition Temp	Basic change in Structure	Reference
$Mn_2P_2O_7$	-	C2/m	<100°K	none	Tondon (1970)
$Cu_2P_2O_7$	C2/c	C2/m	$\sim$353°K	P-O-P bond bends Cu^{++} sites slightly inequiv.	Robertson and Calvo (1967) (1968)
$Co_2P_2O_7$	$B2_1/c$	C2/m	$\sim$573°K	P-O-P bond bends bends Co^{++} ions half five fold coord. half six fold coord.	Calvo and Krishnamachari (1970)
$Ni_2P_2O_7$	$B2_1/c$	C2/m	$\sim$838°K	Same as $Co_2P_2O_7$	Łukaszewicz (1967) (1968)
$Mg_2P_2O_7$	$B2_1/c$	C2/m	$\sim$343°K	Same as $Co_2P_2O_7$	Calvo (1965) (1967)
$Zn_2P_2O_7$	I-c	C2/m	$\sim$405°K	P-O-P bond bends	Calvo (1965a) Robertson and Calvo (1970)

Table 2

Lattice Parameters of the pyrophosphates in the α and β phases

	Phase	a (Å)	b (Å)	c (Å)	β°
$Mn_2P_2O_7$		6.620	8.578	4.538	102.8
$Cu_2P_2O_7$	α	6.876	8.113	9.162	109.5
	β	6.827	8.118	4.516	108.8
$Co_2P_2O_7$	α	13.233	8.318	8.983	104.3
	β	-	-	-	-
$Ni_2P_2O_7$	α	13.093	8.275	8.974	104.9
	β	6.501	8.239	4.480	104.1

compounds have the same C2/m space group the structure is layer like with places of cations, Mn^{++}, Cu^{++} etc, between planes of anions, $P_2O_7^{4-}$, all parallel to the ab plane. The cations are surrounded by six oxygens in a distorted octahedron. However a feature of the α-phase of some of the pyrophosphates is that half of the cations are surrounded by only five oxygens.

CRYSTAL GROWING

$Mn_2P_2O_7$, $Cu_2P_2O_7$, $Co_2P_2O_7$ and $Ni_2P_2O_7$ are all insoluble in water. Their melting points are in the range 1200°C to 1500°C. It was found possible to grow single crystals of $Mn_2P_2O_7$, $Cu_2P_2O_7$ and $Co_2P_2O_7$ from the melt. However attempts to grow single crystals of $Ni_2P_2O_7$ from the melt were unsuccessful. The crystals were grown by heating the respective powder to just above its melting point under vacuum, approximately 5×10^{-4} torr in a shaped quartz crucible. The temperature was then lowered slowly through the melting point. Crystals were then extracted from the solidified mass. Examination by x-rays showed that they were single crystals except in the case of $Ni_2P_2O_7$ where the small crystallites obtained showed twinning.

CRYSTAL ALIGNMENT

Single crystals were aligned using an x-ray precession camera. The aligned crystal was then transferred to a sample holder which depended on the type of experiment. The alignment was checked after the crystal had been transferred to the sample holder and it was found that the alignment could be held to an accuracy of better than 2 degrees.

It was found convenient to choose the following orthogonal set of axes as a reference coordinate system. The a-axis, b-axis and c*-axis, where the b-axis is the two fold crystal axis and $\vec{c}* = \vec{a}\times\vec{b}$. Figure 2 shows the relative directions of these axes. Also shown in Figure 2 is the direction of the c-axis and the a*-axis $(\vec{b}\times\vec{c})$.

Figure 2. Direction of reference coordinate system with respect to the crystallographic axes

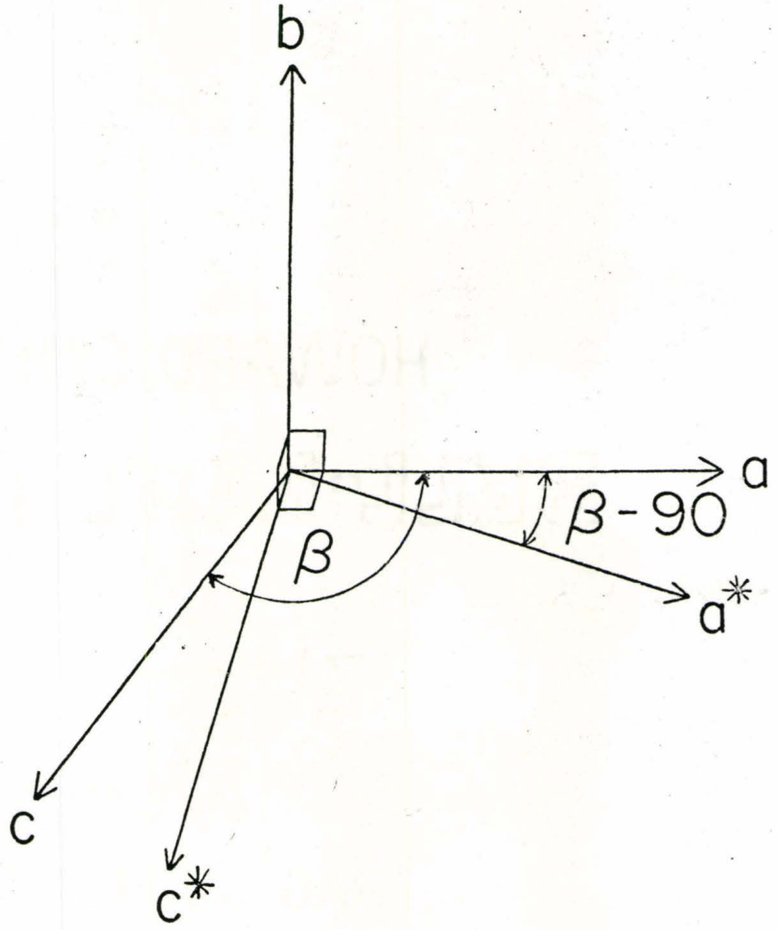
b
a
β-90
a*
β
c
c*

CHAPTER IV

EXPERIMENTAL METHOD

Two different measurement techniques were used, magnetic susceptibility and magnetic resonance. The magnetic resonance measurements can be subdivided into two types Electron spin resonance (E.S.R.) measurements which were made in the paramagnetic range and antiferromagnetic resonance (AFMR) measurements which were made in the ordered state. Although these resonances are different the experimental method of observing them is the same.

The magnetic susceptibility was measured using a Foner Vibrating Sample Magnetometer (F.V.S.M.), Foner (1959) manufactured by Princeton Applied Research Corporation. The principle of the F.V.S.M. is the following. The sample to be measured is vibrated perpendicular to the direction of the applied magnetic field. This induces a voltage in a set of pick-up coils which are attached to the poles-faces of the magnet. This voltage is proportional to the magnetic moment of the sample. At the same time a reference voltage of the same frequency, as that induced in the coils, is produced at a set of vibrating capacitor plates. The reference voltage is varied, by changing the dc voltage on the capacitor system, to produce a null between the reference voltage and that induced in the coils by the vibrating sample. The dc voltage applied to the capacitor system to produce this null is then proportional to the magnetic moment of the sample. The susceptibility can then be determined knowing the applied magnetic field. The magnetometer was calibrated using the saturated magnetic moment of high purity nickel. Danan et al (1968) give the value 58.6 emu/gm.

Measurements were made down to 4.2°K using a low temperature cryostat and up to 600°K using a home made furnace. The temperature was measured using a thermocouple. Different thermocouples were used for different temperature ranges. The thermocouple calibrations were obtained by adjusting the published thermocouple tables to measured fixed points. Magnetic fields up to 14.5 kOe were available from a "Magnion", 9 inch pole face, electromagnet with a 2 inch pole gap.

For the single crystal measurements the aligned crystal was mounted on the end of quartz rod. This was attached to the magnetometer in such a way that the magnetic field could be applied in the plane perpendicular to the direction of alignment. In the case of powders, the powder was packed in an epoxy glass holder. In both the single crystal and powder cases the measurements were corrected for background by repeating the measurements with the sample removed.

The accuracy of the absolute temperature depended on the temperature range. At temperatures close to liquid helium, 4.2°K, we estimated the accuracy of temperature to be better than 0.5°K. The absolute accuracy of the susceptibility measurements is about 2%.

The experimental technique for the E.S.R.and AFMR measurements was the same. Experiments were done in the microwave region at three different frequency ranges, 9 to 12 GHz, 34 to 36.5 GHz and 67 to 72.5 GHz. For all the frequency ranges a microwave bridge was used to measure the reflected power from a shorted waveguide. For the 34 to 36.5 GHz range the bridge from a Varian E.S.R. spectrometer was used. "Magic Tee" bridges were used for the other frequency ranges. Due to high attenuation losses in waveguides appropriate for the high frequency range, 67-72.5 GHz, it was found convenient to use waveguides appropriate to the lower frequency 34-36.5 GHz and to connect to the high frequency bridge with a tapered section. Measurements at the lower frequency were done using the appropriate waveguide. Standard low frequency, 80 Hz, field modulation and phase sensitive detection techniques were employed to measure the resonances.

Measurements were made using a "Varian 15" electromagnet with either a 2" gap giving 0 to 23 kOe or a 1" gap giving 0 to 30 kOe. Additional measurements were made on a 0 to 60 kOe Westinghouse superconducting solenoid. In the case of the Varian magnet the field was measured using a Varian Fieldial which was calibrated by a nuclear resonance gaussmeter. During experiments the calibration was checked against the E.S.R. of

DPPH, g = 2.0036. The field in the case of the superconducting solenoid was determined from a linear current field relationship which was calibrated using DPPH at two frequencies.

The optimum geometry for a magnetic resonance measurement requires that the microwave magnetic field be perpendicular to the dc magnetic field. When the angle between these two fields decreases the sensitivity decreases such that when the two fields are parallel no resonance should be observed.

The aligned single crystal was mounted on the end plate that sealed the waveguide in such a way that the magnetic field could be applied in a plane perpendicular to a desired crystallographic axis. Since the AFMR could usually only be observed over a limited angular range, because of magnetic field limitations, the crystal was positioned so that the angle between the microwave field and the magnetic field was always close to 90 degrees. When the superconducting magnet was used the crystal was mounted on a rotatable pin that was attached to the broad side of the waveguide, 1-1/2 guide wavelengths from the shorting plate. The crystal could be rotated about an axis perpendicular to the dc magnetic field.

For temperatures of 4.2°K and below the sample was immersed in liquid ^{4}He. By pumping on ^{4}He temperatures down to 1°K could be obtained. These temperatures were measured from the helium vapour pressure. Temperatures above 4.2°K were obtained by having a large helium reservoir below the sample.

In this way when the liquid helium level fell below the sample the warming rate was sufficiently slow. The following are typical warming rates, between 4.2°K and 10° K, ∿ 0.05°K per minute, between 10°K and 20°K, ∿ 0.1°K per minute, and between 20°K and 40°K ∿ 0.2°K per minute. These warming rates were slow enough to allow resonance data to be taken. The temperature about 4.2°K was measured using a calibrated Ge resistance thermometer (Texas Instr.) which was corrected for magnetoresistance.

CHAPTER V

EXPERIMENTAL RESULTS AND DISCUSSION

(i) $Mn_2P_2O_7$

Experimental Results

Three different types of measurement were made on single crystals of $Mn_2P_2O_7$. They were magnetic susceptibility measurements, electron spin resonance measurements and antiferromagnetic resonance measurements.

The magnetic susceptibility of a single crystal of $Mn_2P_2O_7$ was measured from 4.2°K to 300°K. This is shown in figure 3 for the applied field parallel to the x and y axes. The directions of the x and y axes with respect to the crystallographic axes are shown in figure 4. The angular dependence of the susceptibility at 4.2°K is shown in figure 5 for the applied magnetic field in the ac plane, H perpendicular to the b-axis, and in the ab plane, H perpendicular to the c* axis. Table 3 lists the principal values of the susceptibility at 4.2°K. At 295°K the susceptibility showed less than one percent deviation from being isotropic.

Electron spin resonance of Mn^{++} in $Mn_2P_2O_7$ was observed at approximately 35 GHz. The g value was isotropic and had the value 2.000(5). At room temperature the linewidth was 0.50 kOe. Figure 6 shows the temperature dependence of the intensity, peak

Figure 3. The temperature dependence of the magnetic susceptibility of $Mn_2P_2O_7$ from 4.2 to 300°K. The magnetic field was applied along the x-direction, 22° from the a axis, and along the y-axis, 22° from the c* axis. The insert shows an enlarged view of the low temperature range.

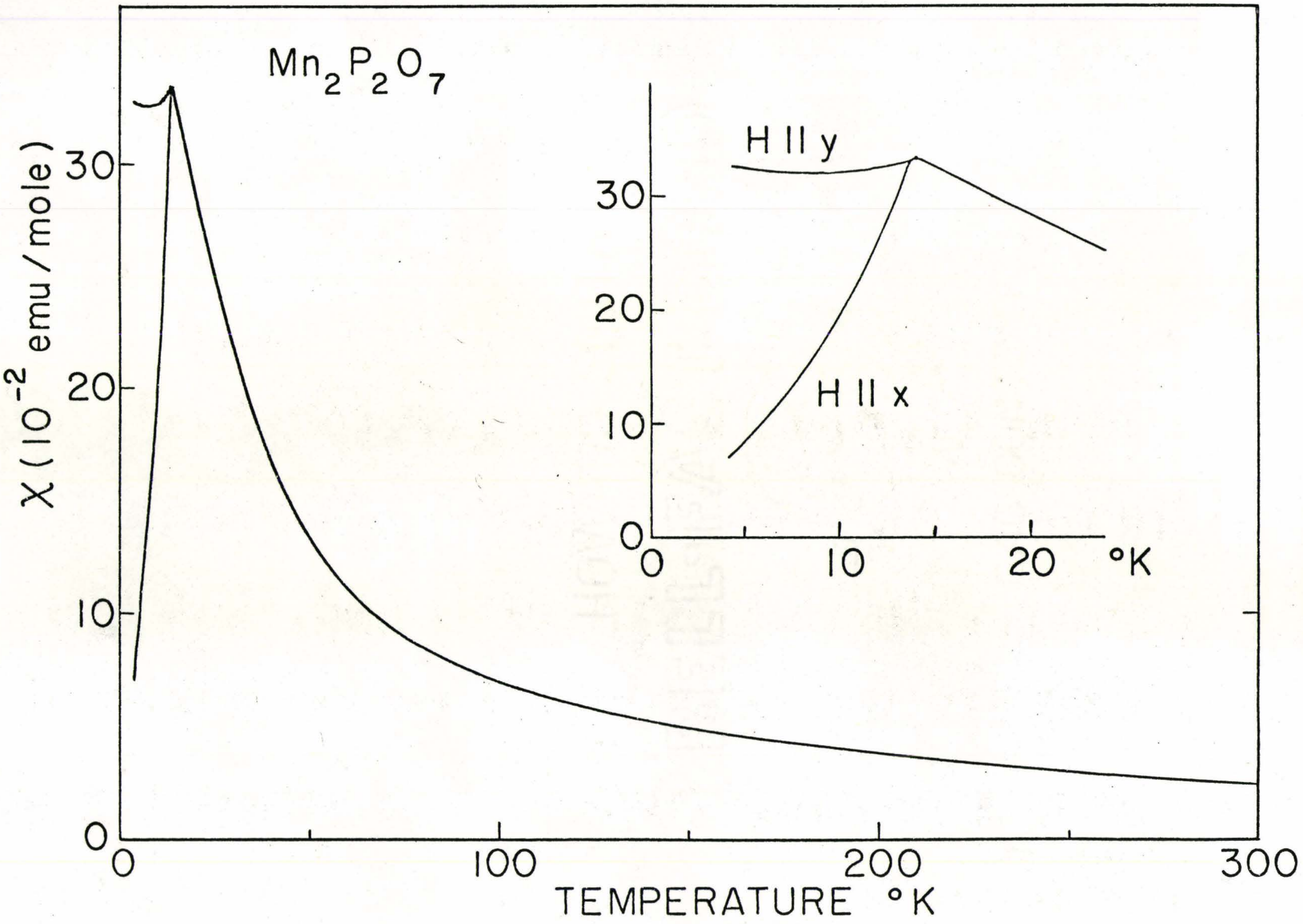
$Mn_2P_2O_7$
χ (10^{-2} emu / mole)
0
10
20
30
0
100
200
300
TEMPERATURE °K
H ll y
H ll x
0
10
20
30
0
10
20
°K

Figure 4. Principal directions of the magnetic susceptibility at 4.2°K. The x axis is along the spin direction. The y axis is perpendicular to the x-axis in the ac* plane. The b axis or z axis is the two fold axis of the crystal.

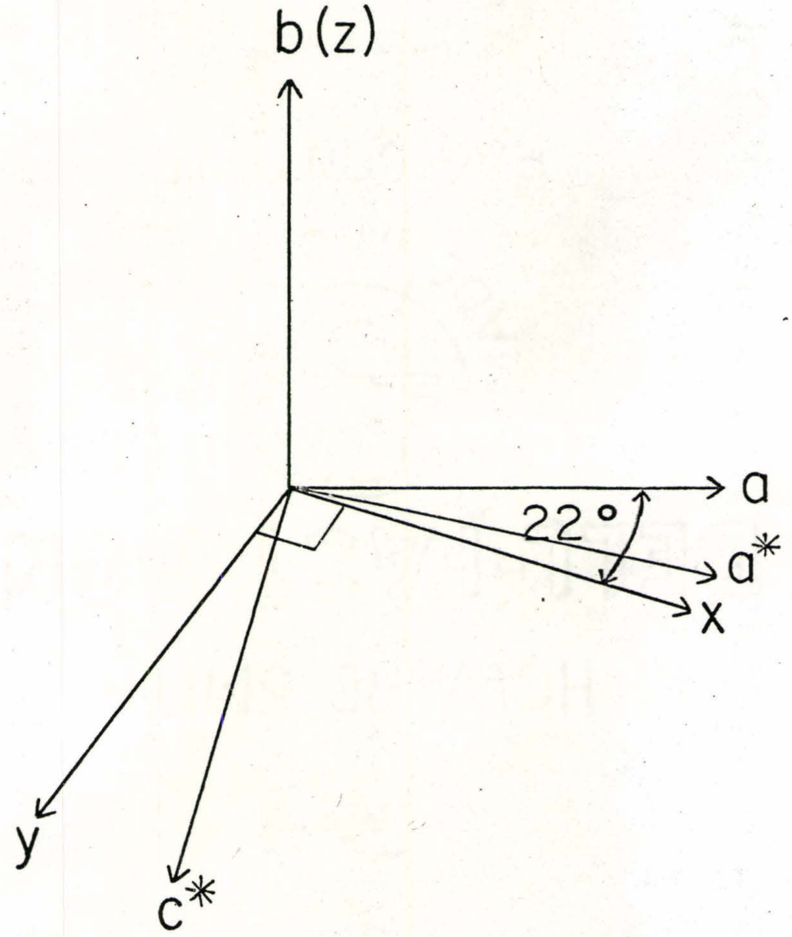

b (z)
a
22°
a*
x
y
c*

Figure 5. The angular dependence of the magnetic susceptibility of $Mn_2P_2O_7$ at 4.2°K, for the magnetic field in the ab plane, i.e. H perpendicular to c* axis and for the magnetic field in the ac plane, i.e. H perpendicular to b axis. The magnetic field was 12.6 kOe. Solid lines are smooth curves through the measured points.

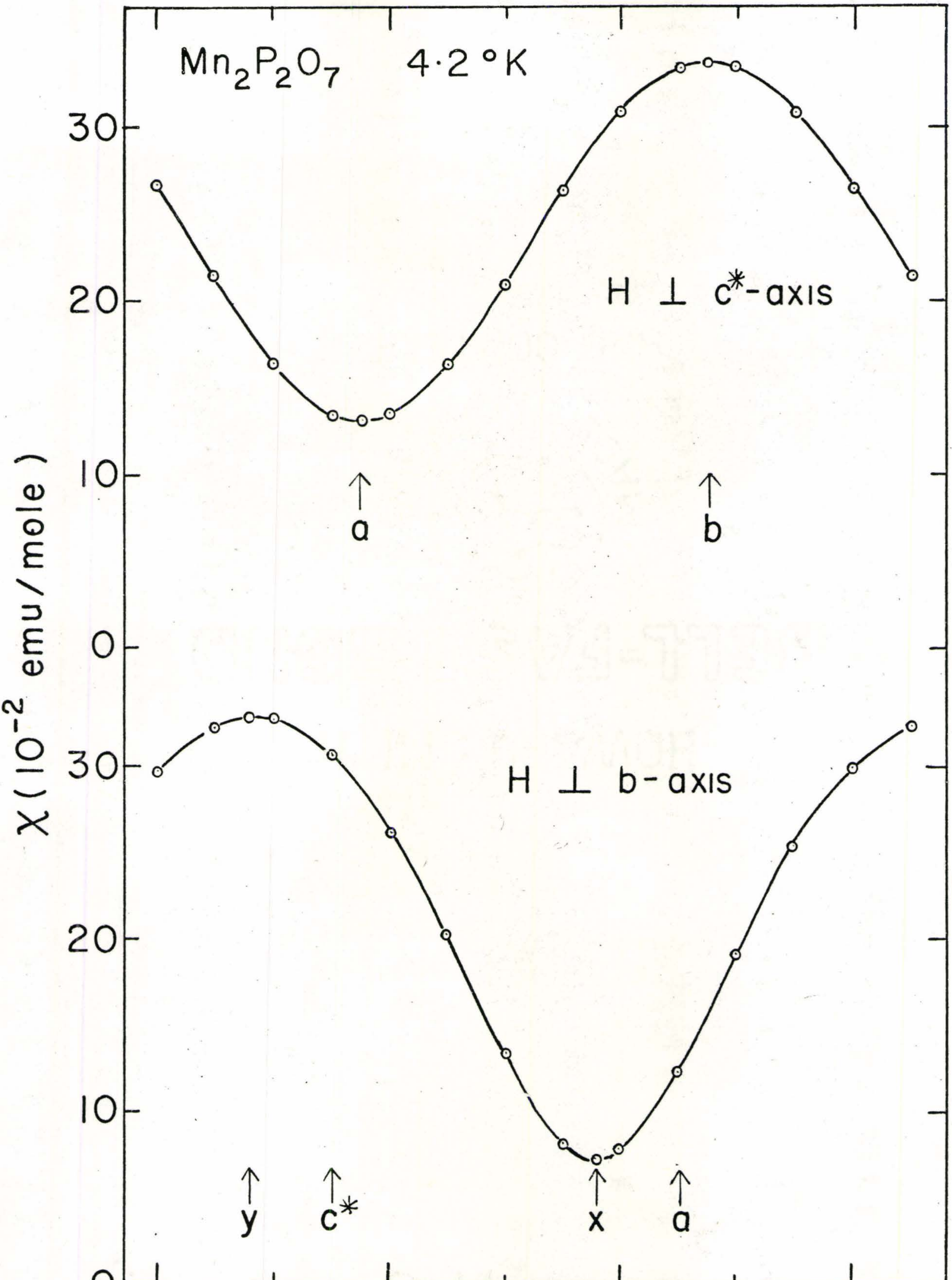
$Mn_2P_2O_7$ 4·2 °K
H ⊥ c*-axis
a
b
H ⊥ b-axis
y
c*
x
a
X (10⁻² emu/mole)
30
20
10
0
30
20
10
0
0
60
120
180
ANGLE °

Table 3

Principal Values of Magnetic Susceptibility of $Mn_2P_2O_7$ at 4.2°K

Direction	Susceptibility (10^{-2} emu/mole)
x-axis	7.0(2)
y-axis	32.9(1)
z-axis	34.0(1)

Figure 6. Temperature dependence of the absorption, peak to peak amplitude and linewidth of the electron spin resonance of Mn^{++} in $Mn_2P_2O_7$. The measurements were made at 35.04 GHz with the applied magnetic field along the x-axis. No absorption was observed below 13.8(2)°K.

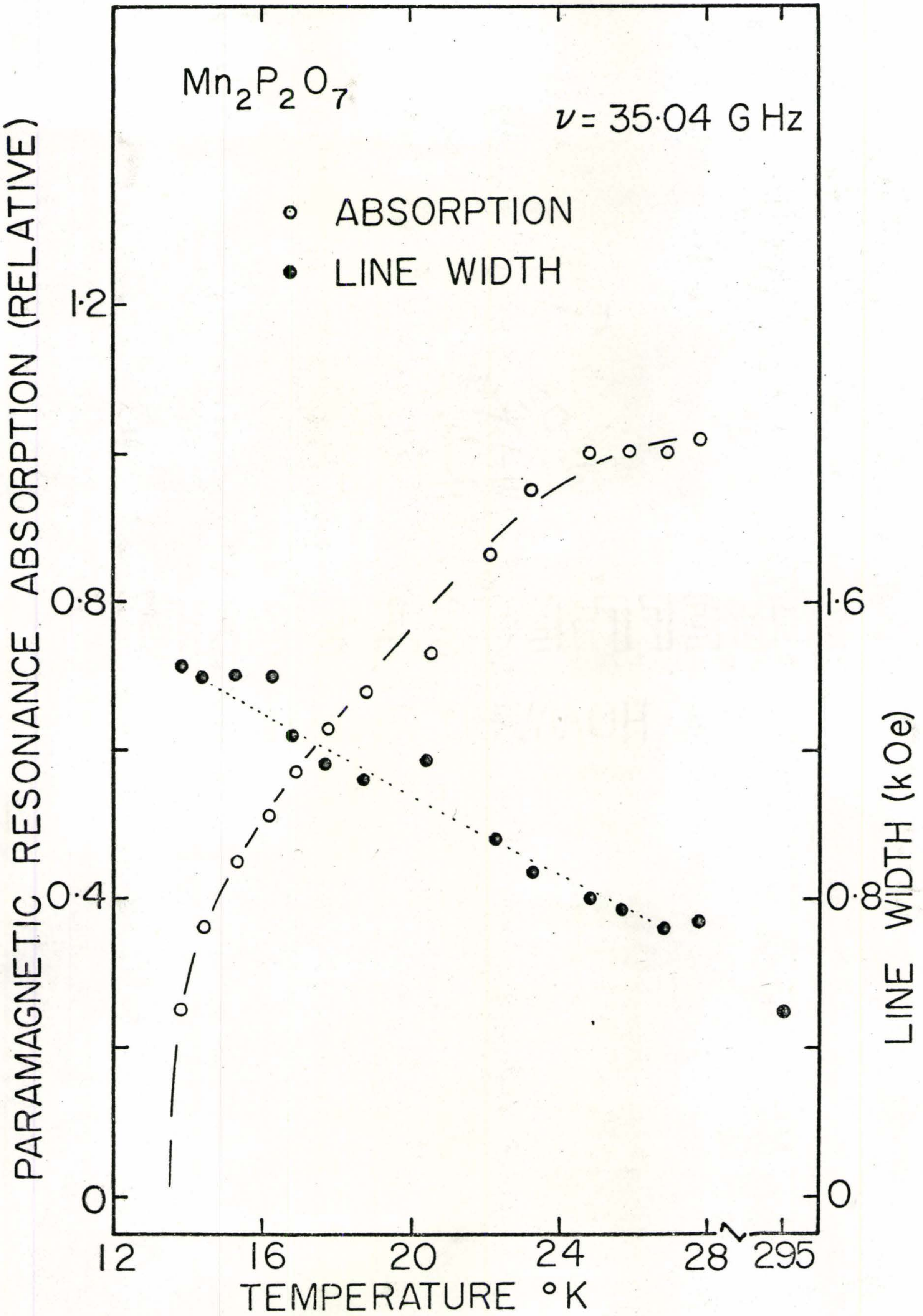
$Mn_2P_2O_7$
ν = 35·04 GHz
○ ABSORPTION
● LINE WIDTH
PARAMAGNETIC RESONANCE ABSORPTION (RELATIVE)
1·2
0·8
0·4
0
LINE WIDTH (kOe)
1·6
0·8
0
12
16
20
24
28
295
TEMPERATURE °K

to peak amplitude , of the resonance and of the linewidth. The resonance could not be observed below 13.8(2)°K.

Antiferromagnetic resonance was observed in $Mn_2P_2O_7$ below 14°K. Measurements were made in two frequency ranges, 34 to 36 GHz and 67 to 72.5 GHz. Figure 7 shows the angular dependence of the resonances in the ac plane at different frequencies. The position of the low frequency minimum is 22(2) degrees from the a-axis. This is the x direction shown in figure 4. The angular dependence of the resonances in the xz plane, where the z direction corresponds to the b-axis, is shown in figure 8. In figure 9 the angular dependence of the resonances in yz plane is shown where the minimum corresponds to the applied field along the y-axis. The frequency versus magnetic field diagram at 4.2°K for the magnetic field along the x and y axes is shown in figure 10. In figure 11 is shown the temperature dependence at constant frequency of the resonance field and the linewidth when the field is along the x axis. The temperature dependence of the antiferromagnetic resonance frequency is shown in figure 12.

Analysis and Discussion

Above 14°K $Mn_2P_2O_7$ is paramagnetic. The susceptibility could be fitted to a Curie-Weiss law,

$$\chi_{mole} = C_M/(T + \Theta)$$

where $C_M = \frac{2N\beta^2\mu^2_{eff}}{3kT}$ with $\mu_{eff} = 5.90(5)$ and $\Theta = 13(1)$°K. The μ_{eff} is in good agreement with the spin only value of

Figure 7. Angular dependence of AFMR in $Mn_2P_2O_7$ as a function of magnetic field at different frequencies. The applied field was in the ac plane, i.e. H perpendicular to b. Measurements were made at 4.2°K. The x direction is 22(2)° from the a axis.

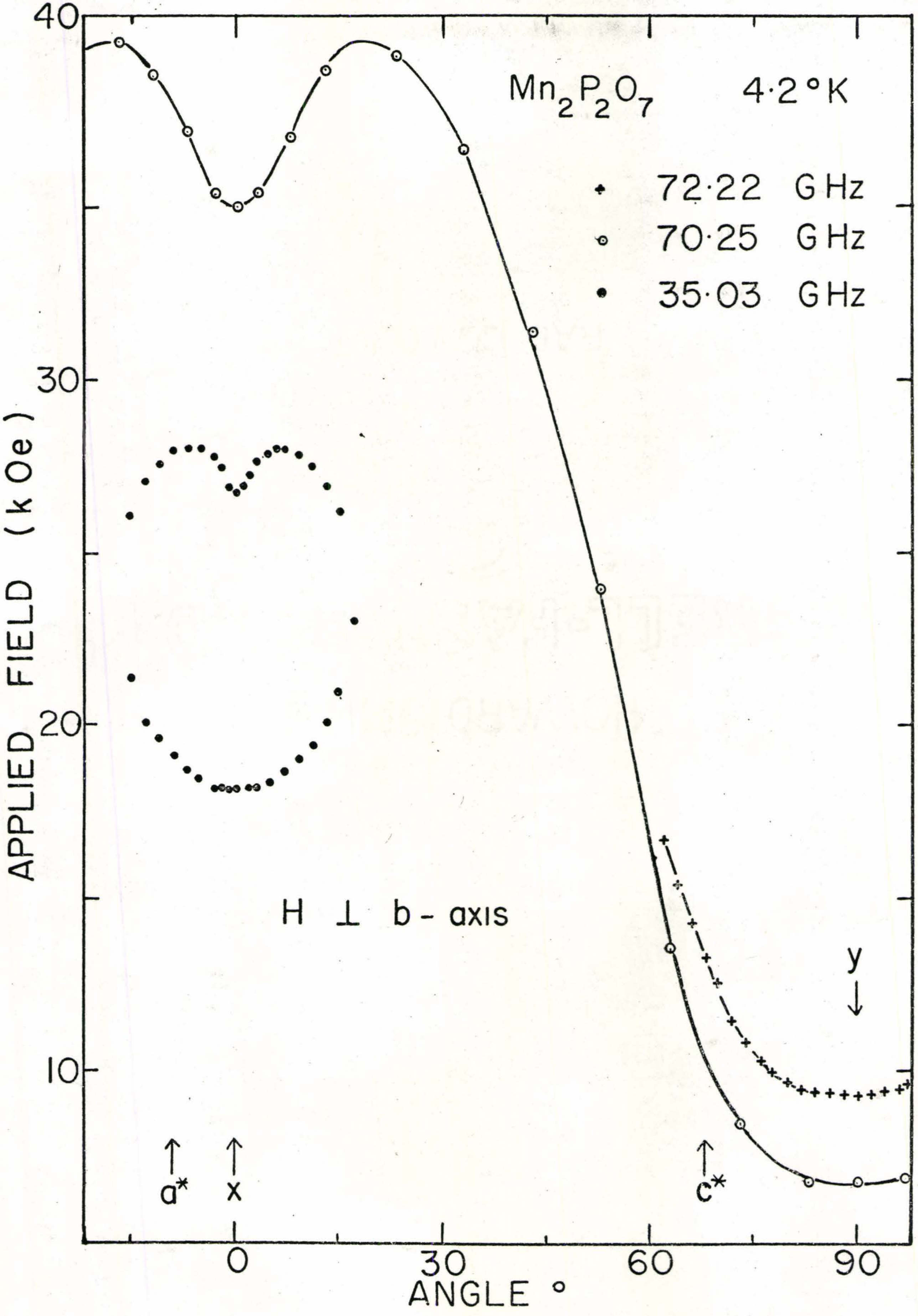
40
30
20
10
0
30
60
90
ANGLE °
APPLIED FIELD (k Oe)
$Mn_2P_2O_7$ 4·2°K
+ 72·22 GHz
⊙ 70·25 GHz
● 35·03 GHz
H ⊥ b - axis
a*
x
c*
y

Figure 8. Angular dependence of AFMR in $Mn_2P_2O_7$ as a function of applied field in the xz plane, i.e H perpendicular to the y direction. The temperature was 4.2°K and the measurements are shown for three different frequencies.

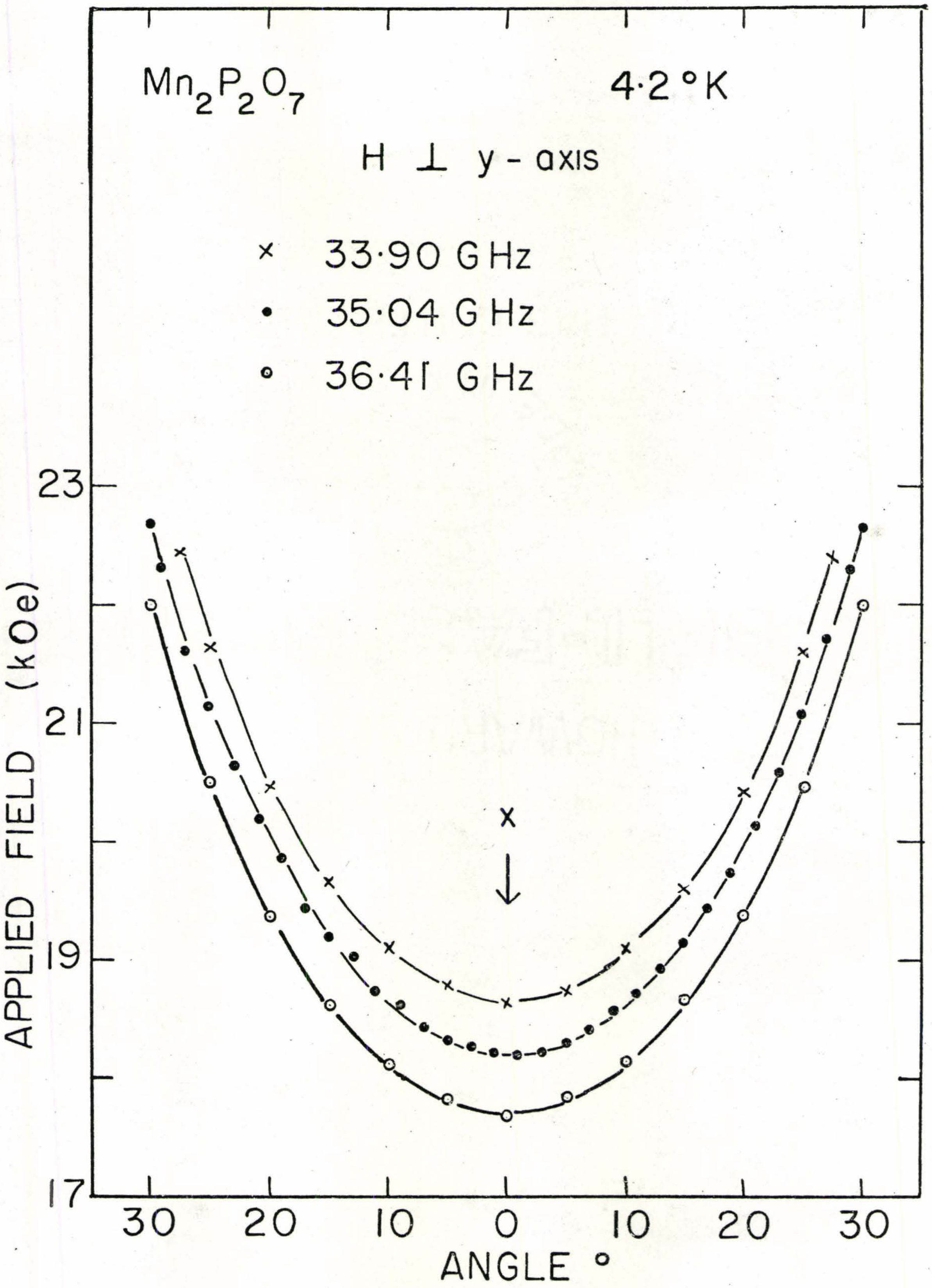
$Mn_2P_2O_7$
4·2 °K
H ⊥ y - axis
× 33·90 GHz
● 35·04 GHz
○ 36·41 GHz
23
21
19
17
APPLIED FIELD (kOe)
30
20
10
0
10
20
30
ANGLE °
x

Figure 9. Angular dependence of AFMR in $Mn_2P_2O_7$ as a function of applied field at constant frequency. The magnetic field was applied in the plane perpendicular to the spin direction, i.e. the x direction. Measurements were made at 4.2°K.

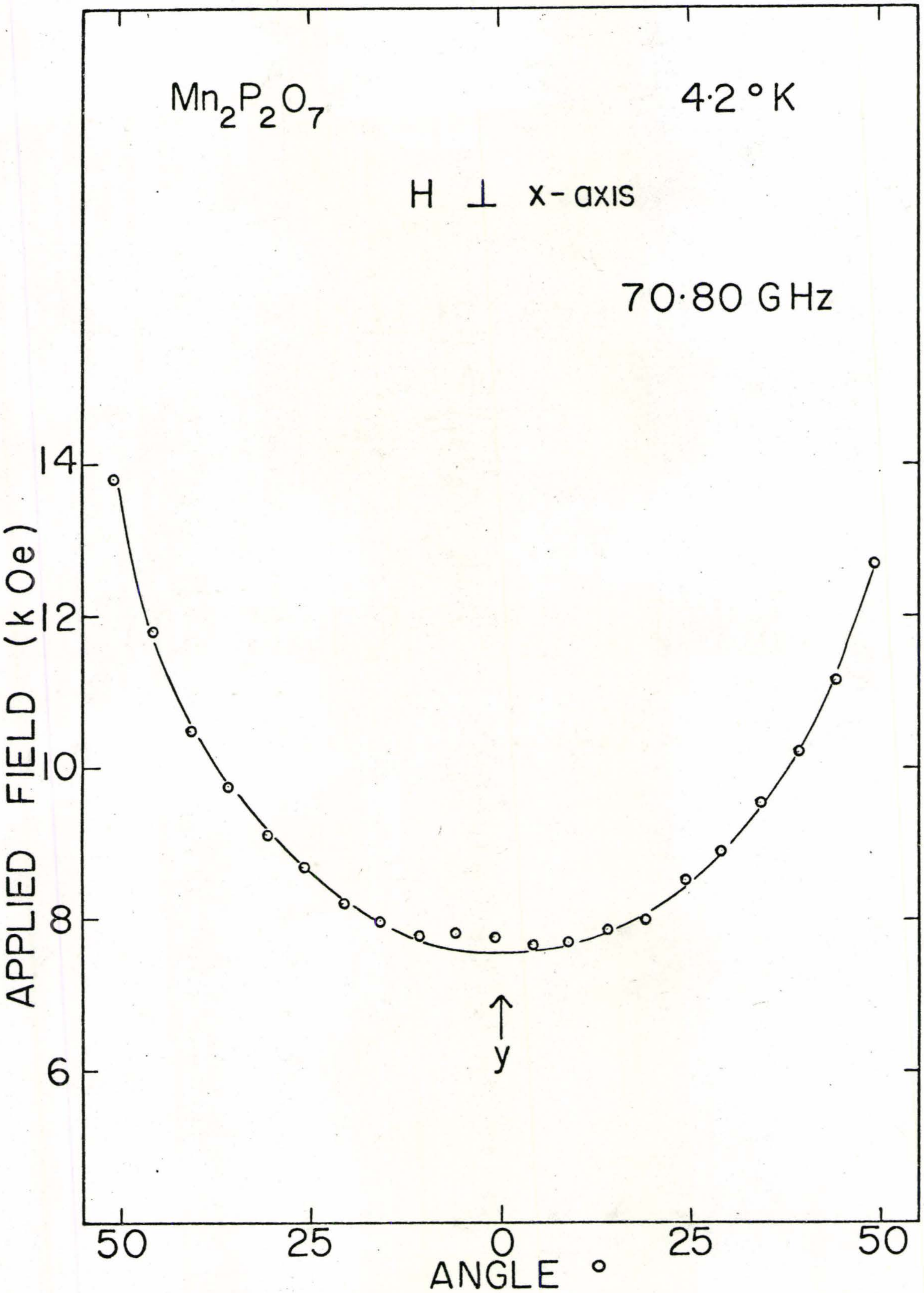
$Mn_2P_2O_7$
4·2 °K
H ⊥ x-axis
70·80 GHz
APPLIED FIELD (k Oe)
14
12
10
8
6
y
50
25
0
25
50
ANGLE °

Figure 10. The frequency versus magnetic field diagram for $Mn_2P_2O_7$ at 4.2°K. The open and closed circles represent the experimental values when the applied field is along the x and y directions respectively. The solid lines represent the calculated frequency versus magnetic field relationship from the Date theory using the molecular field coefficients given in Table 4.

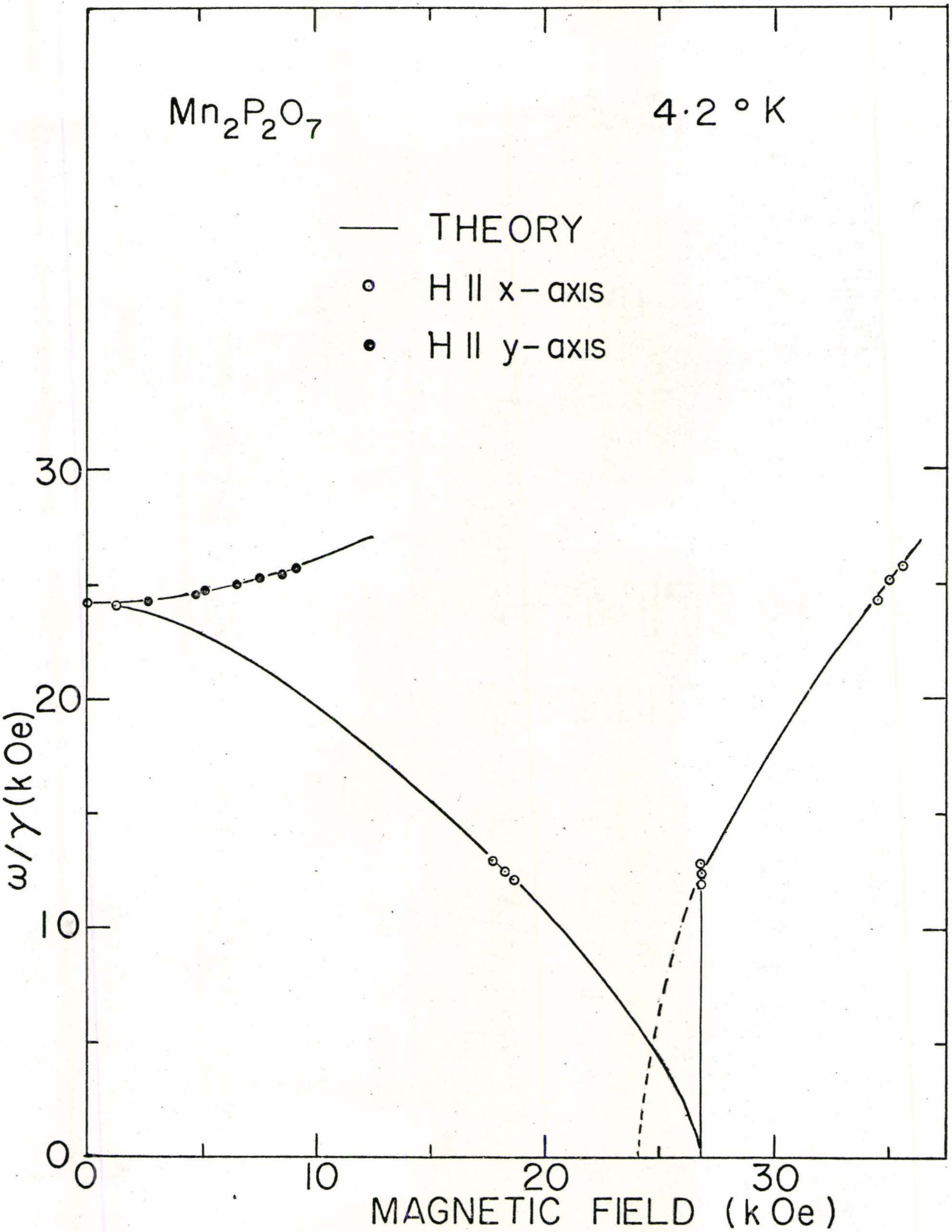

Mn2P2O7
4·2 °K
THEORY
H ll x-axis
H ll y-axis
ω/γ (k Oe)
0
10
20
30
0
10
20
30
MAGNETIC FIELD (k Oe)

Figure 11. Temperature dependence of the applied magnetic field necessary to observe the AFMR in $Mn_2P_2O_7$ at a constant frequency of 35.04 GHz, when the field is along the spin direction, i.e. the x axis. Also shown is the linewidth (FWHM).

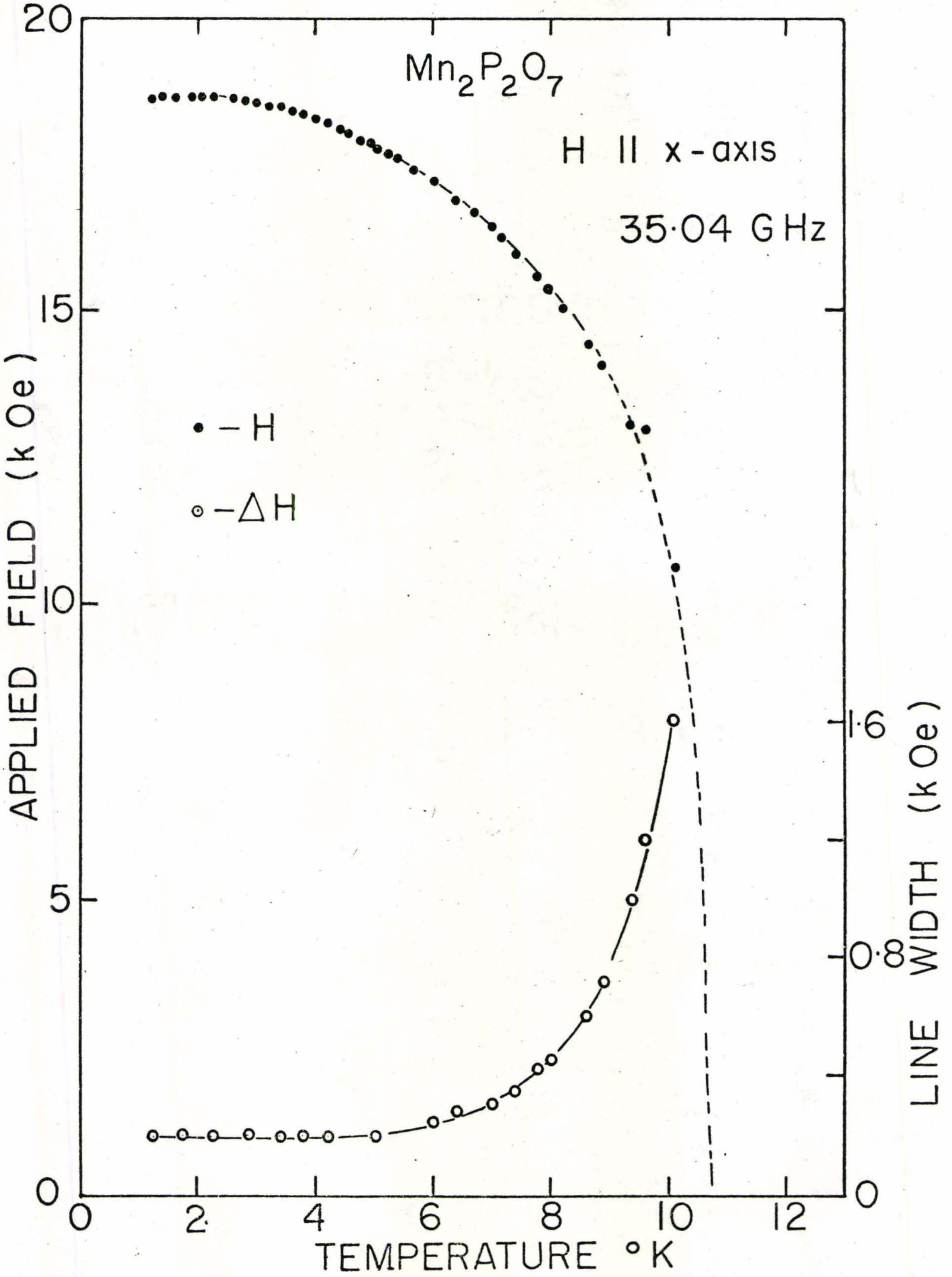
$Mn_2P_2O_7$
H ll x - axis
35·04 GHz
● - H
○ - ΔH
APPLIED FIELD (k Oe)
LINE WIDTH (k Oe)
TEMPERATURE °K
0
5
10
15
20
0
0·8
1·6
0
2
4
6
8
10
12

Figure 12. Temperature dependence of AFMR frequency of $Mn_2P_2O_7$. The open circles were measured with the applied field H approximately equal to zero. The closed circles were measured with applied fields of 6 kOe to 20 kOe along the y-axis. The solid line is a Brillouin function for spin $S = 5/2$ and transition temperature 14°K. The Brillouin function is normalized to the AFMR frequency at 1.2°K, 25.5 kOe (71.4 GHz).

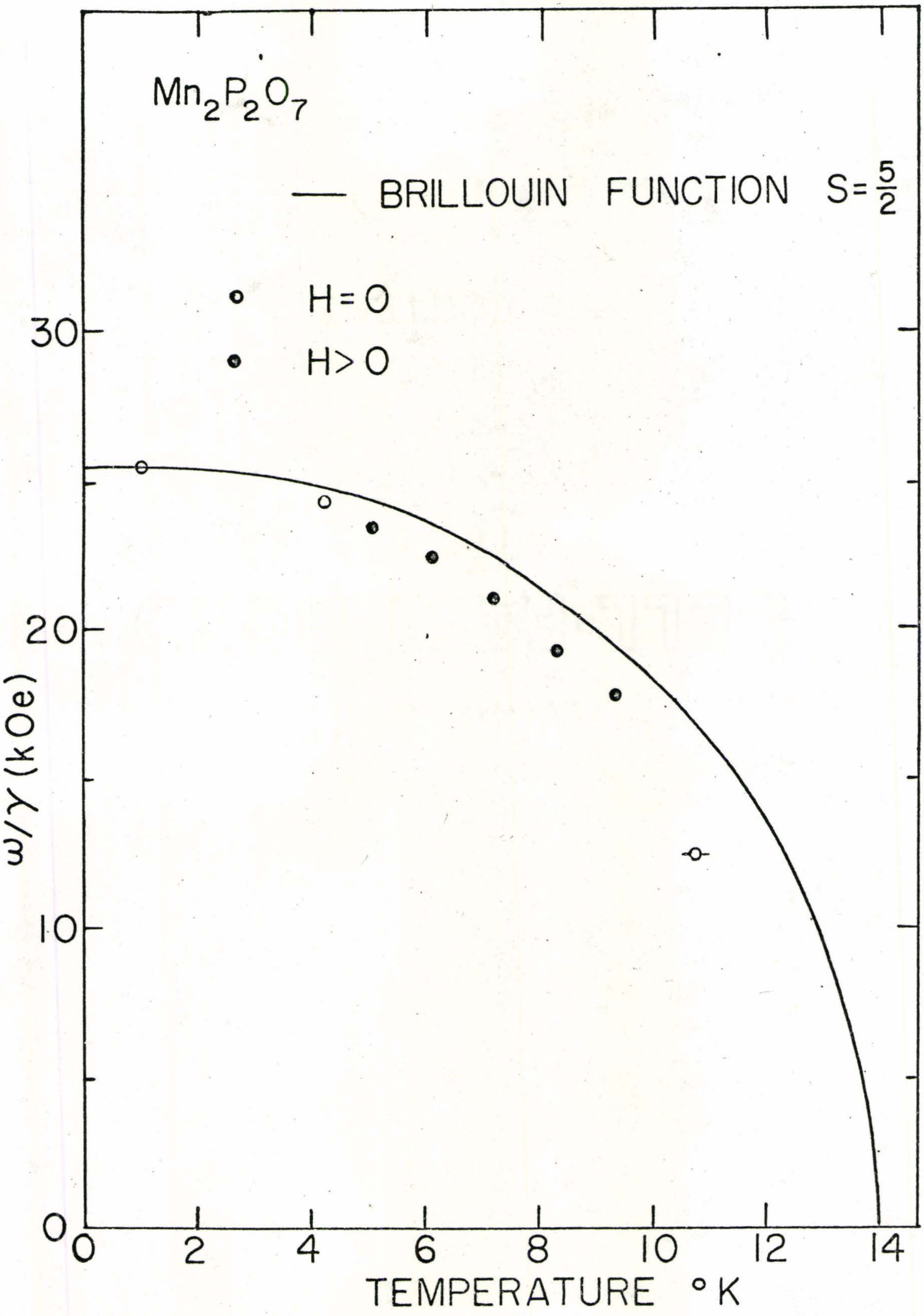
$Mn_2P_2O_7$
— BRILLOUIN FUNCTION $S=\frac{5}{2}$
○ H=0
● H>0
30
20
10
0
ω/γ (kOe)
0
2
4
6
8
10
12
14
TEMPERATURE °K

5.92 expected for a $^6S_{5/2}$ state. An earlier measurement (Lallermand 1935) gives $\mu_{eff} = 5.88$. The ratio Θ/T_N is very nearly unity implying that within the molecular field approximation only nearest neighbour exchange interactions are important.

Below 14°K $Mn_2P_2O_7$ becomes magnetically ordered. From the susceptibility and resonance measurements it is concluded that the ordering is antiferromagnetic. Both AFMR and susceptibility give the spin direction 22(2) degrees from the a-axis. It was noted that the perpendicular susceptibility was anisotropic having its maximum value along the b axis and its minimum value along the y-axis. The amount of anisotropy in the perpendicular susceptibility is 3.5 percent. From the general behaviour of the angular dependence of the AFMR results it is concluded that the anisotropy energy has the orthorhombic form and that the y axis is the intermediate direction and the b axis is the hard direction.

An attempt was made to fit the resonance and susceptibility results using the energy for a two sublattice system given by equation (22). The AFMR equations are then just those of the Nagamiya Yosida theory. Since the AFMR results give the b axis as the hard direction, the perpendicular susceptibility along the b axis should be smaller than the perpendicular susceptibility along the y axis. This is contrary to what is experimentally observed.

It was found that the susceptibility and AFMR measurements could be fitted consistently with the energy of a two sublattice system given by equation (11). The perpendicular susceptibilities are then given by equations (13a) and (14a), and the resonance equations are just those developed by Date (1961) and given by equations (17) to (20). Table 4 lists the determined principal values of the P , Q, A' and Γ' tensors, expressed in terms of the isotropic intersublattice exchange coefficient A. The measured value of the zero field AFMR frequency at 4.2°K was 68.0(1) GHz and from the resonance measurements the spin flop field at 4.2°K was 26.7(2) kOe. The value of the sublattice magnetization at 4.2°K was taken as 95 percent of the saturated value. The value of the parallel susceptibility $\chi_{||}$ needed to fit the resonance measurement was 5.4×10^{-2} emu/mole. This is compared to the measured value of $\chi_{||} = 7.0 \times 10^{-2}$ emu/mole and the value calculated from equation (15) $\chi_{||} = 3.9 \times 10^{-2}$ emu/mole. The value of the intersublattice exchange field at 4.2°K is determined to be 77.5(8) kOe.

A calculation of the anisotropy energy was made for $Mn_2P_2O_7$. The spin configuration in $Mn_2P_2O_7$ has recently been determined by neutron diffraction (Gill et al 1970). The measurements were made on a powder sample at 4.2°K. Their proposed spin configuration is shown in figure 13. Using

Table 4

Molecular field coefficients and crystal field parameters for $Mn_2P_2O_7$

Molecular Field Coefficients (in units of A)

Experimentally determined

$Q_x = +0.057(2)$	$P_x = 0.00(1)$	$A'_x = +0.028(5)$	$\Gamma'_x = -0.028(5)$
$Q_y = +0.008(1)$	$P_y = +0.05(1)$	$A'_y = +0.028(5)$	$\Gamma'_y = +0.020(5)$
$Q_z = -0.065(2)$	$P_z = -0.05(2)$	$A'_z = -0.057(5)$	$\Gamma'_z = +0.008(5)$

Calculated

	$P_y = -0.006$	$A'_x = +0.026$	$\Gamma'_x = -0.031$
	$P_y = +0.044$	$A'_y = +0.026$	$\Gamma'_y = +0.017$
	$P_z = -0.038$	$A'_z = -0.052$	$\Gamma'_z = +0.013$

Crystal Field Parameters

Mn^{++} in $Mn_2P_2O_7$ (Best fit to experiment)	Mn^{++} in $Mg_2P_2O_7$ (From E.S.R.)
$D = +1140 \times 10^{-4}$ cm^{-1}	$D = -1100 \times 10^{-4}$ cm^{-1}
$E = -313 \times 10^{-4}$ cm^{-1}	$E = +5 \times 10^{-4}$ cm^{-1}
$\theta = 48°$	$\theta = 51°$

θ is measured from c* away from a*.

Figure 13. The spin configuration, as determined by neutron diffraction in $Mn_2P_2O_7$. The magnetic unit cell is equal to the chemical unit cell. The open circles are the magnetic ions on one sublattice, the closed circles are those on the other. The fractional coordinates of the ions are 1(0.00,0.31,0.50) ; 2(0.50,0.81,0.50) ; 3(0,00, 0.69,0.50) ; 4(0.50,0.19,0.50). Planes parallel along the c axis have the same spin arrangement. The dashed line indicates the mirror plane.

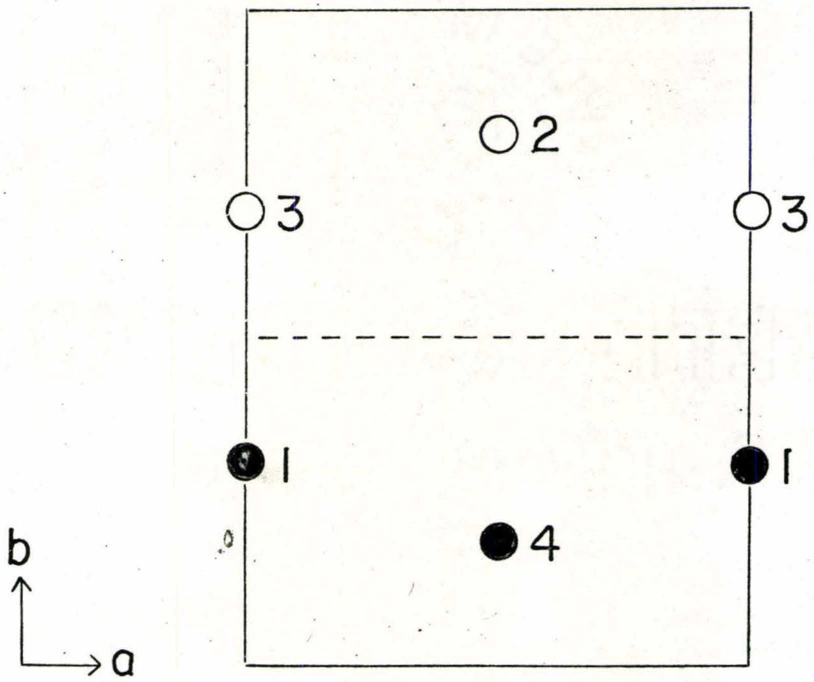
2
3
3
1
1
4
b
a

this spin configuration the anisotropy energy was calculated. It was assumed that the exchange interaction is isotropic and that there were two contributions to the energy, a dipole field term and a crystal field term.

The energy due to the dipole field E_d may be written in the following form (Kanamori 1963)

$$E_d = \frac{1}{2} \vec{M}^{+} \cdot \overline{\overline{\phi}} \cdot \vec{M}^{+} + \frac{1}{2} \vec{M}^{-} \cdot \overline{\overline{\phi}} \cdot \vec{M}^{-} + \vec{M}^{+} \cdot \overline{\overline{\phi}}' \cdot \vec{M}^{-}$$

where ϕ and ϕ' are tensors. The energy was calculated using an Ewald sum method. The computer program was written by E. R. Cowley. The program gave the same result for MnF_2 as that obtained by Keffer (1952). The energy due to the crystal field term $E_{C.F}$ in $Mn_2P_2O_7$ may be written as

$$E_{CF} = \frac{1}{2} \vec{M}^{+} \cdot \overline{\overline{\phi}}'' \cdot \vec{M}^{+} + \frac{1}{2} \vec{M}^{-} \cdot \overline{\overline{\phi}}'' \cdot \vec{M}^{-}$$

where ϕ'' is a tensor. The crystal field term was taken from the E.S.R. measurements of Mn^{++} as a dilute substitutional impurity in $Mg_2P_2O_7$ (Chambers et al 1964).

The energy was then calculated from the sum of the dipole and crystal field energies assuming an arbitrary antiferromagnetic spin direction. The spin direction was then varied to minimize the energy. It was found that the spin direction which minimized the energy did not correspond to the experimentally observed spin direction. The calculation was redone with the crystal field as a parameter. Since the crystal field used was orthorhombic and its orientation was allowed to be arbitrary it was necessary to use the measured spin direction and the components of the Q tensor as determined experimentally. The result of this calculation is compared with the measured values in Table 4. The crystal field term used is also shown in Table 4 as is that determined by Chambers et al (1964).

It was found that using the following effective molecular field

$$\vec{H}^{\pm} = -\bar{\bar{A}}\vec{M}^{\mp} - \bar{\bar{\Gamma}}\vec{M}^{\pm} - \bar{\bar{A}}'\vec{M}^{\mp} - \bar{\bar{\Gamma}}'\vec{M}^{\pm}$$

the susceptibility and resonance measurements could be satisfactorally explained; the only major discrepancy being the value of the parallel susceptibility. The experimentally measured value of 4.2°K is 23 percent larger than that needed to fit the resonance data. The value needed to fit the resonance data is determined in our case from the spin flop field resonance. The linewidth of this resonance was large, approximately 1.0 kOe. One would have expected a narrower line since the frequency versus magnetic field relation is very steep at this point. Misalignment of the crystal in the resonance measurements would only tend to increase the discrepancy, but misalignment of the crystal in the susceptibility determination would decrease the discrepancy. It must be noted that a large oblate single crystal, with extremal diameters 5 mm; 5 mm; 3.5 mm, was used for the susceptibility measurements whereas a small nearly spherical single crystal, approximately 1 mm in diameter, was used for AFMR measurements. Both were a regular shape so that proper account of the demagnetizing field could be taken in each case. The perpendicular susceptibility was not quite constant as a function of temperature but showed a one percent increase at low temperatures. If this were due to paramagnetic impurities then, assuming the effect to be isotropic, the result would be a parallel susceptibility approximately 5 percent larger than it should be. Another effect which might produce a larger parallel susceptibility would be imperfections such as vacancies in the crystal. The parallel susceptibility since it measures the sublattice imbalance would be most influenced by such effects. It is difficult to estimate the total result of the above effects. It would appear that such effects might account for some of the discrepancy but certainly not the 23 percent observed.

It was noted that the crystal field term necessary to give agreement between the measured and calculated anisotropy energy had approximately the same principal axes and magnitude, but opposite sign as that determined from E.S.R. Differences in crystal field terms as measured from E.S.R. of a magnetic ion as a dilute impurity in an isomorphic host to that needed to give the correct anisotropy energy have been reported before. Foner (1963) found that the crystal field term contribution to the anisotropy energy in Cr_2O_3 was about 1/9 and of the opposite sign as that observed from E.S.R. of Cr^{3+} as a dilute impurity in Al_2O_3, which is isomorphic to Cr_2O_3.

The temperature dependence of the zero field AFMR was found to decrease faster than the Brillouin function for $S = 5/2$, see figure 12. This resonance depends on the square root of the product of the exchange and anisotropy fields. The exchange and anisotropy might be expected to each have the same temperature dependence as the sublattice magnetization. Thus the resonance frequency would also have the same temperature dependence as the magnetization and therefore be expected to follow the Brillouin-function. However Kanamori (1963) has shown that the crystal field would decrease faster with temperature than the Brillouin function. In our case the crystal field is of comparable magnitude to the dipole field. The temperature dependence of the crystal field term might explain the observed deviation from the Brillouin function.

Date (1961) used the effective field given in equation (12) to explain the A.F.M.R. in $CoCl_2 6H_2O$. In this case the predominant contribution to A' tensor comes from anisotropic exchange. This is understandable in $CoCl_2 6H_2O$ since the g value deviates markedly from 2 and is highly anisotropic. However in $Mn_2P_2O_7$ the g value is isotropic and equal to 2 thus one would not expect any contribution to A' from anisotropic exchange. The calculation shows that the A' tensor in $Mn_2P_2O_7$ can be accounted for from the dipole field.

(ii) $Cu_2P_2O_7$

Experimental Results

Magnetic susceptibility, electron spin resonance and antiferromagnetic resonance measurements were made on single crystals of $Cu_2P_2O_7$.

The magnetic susceptibility of a single crystal of $Cu_2P_2O_7$ was measured from 4.2°K to 300°K. The angular dependence of the susceptibility was measured at 4.2°K, 36°K and 295°K. Figure 14 shows the temperature dependence of the susceptibility for the applied magnetic field in three different directions. These directions are shown with respect to the crystallographic axes in Figure 15. The angular dependence of the susceptibility at 295°K and 4.2°K is shown in figures 16 and 17 for the applied magnetic field perpendicular to the x axis and perpendicular to the y axis (b-axis). At 36°K the angular dependence of the susceptibility had the same behaviour as at 295°K. The field dependence of the magnetization at 4.2°K is shown in figure 18 when the applied field is parallel to the x axis. In Table 5 the measured principal values of the susceptibility are tabulated for 4.2°K, 36°K and 295°K.

Electron spin resonance of Cu^{++} in $Cu_2P_2O_7$ was measured at approximately 35 GHz. The g value was found to be anisotropic. Figure 19 shows the angular dependence of the g value in the ac plane. The principal valuesof the g tensor are listed in Table 5. The temperature dependence of the resonance absorption and linewidth are shown in figure 20. The resonance could

Figure 14. Temperature dependence of the magnetic susceptibility of $Cu_2P_2O_7$ from 4.2°K to 200°K. The magnetic field was applied along the x axis, the b axis (y axis) and the z axis.

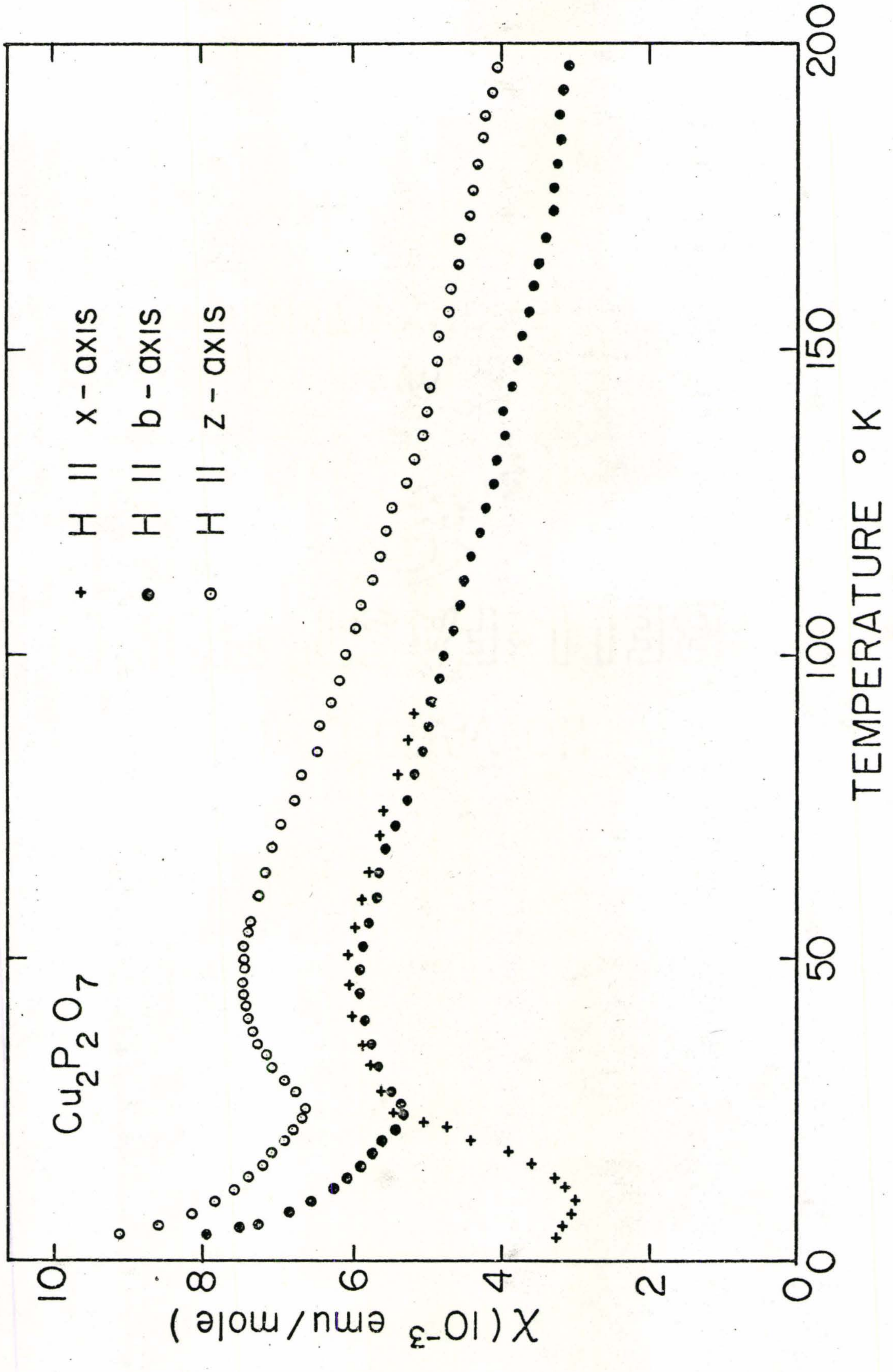
$Cu_2P_2O_7$
+ H ∥ x-axis
● H ∥ b-axis
○ H ∥ z-axis
χ (10^{-3} emu / mole)
0
2
4
6
8
10
TEMPERATURE °K
0
50
100
150
200

Figure 15. The directions of the principal values of the paramagnetic susceptibility of $Cu_2P_2O_7$ in the ac plane i.e. the x' and z' directions and the principal directions of the antiferromagnetic state of $Cu_2P_2O_7$ in the ac plane i.e. the x and z directions. In both cases the third principal direction is the b axis (y' or y direction). The x direction is the antiferromagnetic spin direction.

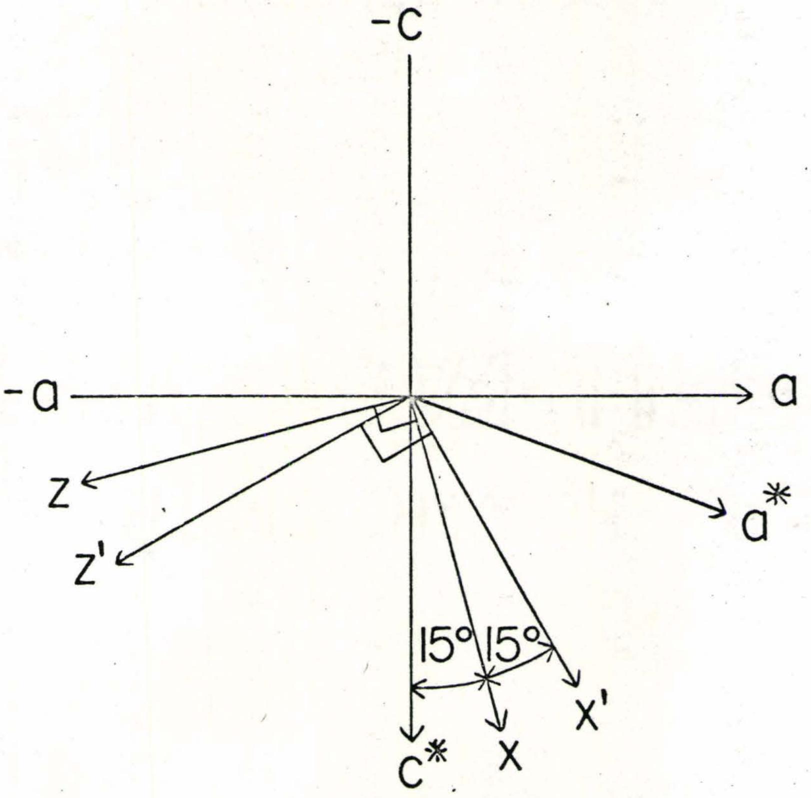
-c
-a
a
z
z'
a*
15°
15°
c*
x
x'

Figure 16. Angular dependence of the magnetic susceptibility of $Cu_2P_2O_7$ at 295°K, for the applied field perpendicular to the x axis and for the applied field perpendicular to the b axis. The solid lines are least squares fits to a cos 2θ angular dependence.

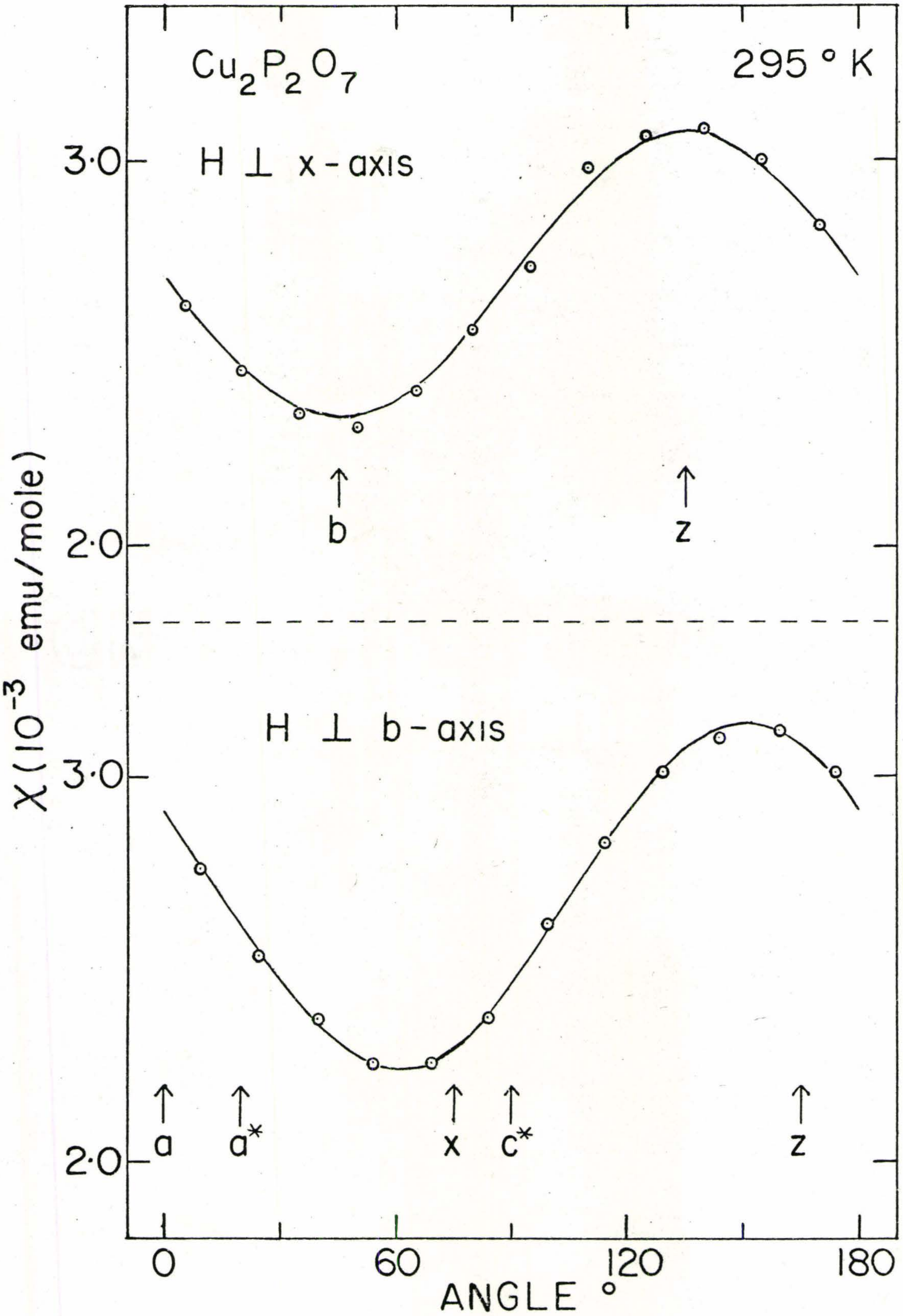
$Cu_2P_2O_7$
295 ° K
H ⊥ x - axis
b
z
H ⊥ b - axis
a
a*
x
c*
z
3·0
2·0
3·0
2·0
$\chi (10^{-3}$ emu/mole)
0
60
120
180
ANGLE °

Figure 17. Angular dependence of the susceptibility of $Cu_2P_2O_7$ at 4.2°K, for the applied field perpendicular to the x and b axes. The solid lines are least square fits to a cos 2θ angular dependence.

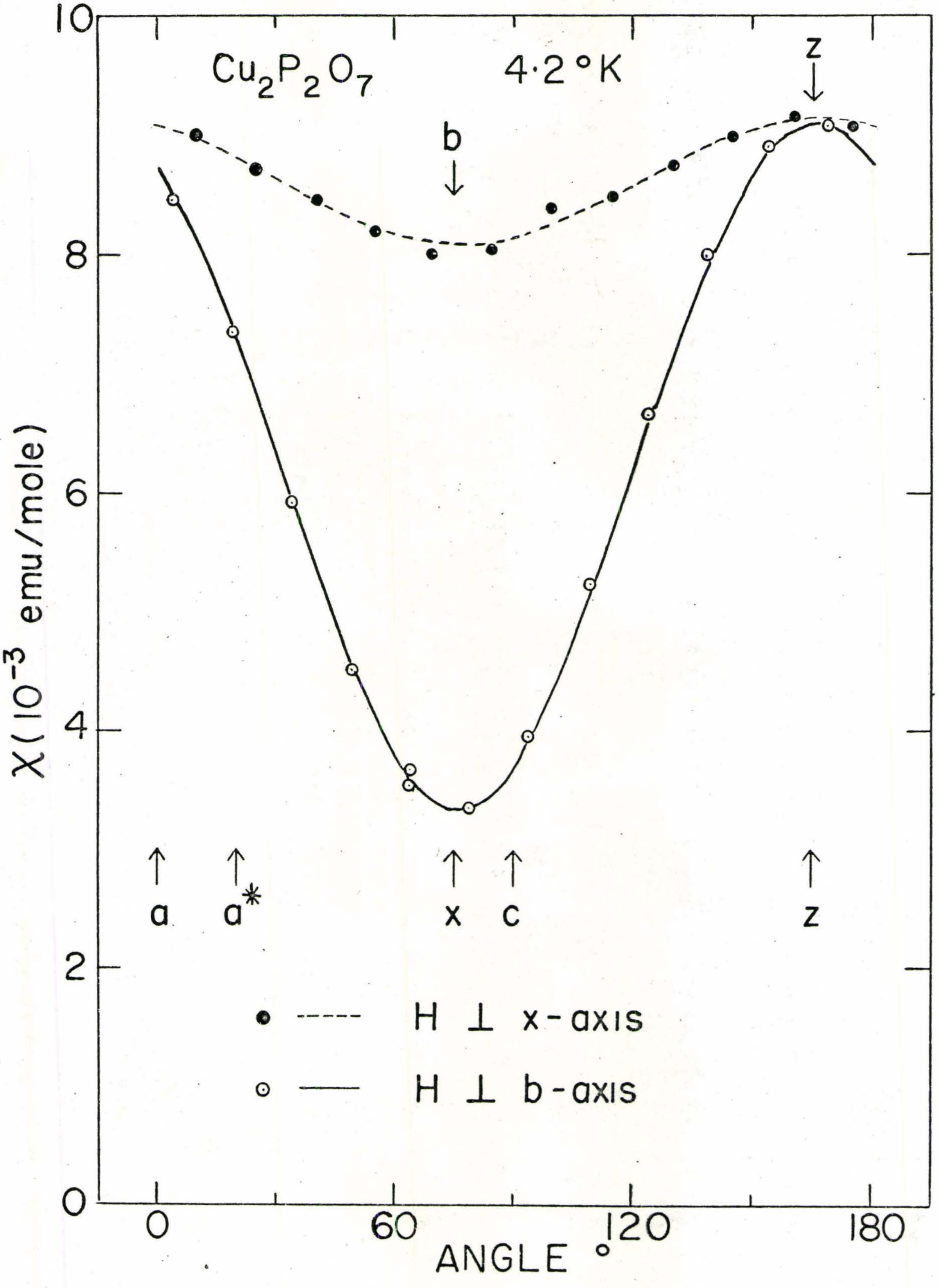
$Cu_2P_2O_7$
4·2 °K
z
b
χ (10^{-3} emu/mole)
10
8
6
4
2
0
a
a^*
x
c
z
● - - - - H ⊥ x-axis
⊙ —— H ⊥ b-axis
0
60
120
180
ANGLE °

Figure 18. Field dependence of the magnetization of $Cu_2P_2O_7$ at 4.2°K, for the magnetic field along the x axis (spin direction). These measurements were made on a small $Cu_2P_2O_7$ crystal so that it was difficult to determine the absolute value of the magnetization.

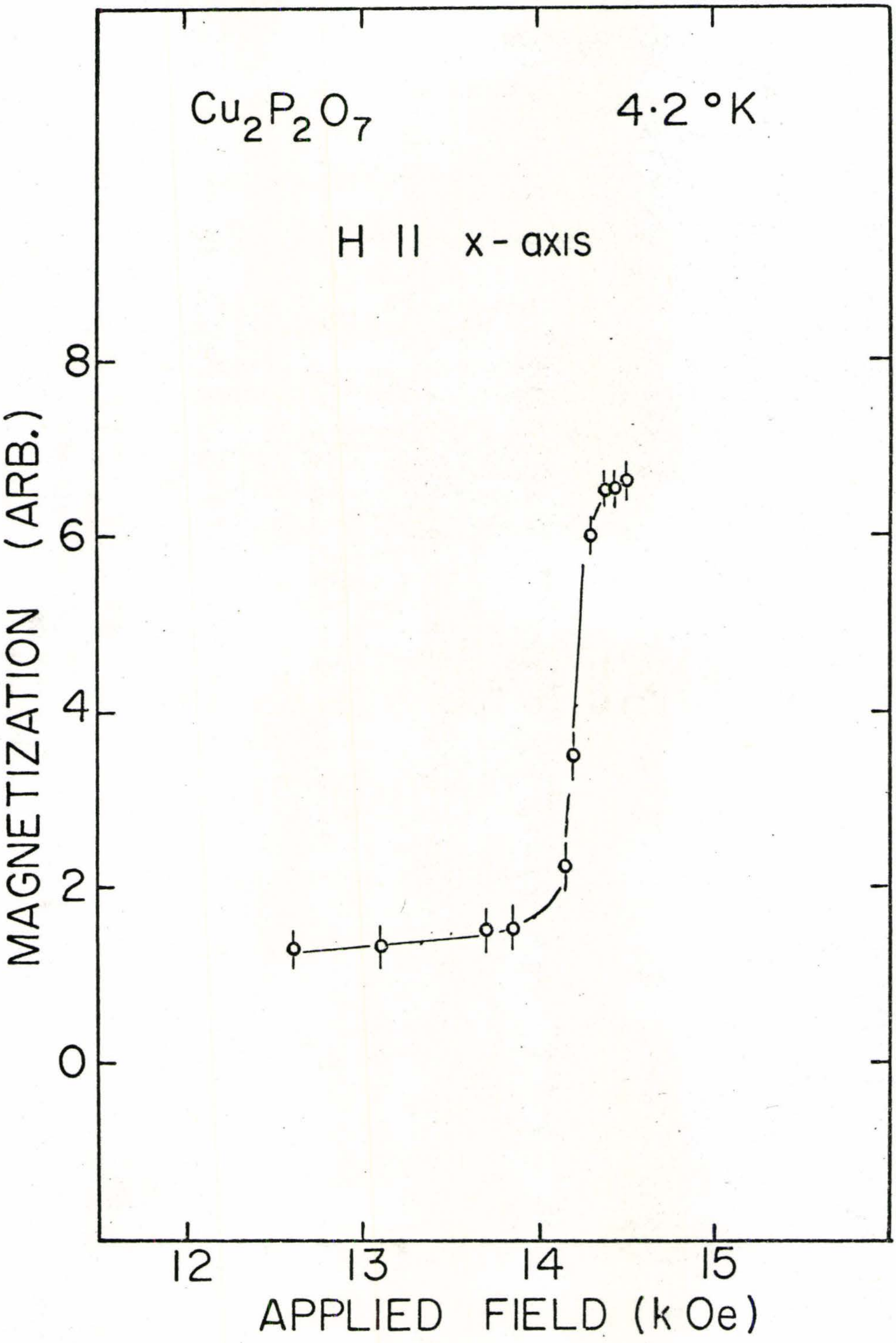
$Cu_2P_2O_7$
4·2 °K
H ll x-axis
MAGNETIZATION (ARB.)
0
2
4
6
8
12
13
14
15
APPLIED FIELD (k Oe)

Table 5

Principal Values of Susceptibility and g tensors of $Cu_2P_2O_7$

Temperature (°K)		Susceptibility (10^{-3} emu/mole)	g-value
	x'-axis	2.24(6)	2.095(5)
295°K	y'-axis	2.33(6)	2.090(5)
	z'-axis	3.14(7)	2.480(5)
	x'-axis	5.85(10)	2.095(5)
36°K	y'-axis	5.75(10)	2.090(5)
	z'-axis	7.38(10)	2.480(5)
			Modified Susceptibility
	x-axis	3.35(10)	2.98(10)
4.2°K	y-axis	8.09(10)	7.42(10)
	z-axis	9.12(10)	6.12(10)

Figure 19. Angular dependence of the g value of Cu^{++} in $Cu_2P_2O_7$ as determined by electron spin resonance at approximately 35 GHz. The magnetic field was applied in the ac plane i.e. perpendicular to b axis. Measurements were taken at 295°K. The solid line is a least squares fit to a cos 2θ angular dependence.

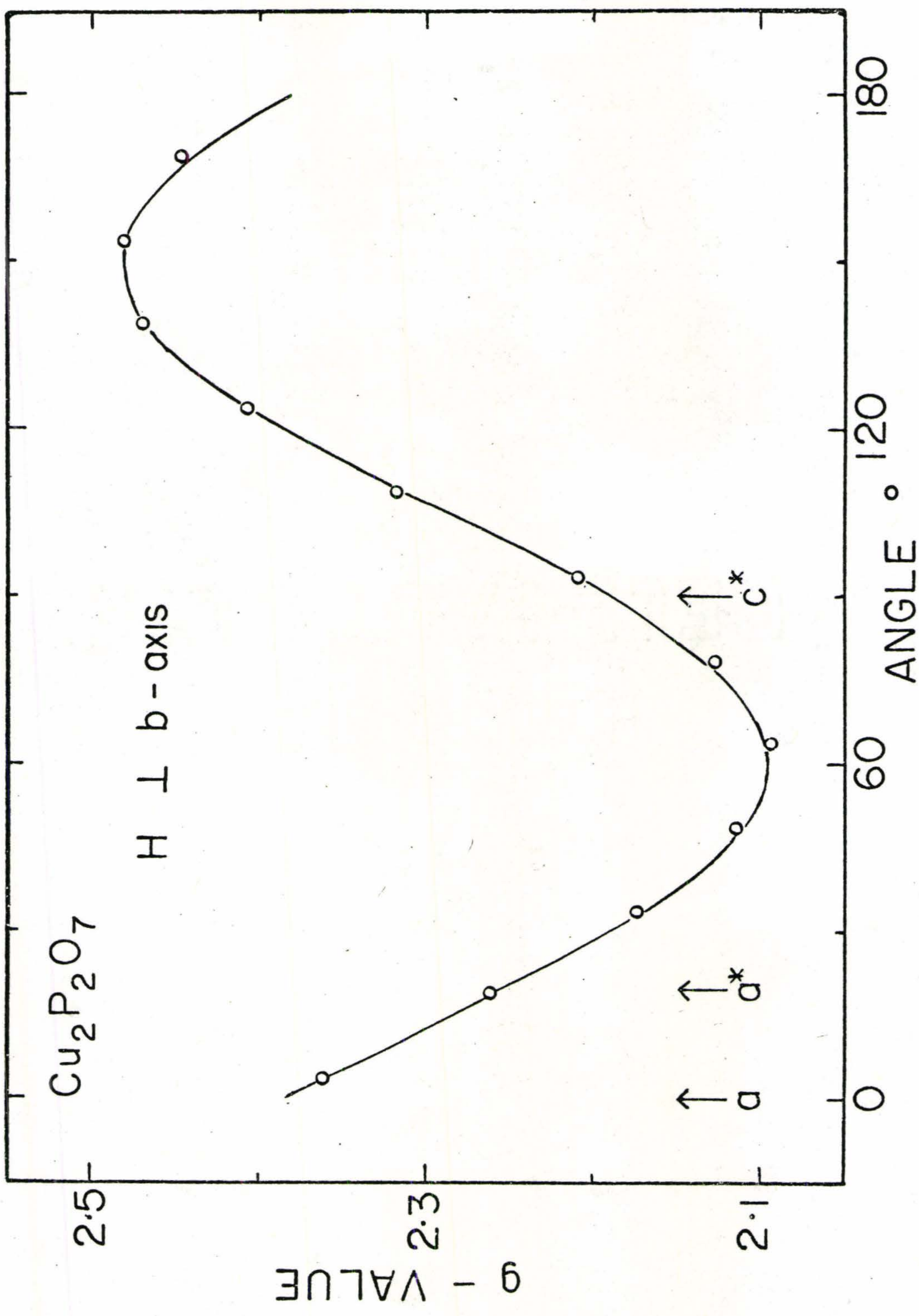
$Cu_2P_2O_7$
H ⊥ b-axis
a
a*
c*
2·5
2·3
2·1
g - VALUE
0
60
120
180
ANGLE °

Figure 20. Temperature dependence of the absorption, peak to peak amplitude, and linewidth of the electron spin resonance of Cu^{++} in $Cu_2P_2O_7$. Measurements were made at 35.03 GHz with the magnetic field applied along the x direction. No absorption was observed below 26(1)°K.

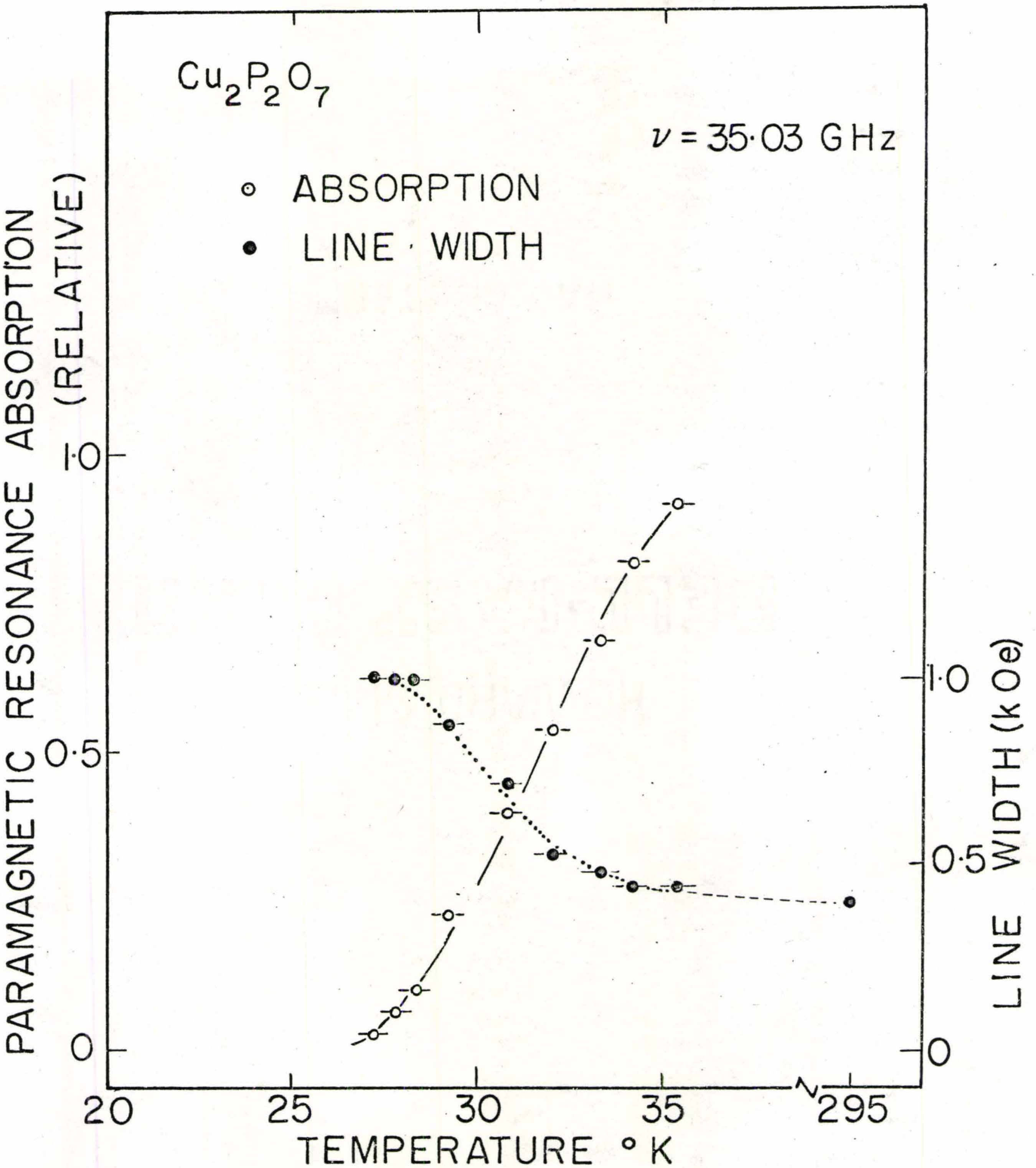
$Cu_2P_2O_7$
$\nu = 35{\cdot}03$ GHz
○ ABSORPTION
● LINE · WIDTH
PARAMAGNETIC RESONANCE ABSORPTION (RELATIVE)
0
0·5
1·0
LINE WIDTH (k Oe)
0
0·5
1·0
20
25
30
35
295
TEMPERATURE °K

not be observed below 26(1)°K.

Antiferromagnetic resonance was measured below 25°K. Measurements were made at three frequency ranges. In addition the temperature dependence was measured along the x axis. Figures 21 and 22 show the angular dependence of the resonance as a function of magnetic field in the ac plane, ie H perpendicular to the b axis, at different frequencies. The angular dependence of the resonance in the xy plane, ie the applied field perpendicular to the z axis is shownin figures 23 and 24. In both planes the results are shown for the temperature equal to 4.2°K. Figures 25 and 26 show the temperature dependence of the applied magnetic field along the x-axis necessary to observe the antiferromagnetic and spin flop resonance respectively when the frequency is held constant. Also shown is their respective linewidths. The frequency versus "modified" magnetic field diagram for the field along the x and y axes is shown in figure 27.

Analysis and Discussion

Above about 100°K $Cu_2P_2O_7$ behaves like a regular paramagnet. The inverse of the high temperature susceptibility versus temperature extrapolates to -70(5)°K, indicating that the predominant exchange is antiferromagnetic. At 295°K and 36°K the measured susceptibility and measured g tensor have the same principal axes, one of these axes being along the b-axes and the other two in the ac plane. These directions

Figure 21. Angular dependence of the AFMR in $Cu_2P_2O_7$ at different frequencies for the applied magnetic field in the ac plane, i.e. H perpendicular to the b-axis. The higher field measurements at 35.07 GHz correspond to Spin Flop Resonance (S.F.M.). The measurements were taken at 4.2°K.

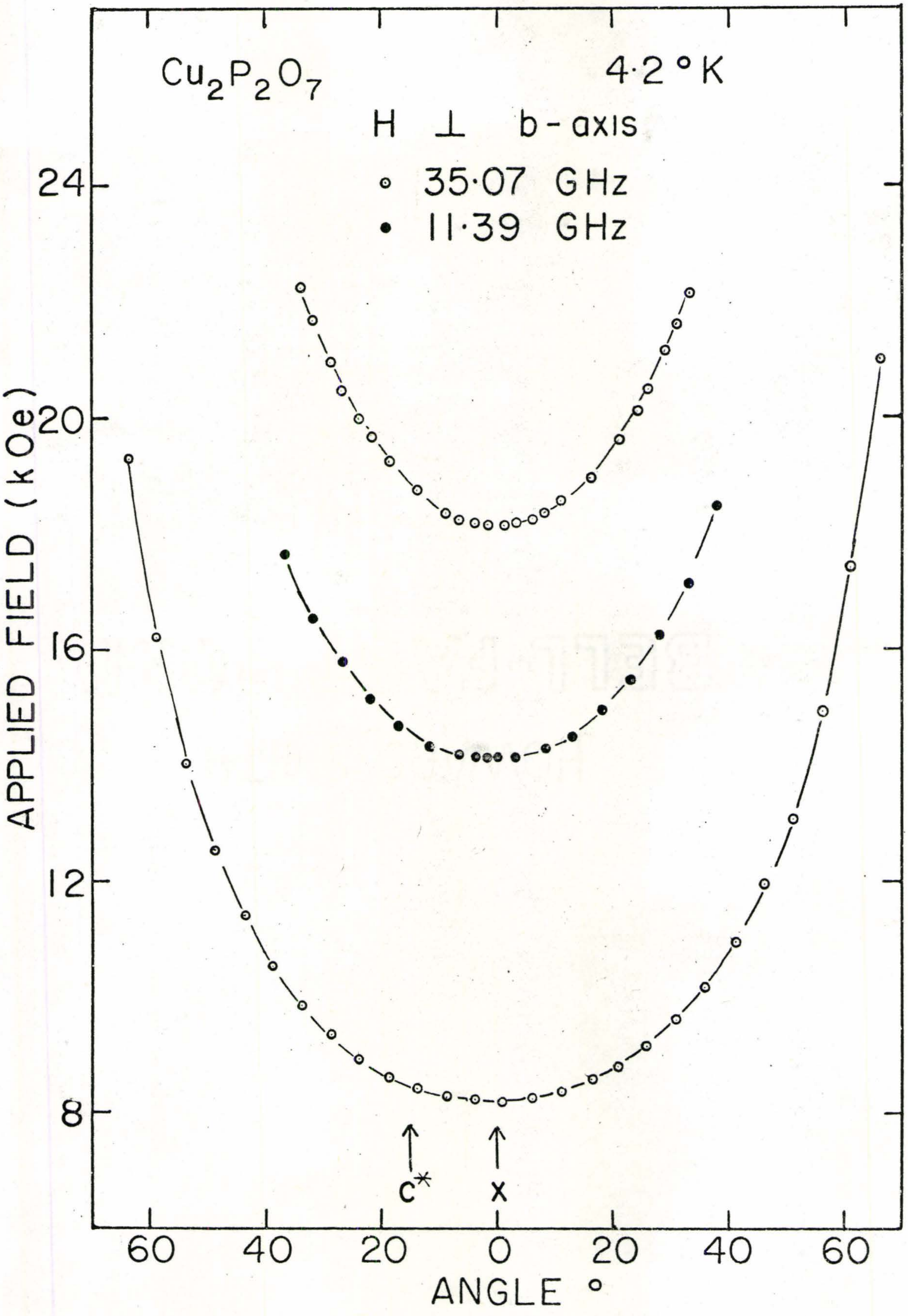

$Cu_2P_2O_7$
4·2 °K
H ⊥ b-axis
○ 35·07 GHz
● 11·39 GHz
APPLIED FIELD (kOe)
24
20
16
12
8
c*
x
60
40
20
0
20
40
60
ANGLE °

Figure 22. Angular dependence at 4.2°K of S.F.M. in $Cu_2P_2O_7$ at high frequencies for the applied field in the ac plane, i.e. H perpendicular to the b-axis.

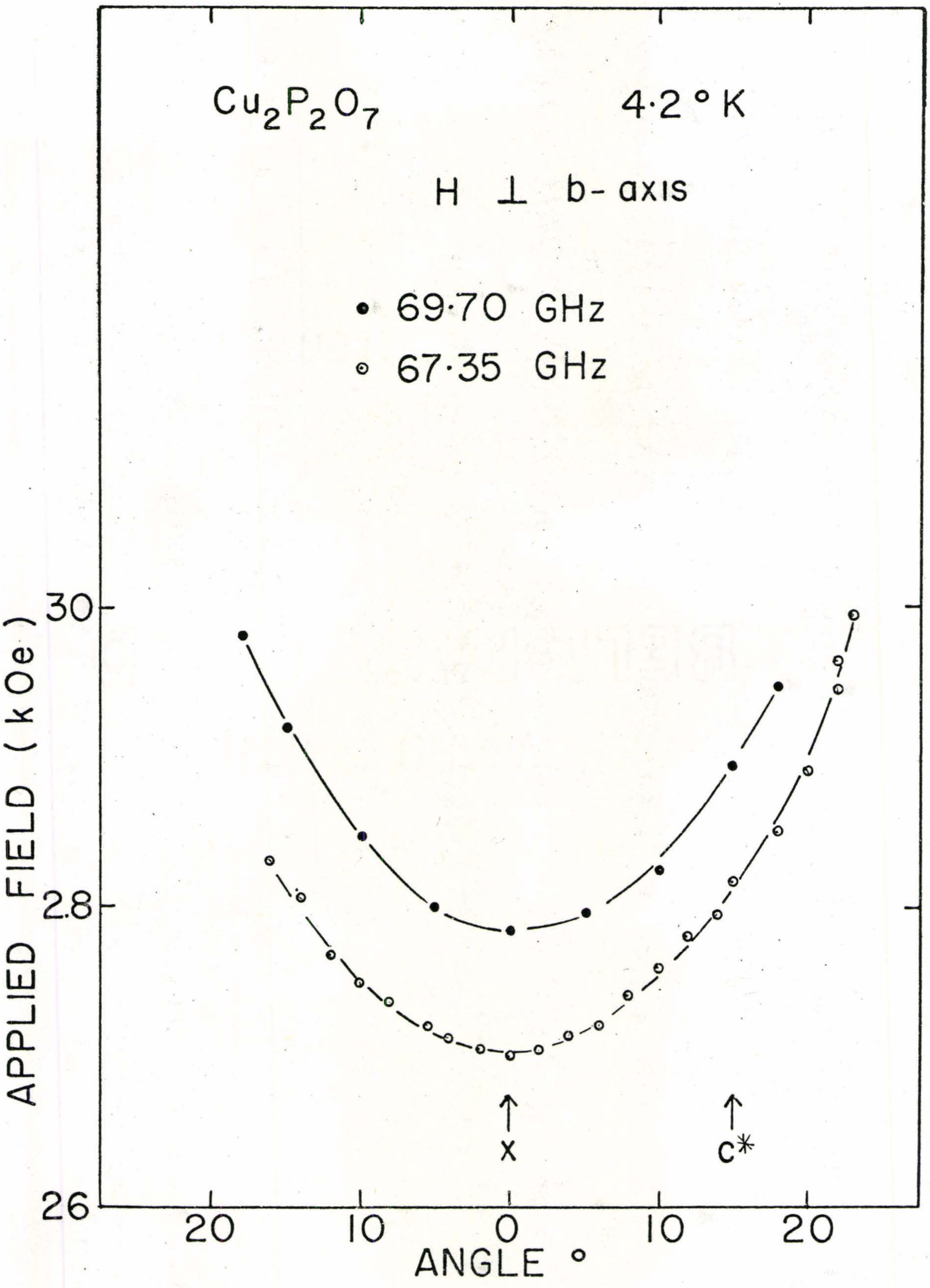
$Cu_2P_2O_7$
4·2 °K
H ⊥ b- axis
● 69·70 GHz
○ 67·35 GHz
APPLIED FIELD (k Oe)
30
2.8
26
20
10
0
10
20
ANGLE °
x
c*

Figure 23. Angular dependence of AFMR in $Cu_2P_2O_7$ for the magnetic field in the xy plane i.e. H perpendicular to the z axis for different frequencies. The measurements were taken at 4.2°K.

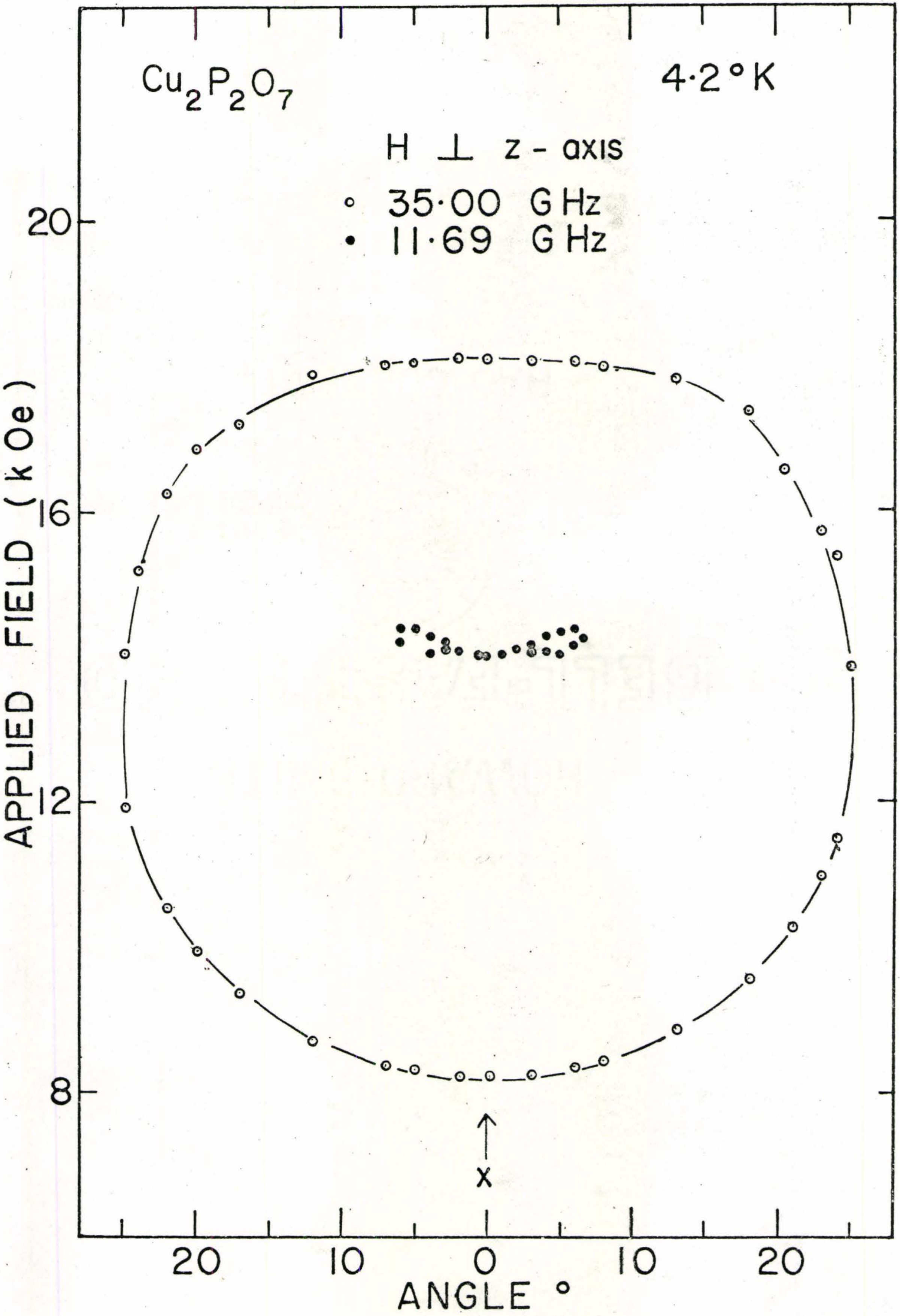
$Cu_2P_2O_7$
4·2°K
H ⊥ z - axis
○ 35·00 GHz
● 11·69 GHz
APPLIED FIELD (k Oe)
20
16
12
8
X
20
10
0
10
20
ANGLE °

Figure 24. Angular dependence of AFMR in $Cu_2P_2O_7$ for the applied magnetic field in the xy plane at 69.85 GHz and at 4.2°K.

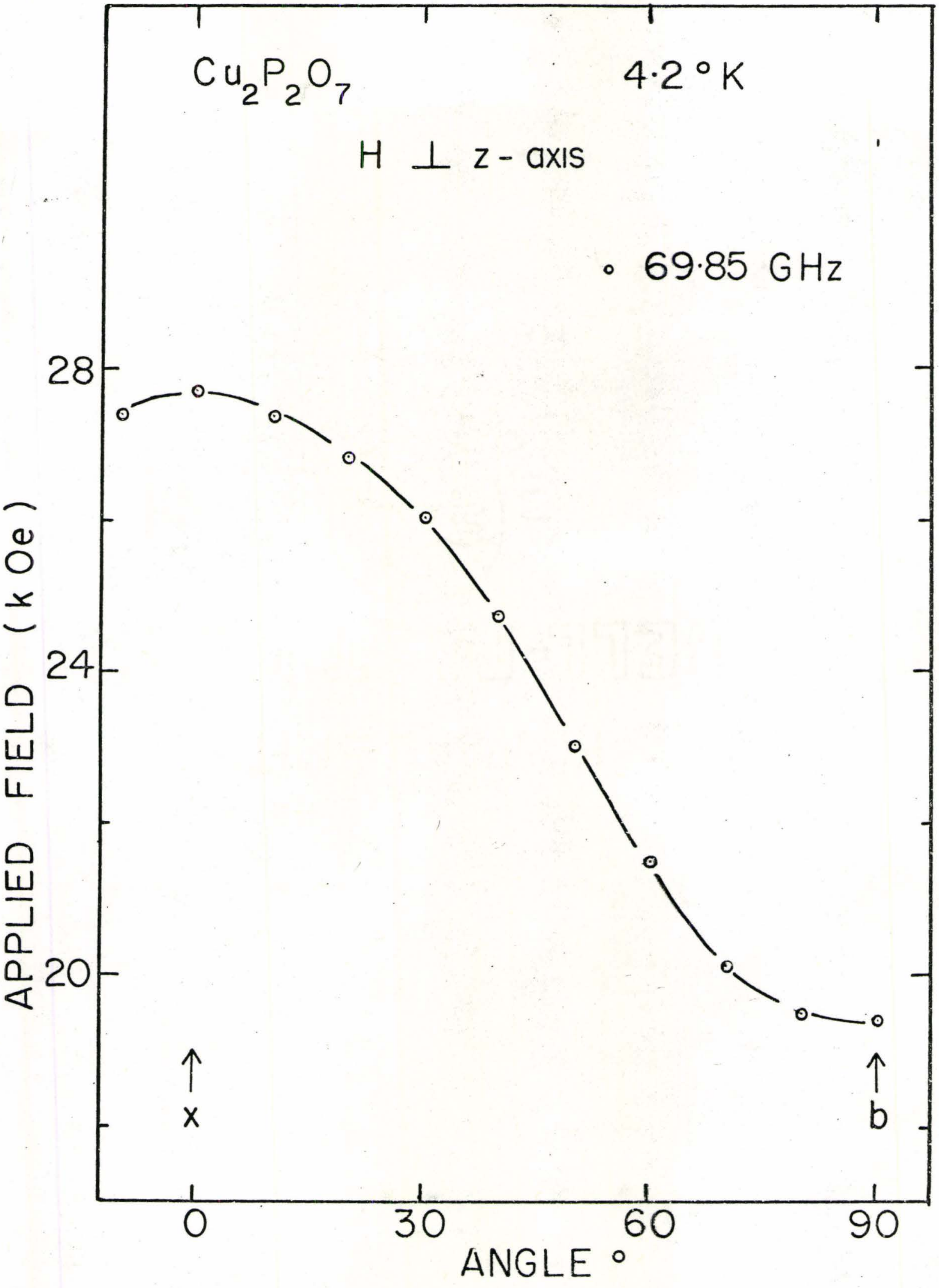
$Cu_2P_2O_7$
4·2 °K
H ⊥ z - axis
○ 69·85 GHz
APPLIED FIELD (k Oe)
28
24
20
↑ x
↑ b
0
30
60
90
ANGLE °

Figure 25. Temeprature dependence of the magnetic field along the x-axis necessary to observe the AFMR in $Cu_2P_2O_7$ at 35.04 GHz. Also shown is the temperature dependence of the linewidth.

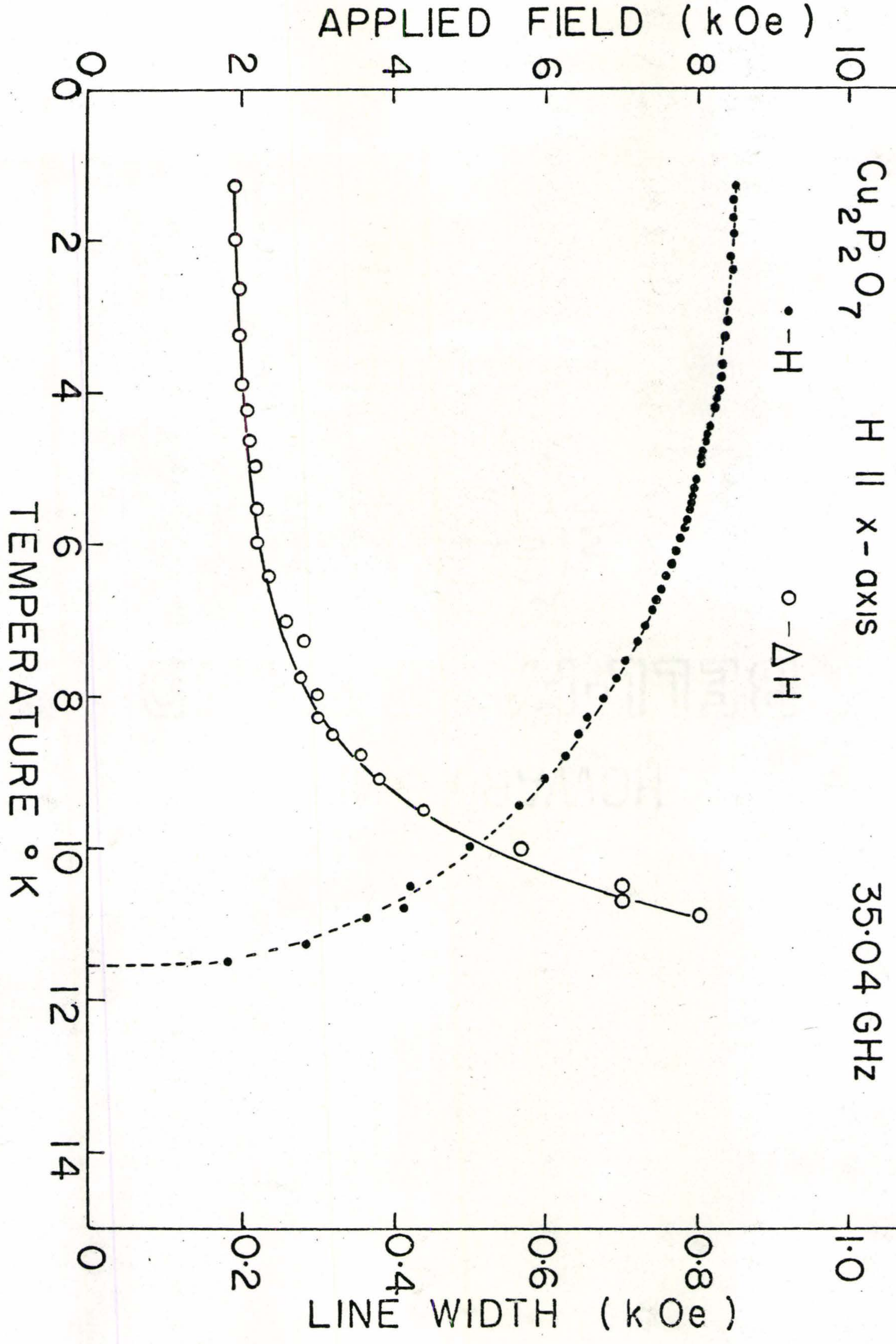
APPLIED FIELD (kOe)
0
2
4
6
8
10
$Cu_2P_2O_7$
H ll x-axis
35·04 GHz
• - H
○ - ΔH
TEMPERATURE °K
0
2
4
6
8
10
12
14
LINE WIDTH (kOe)
0
0·2
0·4
0·6
0·8
1·0

Figure 26. Temperature dependence of the magnetic field and its linewidth along the x axis necessary to observe the S.F.M. resonance in $Cu_2P_2O_7$ at 34.98 GHz.

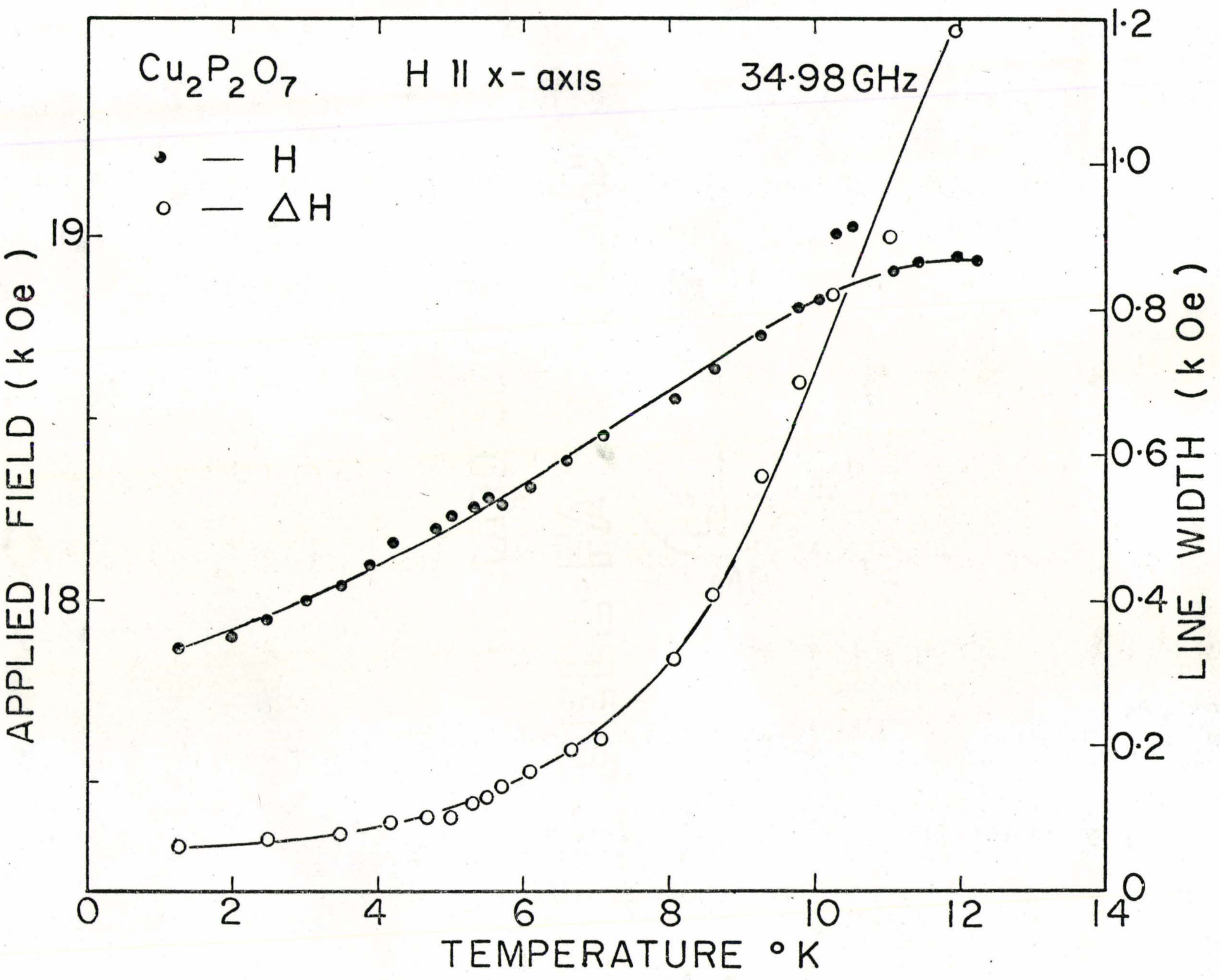
Cu$_2$P$_2$O$_7$
H ll x - axis
34·98 GHz
● — H
○ — ΔH
APPLIED FIELD (k Oe)
19
18
LINE WIDTH (k Oe)
1·2
1·0
0·8
0·6
0·4
0·2
0
TEMPERATURE °K
0
2
4
6
8
10
12
14

Figure 27. Frequency versus modified magnetic field diagram for $Cu_2P_2O_7$ at 4.2°K. The modified field $H_{mod} = g/2\ H$, where H is the applied field and g the respective g-value. The open circles are for the field along the spin direction and the closed circles for the field along the b axis. The solid line is the best fit to the Nagamiya Yosida theory of antiferromagnetic resonance using the zero field AFMR frequency of 42.0 GHz, an anisotropy ratio of 100:1 and $\chi_{\parallel} / \chi_{\perp} = 0.02$.

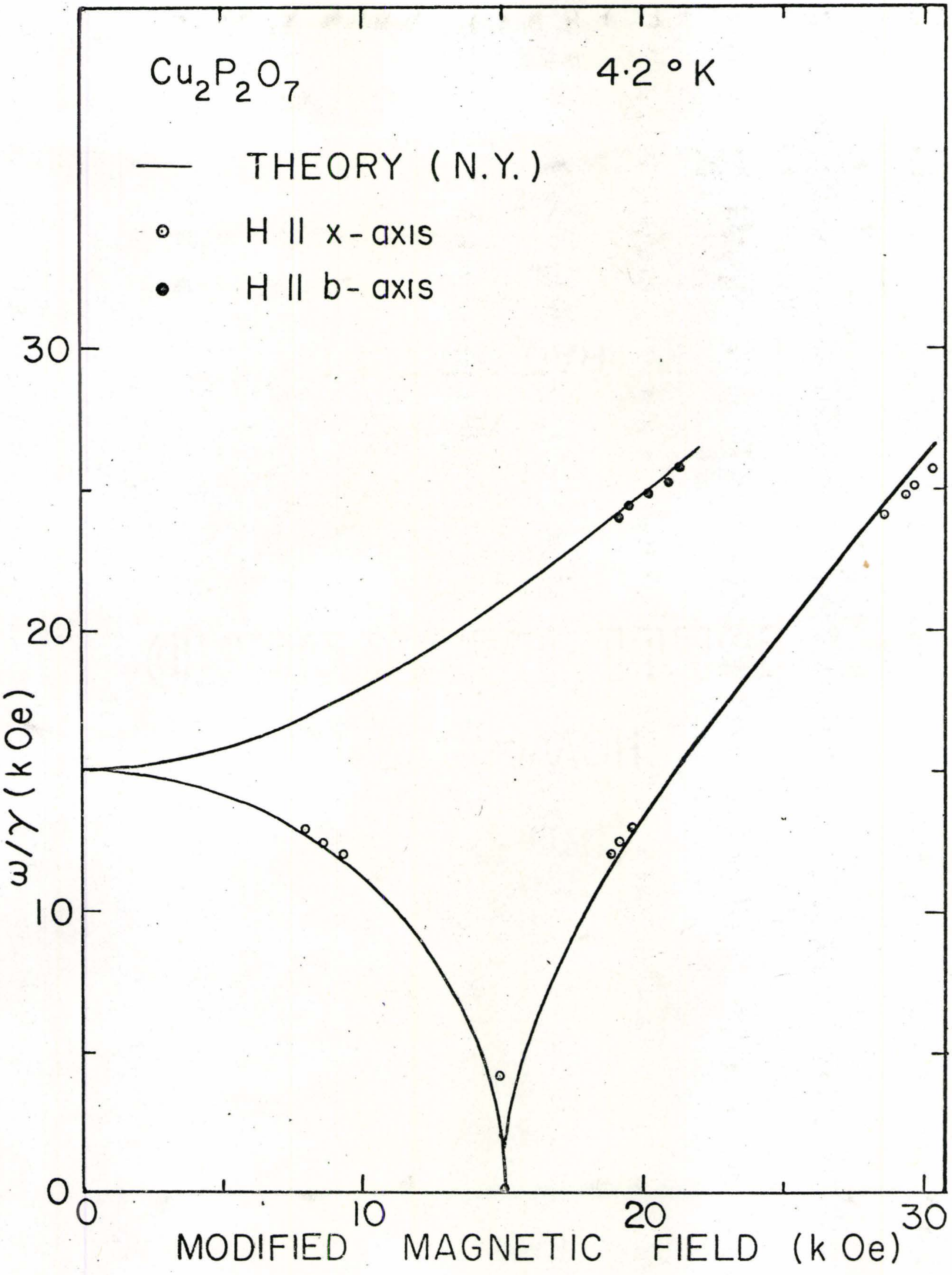
$Cu_2P_2O_7$
4·2 °K
THEORY (N.Y.)
○ H ll x-axis
● H ll b-axis
30
20
10
0
ω/γ (k Oe)
0
10
20
30
MODIFIED MAGNETIC FIELD (k Oe)

agree with what one might expect from symmetry arguments. No change in the g value was observed down to 26(1)°K. The maximum in the susceptibility occurred at 50(3)°K. It is clear from the general shape of the temperature dependence of the magnetic susceptibility that these measurements could not be explained in terms of the molecular field approximation. The measurements were repeated on the same crystal that the g values were measured on, and within experimental accuracy, since the crystal was small, it gave the same susceptibility behaviour except along the x axis at low temperature, less than 10°K. In the small crystal the susceptibility along the x axis approached zero as the temperatures approached zero. The spin flop, figure 18, could not be observed in the large crystal. It was felt that these differences might be due to strains in the large crystals which would produce the largest effect on the parallel susceptibility. Examination of different parts of the large crystal by x-rays showed it to be one single crystal of $Cu_2P_2O_7$.

Electron spin resonance of Cu^{++} in $Cu_2P_2O_7$ could be observed down to 26(1)°K. However below this temperature no electron spin resonance was observed indicating that $Cu_2P_2O_7$ had become magnetically ordered. Atkinson (1969) measured the temperature dependence of the shift of the ^{31}P N.M.R. in $Cu_2P_2O_7$ powder. It showed the same temperature behaviour as the measured susceptibility down to 26°K. Below 26(1)°K the ^{31}P resonance could not be observed in a powder sample.

Stiles (1970) has recently observed highly anisotropic ^{31}P N.M.R. in a single crystal of $Cu_2P_2O_7$ at 4.2°K. Although the maximum in the susceptibility occurs at 50(3)°K there is a definite change in the behaviour of the susceptibility at 25(1)°K. This is most pronounced when the field is along the b and z axis, figure 14. It is concluded from all the evidence that $Cu_2P_2O_7$ becomes magnetically ordered in these dimensions at 26(1)°K.

It is now recognized that the susceptibility maximum in antiferromagnets occurs at a temperature somewhat higher than that for which long range magnetic order sets in (Fisher 1962), (Sykes and Fisher 1962). The exact difference in temperature depending on the details of the lattice. For three dimensional antiferromagnetic lattices the susceptibility maximum occurs at a temperature of the order of 5 percent above the Néel temperature. However systems have been observed where the susceptibility maximum occurs at approximately twice the temperature at which long range magnetic order sets in. Strivastava (1963) found that the susceptibility maximum in K_2NiF_4 occurred at 250°K. Using elastic neutron diffraction techniques Birgeneau et al (1969) determined the Néel temperature to be 97.1°K. Lines (1967) examined K_2NiF_4 and has shown that its susceptibility behaviour can be explained in terms of two dimensional antiferromagnetic ordering. In such systems the structure is layer like with a large separation between the layers. However the crucial point about two dimensional antiferromagnets is that the coupling within the layers is antiferromagnetic. Lines (1967) has argued that the intralayer antiferromagnetic coupling would tend to oppose ordering in the third dimension. In layer structures where the intralayer coupling is ferromagnetic and the interaction in the third dimension is weak there is a single temperature at which long range magnetic order sets in simultaneously in all three dimensions.

Since the measured magnetic susceptibility of $Cu_2P_2O_7$ suggests two dimensional antiferromagnetic ordering it is compared with the High Temperature Series Expansion for a quadratic layer lattice. The comparison is shown in figure 28 for the applied field in different directions. It is equivalent to an inverse susceptibility versus temperature plot. Since the maximum in the measured susceptibility occurs at 50(3)°K then the best fit at low temperatures to the H.T.S.E. requires $J = 55°K$. The calculation shown in figure 28 was done for $J = 55°K$.

The Van Vleck temperature independent contribution to the susceptibility in $Cu_2P_2O_7$ was calculated. It was found to have the following values, along the x axis 8.6×10^{-5} emu/mole, along the y axis 7.2×10^{-5} emu/mole and along the z axis 29.2×10^{-5} emu/mole. From Pascal's rule we estimate the diamagnetic susceptibility of $Cu_2P_2O_7$ to be -7.0×10^{-5} emu/mole. The total temperature independent contributions to

Figure 28. The modified inverse of the magnetic susceptibility χ of $Cu_2P_2O_7$ as a function of temperature for the applied magnetic field along the x, y and z axes. The solid line is the calculated modified magnetic susceptibility of a quadratic layer antiferromagnet using a High Temperature Series Expansion with nearest neighbour exchange J = 55°K and spin S = 1/2

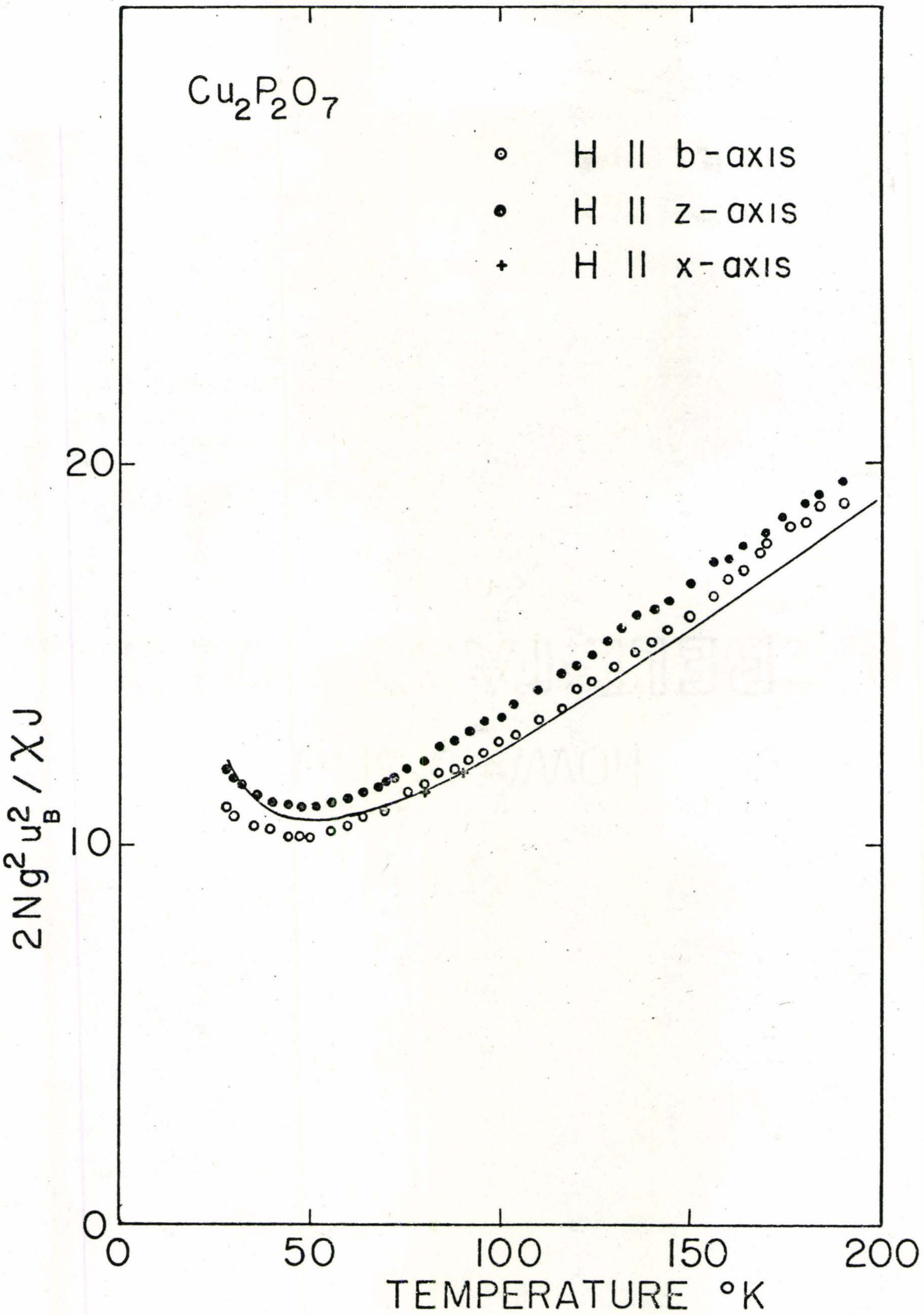
$Cu_2P_2O_7$
○ H ǁ b-axis
● H ǁ z-axis
+ H ǁ x-axis
$2Ng^2u_B^2/\chi J$
0
10
20
0
50
100
150
200
TEMPERATURE °K

the susceptibility along the x and y axes are less than one percent of the measured values. However along the z axis the temperature independent contribution is approximately six percent of the measured value at 295°K.

Below 26(1)°K $Cu_2P_2O_7$ becomes magnetically ordered in three dimensions. From the behaviour of susceptibility and the magnetic resonances observed below 26°K it is concluded that the ordering is antiferromagnetic. From the angular dependence of the susceptibility at 4.2°K, shown in figure 17, the antiferromagnetic spin direction is determined to be at 15(2) degrees from the c* axis. This is the x axis shown in figure 15. The principal perpendicular directions are determined to be the b axis (y axis) and the z axis. These directions are also shown in figure 15. At 4.2°K spin flop is observed in $Cu_2P_2O_7$ for the applied field along the x axis and at a field of 14.20(5) kOe. The principal values of susceptibility at 4.2°K are listed in Table 5. Also shown in Table 5 is the modified principal values of the susceptibility at 4.2°K. The modified value χ_{mod} is defined as

$$\chi_{mod} = (g/2)^2 \chi_{measured}.$$

The values of the susceptibility quoted are for the large $Cu_2P_2O_7$ crystal. For the small crystal of $Cu_2P_2O_7$ the parallel susceptibility is $17(10) \times 10^{-4}$ emu/mole. The parallel susceptibility calculated using equation (15) is 3.2×10^{-6} emu/mole.

The exchange field may calculated from the perpendicular susceptibility. Assuming the exchange field very much greater than the anisotropy fields then from the perpendicular susceptibility along the y axis the exchange field H_{ex} equals 800(80) kOe. It may also be determined from the high temperature susceptibility using the molecular field approximation. This gives H_{ex} = 980(80) kOe.

From the overall behaviour of the AFMR in $Cu_2P_2O_7$ it appears that the anisotropy energy has the orthorhombic form. The resonance measurements give the spin direction along the x axis. This is in agreement with the spin direction as determined by the susceptibility results. The b axis (y axis) is the intermediate axis and the z axis the hard direction. The antiferromagnetic resonance measurements have been compared to the Nagamiya Yosida theory for orthorhombic anisotropy. The experimental results along the x and y axis were compared to equations (23) through (26). The best fit was determined using the zero field AFMR as 42.0(1) GHz, ratio of anisotropy fields 100 to 1, and $(1 - \chi_{\parallel}/\chi_{\perp}) = 0.98$. The comparison between the measured values and those calculated using the Nagamiya Yosida theory with the above parameters is shown in figure 27. The solid line is the result of the theory. In the analysis the modified magnetic field was used where $H_{mod} = g/2\ H$, where H is the applied field and g the g value in the direction of the applied field.

From the exchange field determined above and the zero field antiferromagnetic resonance, the anisotropy field along the y-axis is 0.12(1) kOe and from the anisotropy ratio, the anisotropy field along the z-axis is 12(1) kOe. The modified perpendicular susceptibilities are such that the largest value is along the b-axis. This is consistent with the b-axis being the intermediate axis but the difference between the susceptibility along the y and z axes cannot be accounted for by the anisotropy fields determined from AFMR.

The spin configuration in $Cu_2P_2O_7$ is not known. Since the resonance measurements indicate a large anisotropy ratio an attempt was made to see if such a large difference in anisotropy energies could be accounted for. The dipole energy was calculated for various spin configurations. None of the spin configurations tried gave a dipole contribution with an anisotropy ratio greater than 4 to 1. It was noted, however, that the spin configuration which gave an antiferromagnetic layer structure had its dipole energy minimum when the spin direction is approximately along the c* axis, ie close to the experimentally observed direction.

It would appear that $Cu_2P_2O_7$ may not be a simple two sublattice antiferromagnet. We know of no other system which has as large a ratio of anisotropy energies. It will take additional measurements to understand this compound more fully.

(iii) $Co_2P_2O_7$

Experimental Results

The magnetic susceptibility of a single crystal of $Co_2P_2O_7$ has been measured from 4.2°K to 600°K. The complete susceptibility tensor has been determined at 4.2°K, 77°K, 295°K and 563°K. This was done by applying the magnetic field in three mutually perpendicular planes. Figure 29 shows the temperature dependence of the susceptibility from 4.2°K to 300°K with the applied field parallel to the c* and b axes. The principal values of the susceptibility at 4.2°K, 77°K, 295°K and 563°K are listed in Table 6. Figure 30 shows the orientation of the principal values with respect to the crystal axes. Figure 31 shows the angular dependence of the susceptibility at 4.2°K in three mutually perpendicular planes. The low temperature dependence of the susceptibility along the principal directions, determined at 4.2°K, are shown in figure 32.

Analysis and Discussion

From the general behaviour of the magnetic susceptibility $Co_2P_2O_7$ is paramagnetic above 11.0(3)°K and magnetically ordered below.

In the paramagnetic region the measured susceptibility has its principal axes along the b-axis and in the ac plane. This is what one would predict from symmetry. The principal axes in the ac plane rotate slightly as a function of temperature.

Figure 29. Temperature dependence of the magnetic susceptibility of $Co_2P_2O_7$ for the magnetic field along the b and c* axes.

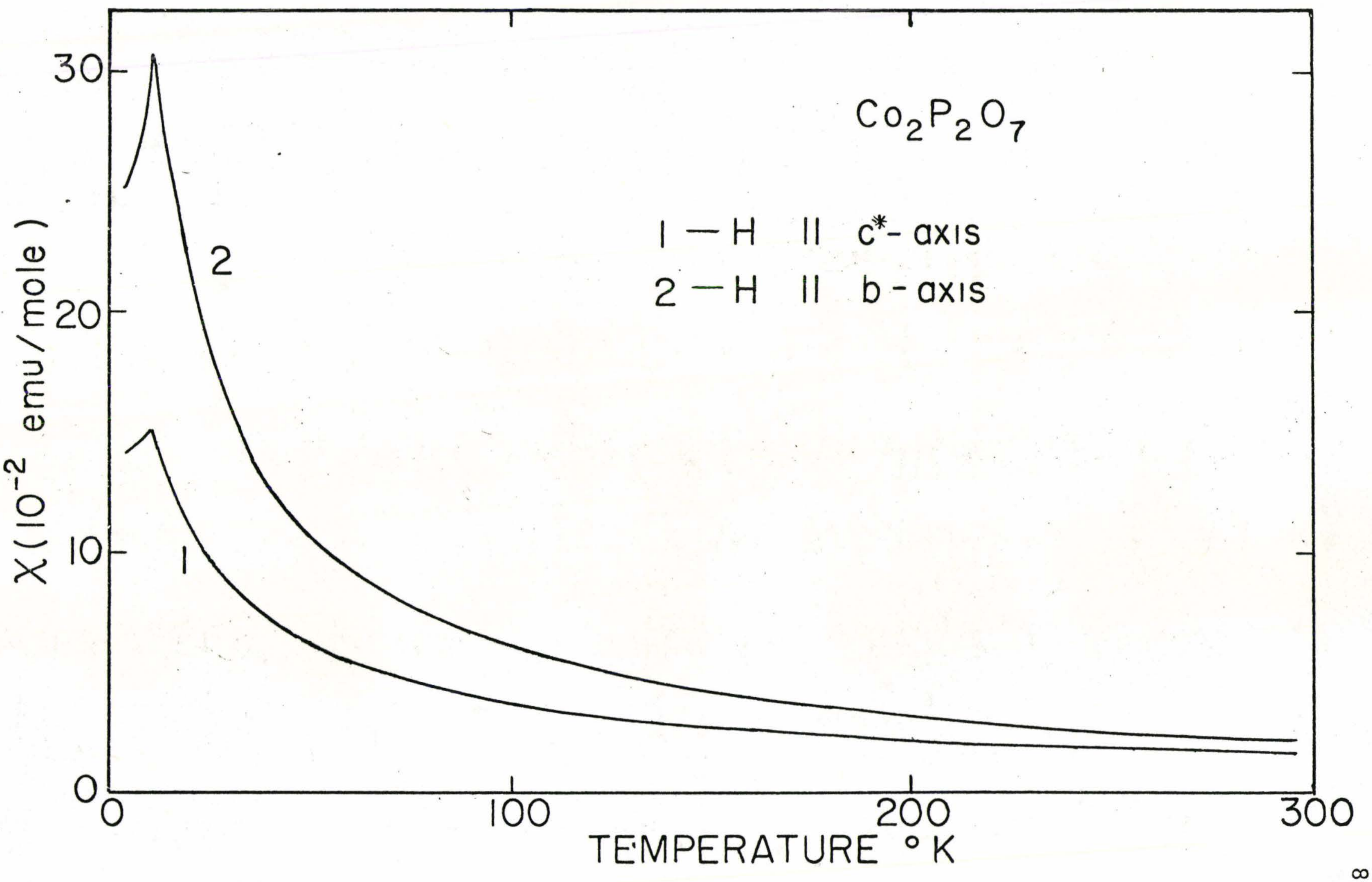
$Co_2P_2O_7$
1 — H ∥ c*- axis
2 — H ∥ b - axis
2
1
χ (10⁻² emu/mole)
30
20
10
0
0
100
200
300
TEMPERATURE °K

Table 6

Principal values of susceptibility of $Co_2P_2O_7$

Temperature (°K)		Susceptibility (10^{-3} emu/mole) Measured	Calculated	% error
	x-axis	10.9(2)	11.6	+6
563	y-axis	12.0(2)	11.5	-4
	z-axis	8.6(2)	9.2	+7
	θ°	31(3)	30.0	
	x-axis	21.2(2)	23.6	+11
295	y-axis	22.7(2)	22.8	0
	z-axis	15.3(2)	15.9	+4
	θ°	27(2)	28.1	
	x-axis	75.8(5)	76.5	+1
77	y-axis	76.4(5)	72.7	-5
	z-axis	41.0(5)	37.2	-9
	θ°	24(2)	27.4	
	x-axis	118.1(5)		
4.2	y-axis	250.6(5)		
	z-axis	143.5(5)		
	θ°	-10(2)		

Figure 30. Directions of principal values of the susceptibility of $Co_2P_2O_7$. The x and z axes are in the ac plane. The angle θ is measured from a towards c*. The y axis is along the b-axis.

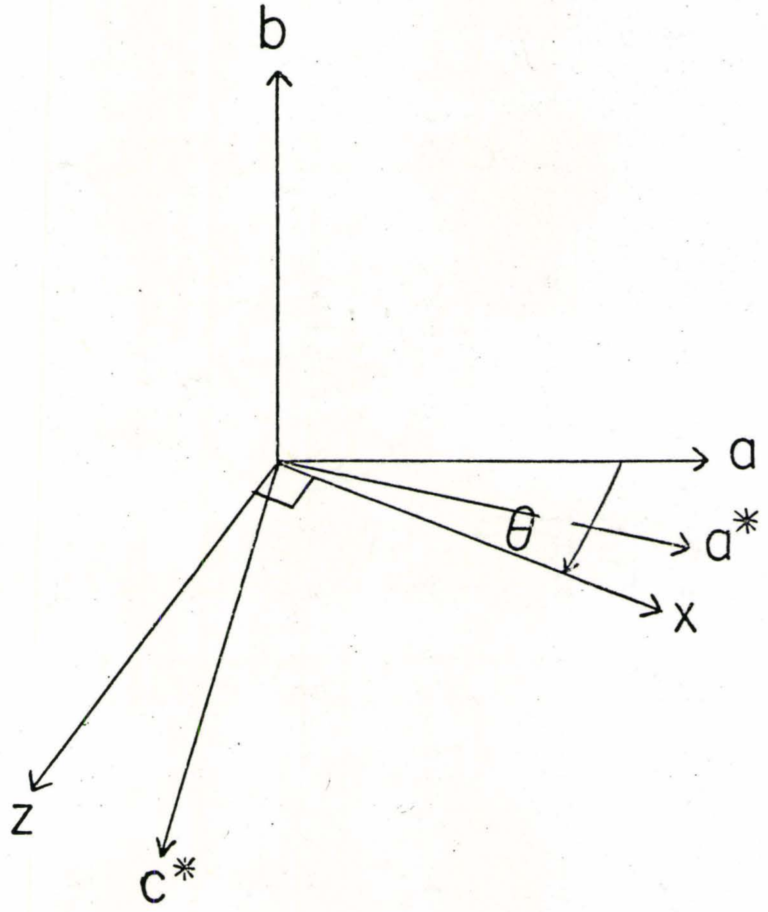
b
a
θ
a*
x
z
c*

Figure 31. Angular dependence of the magnetic susceptibility of $Co_2P_2O_7$ at 4.2°K. The magnetic field H was applied in three mutually perpendicular planes, bc* plane, ab plane and ac* plane. The susceptibility minimum was found to be 10° from the a-axis in the ac* plane, labelled || in the figure.

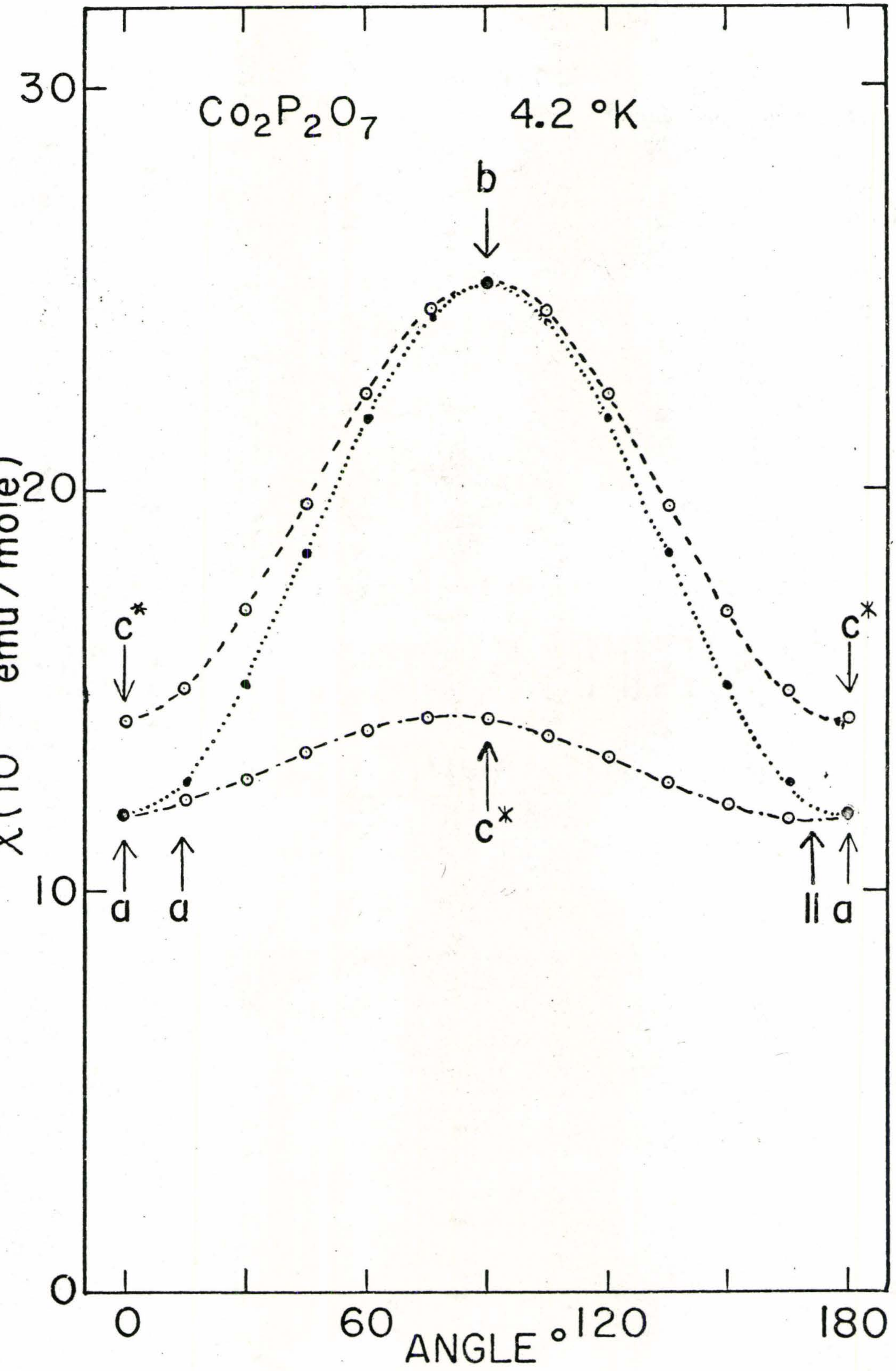
30
20
10
0
$Co_2P_2O_7$
4.2 °K
b
c^*
c^*
c^*
a
a
‖ a
a
χ (10^{-2} emu/mole)
0
60
120
180
ANGLE °

Figure 32. Low temperature dependence of the magnetic susceptibility of $Co_2P_2O_7$. The magnetic field was applied along the three principal directions as determined at 4.2°K, 10° from a, 10° from c* and the b-axis.

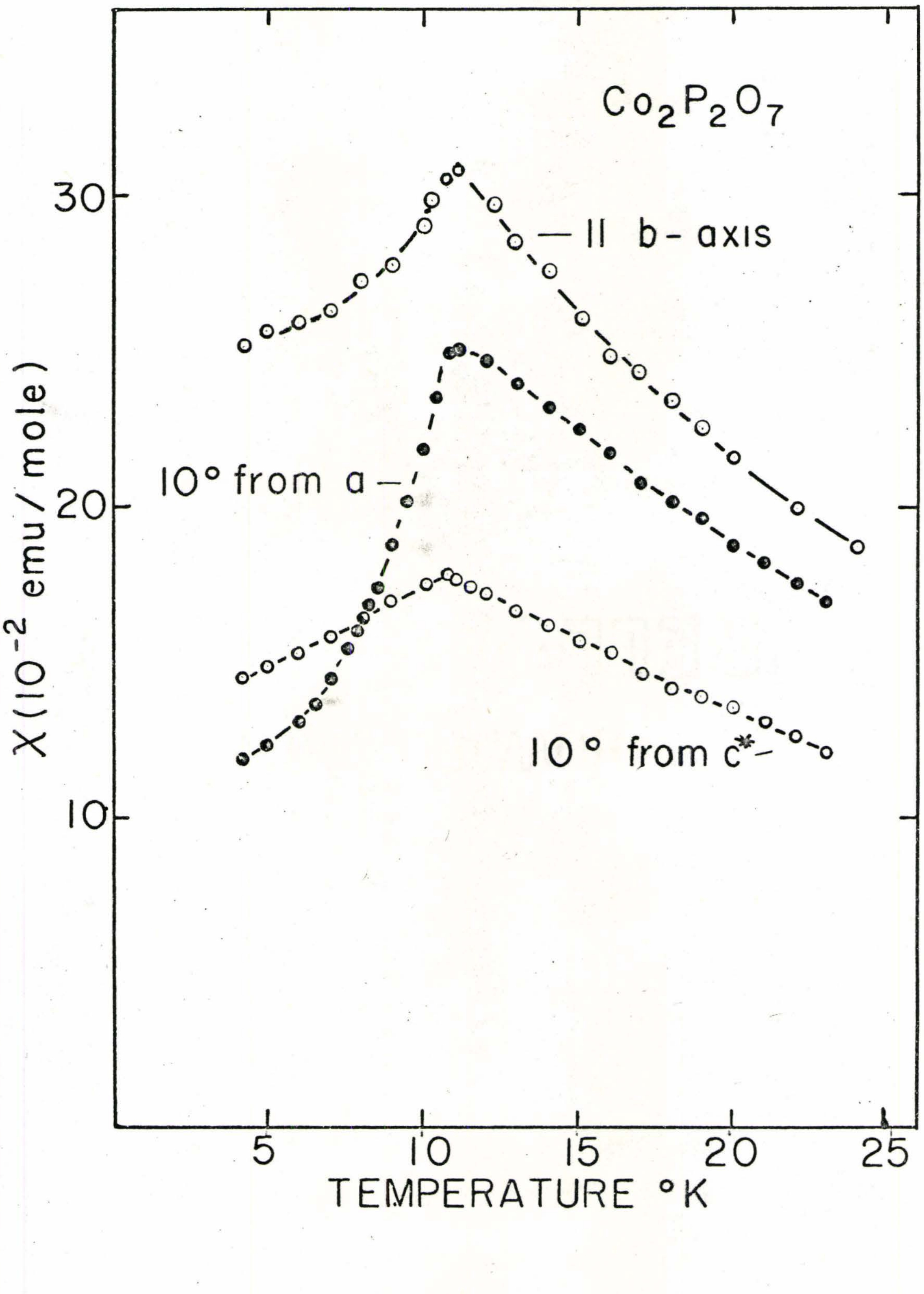
Co₂P₂O₇
— ∥ b- axis
10° from a —
10° from c* —
X (10⁻² emu/ mole)
30
20
10
5
10
15
20
25
TEMPERATURE °K

The paramagnetic susceptibility of $Co_2P_2O_7$ was calculated. The calculation is based on the measured g values of Co^{++} as a dilute substitutional impurity in $Mg_2P_2O_7$ as determined by Atkinson et al (1970). The α phase of $Mg_2P_2O_7$ is isomorphic to the α-phase of $Co_2P_2O_7$. Under a low symmetry crystal field the Co^{++} ion has as its lowest levels 6 Kramer's doublets. Uryu et al (1966) have shown that the crystal field parameters may be determined from the g-values of the lowest doublet. Knowing the crystal field parameters and the spin orbit coupling constant the wave functions of the 6 doublets can be determined. Atkinson et al (1970) observed four Co^{++} sites in $Mg_2P_2O_7$ however they were related in pairs by a two fold axis. Table 7 lists the measured principal g values for the sites. The wave functions for the 6 doublets for each Co^{++} site were calculated by the method due to Uryu et al (1966). Table 7 shows the calculated energy separation of the doublets. The magnetic susceptibility for each site was then calculated using the determined wave functions in equation (3). The total susceptibility of the crystal was then calculated by adding the contributions from each site. In figure 33 the percentage deviation between the calculated and measured susceptibility is shown for the applied field along the c* and b-axes over the temperature range 12°K to 200°K. It was noted that the calculated values were larger than the measured values by as much as 50 percent at low temperatures. The calculation

Table 7

Energy of 6 lowest doublets, and g-value of lowest doublet of Co^{++} in $Mg_2P_2O_7$ after Atkinson et al (1970)

Sites 1 & 2		Sites 3 & 4	
Doublet		Doublet	
1	$g_x = 7.967$ $g_y = 2.410$ $g_z = 1.887$	1	$g_{x'} = 6.366$ $g_{y'} = 2.683$ $g_{z'} = 3.684$
	Energy cm^{-1}		Energy cm^{-1}
6	1760	6	1258
5	1702	5	1185
4	822	4	879
3	531	3	513
2	221	2	242
1	0	1	0

Figure 33. The percentage deviation between the calculated and the measured susceptibility of $Co_2P_2O_7$ for the magnetic field along the b and c* axes. The solid lines give the result when the exchange interaction between the magnetic ions was not included. The dotted lines are the result with exchange included. The molecular field approximation was used such that the exchange interaction had the form $J\langle S\rangle S_i$ for the ith ion. The calculation was done for an anisotropic J such that along the b-axis $J = 2\ cm^{-1}$ and in the ac plane $J = 4\ cm^{-1}$.

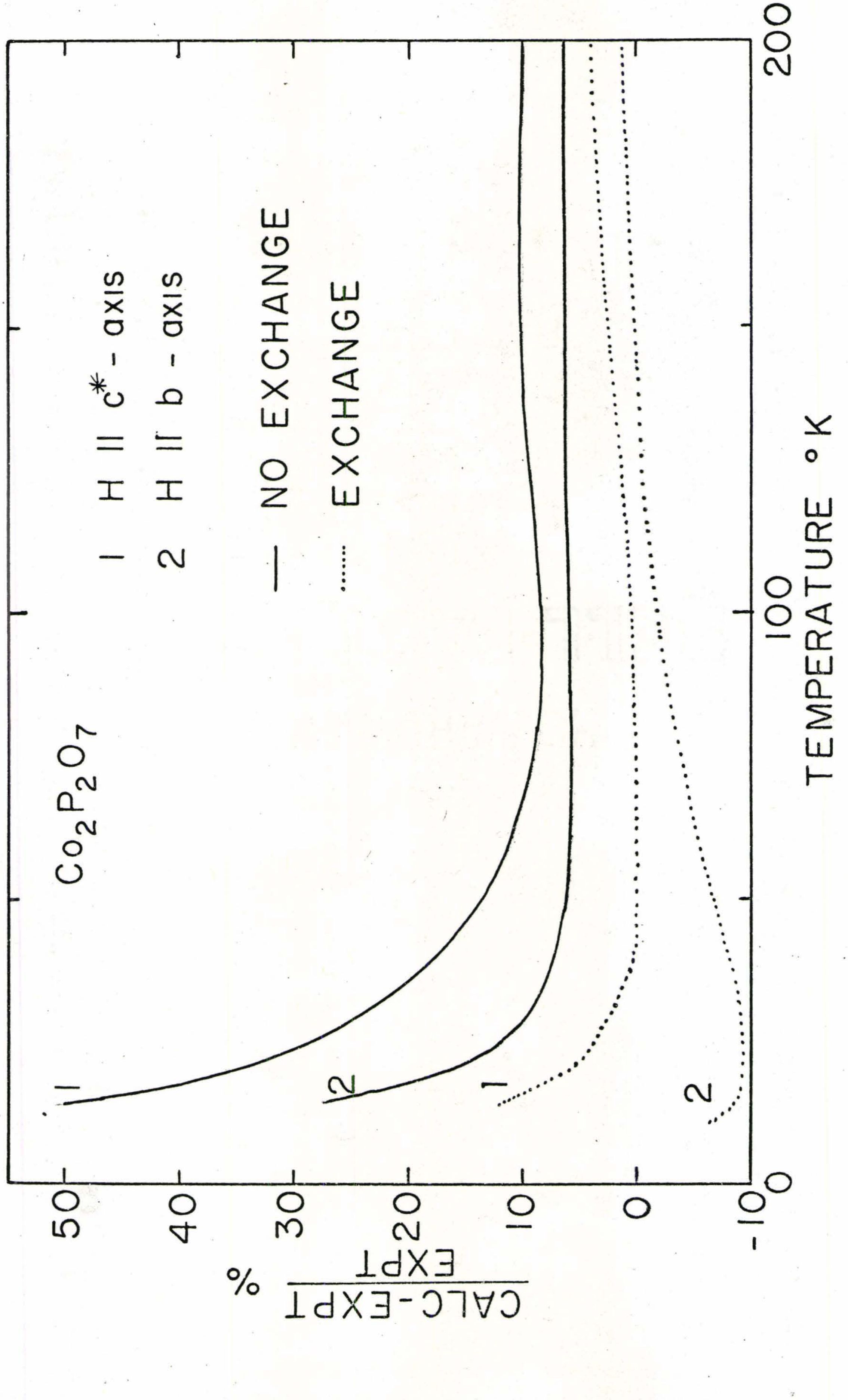
Co$_2$P$_2$O$_7$
1 H ‖ c* - axis
2 H ‖ b - axis
NO EXCHANGE
EXCHANGE
1
2
1
2
$\frac{\text{CALC-EXPT}}{\text{EXPT}}$ %
-10
0
10
20
30
40
50
0
100
200
TEMPERATURE °K

was redone using equation (7) which allowed exchange to be included. Figure 33 shows the percentage deviation between calculated and measured with antiferromagnetic exchange included in the calculation. The amount of exchange was J equal to 2 cm^{-1} along the b axis and J equal to 4 cm^{-1} in the ac plane. Figures 34 and 35 show the comparison between experiment and calculation for the susceptibility in the ac plane at 77°K and in the bc* plane at 295°K. In Table 6 the calculated principal values of the susceptibility and their percentage deviation from experiment are tabulated for 77°K, 295°K and 563°K.

In the calculation the amount of antiferromagnetic exchange was varied to give a reasonable fit over the whole temperature range. It is hard to estimate the accuracy of the calculated susceptibility since it is based on the g-values of Co^{++} as a dilute substitutional impurity in $Mg_2P_2O_7$. However it would appear that the results agree in most cases to within 10 percent. It is interesting to note that the calculated directions of the principal axes in the ac plane agree very well with experiment.

Below 11.0°K $Co_2P_2O_7$ becomes magnetically ordered. From the behaviour of the low temperature susceptibility shown in figures 31 and 32, we conclude that the ordering is antiferromagnetic. From the angular dependence at 4.2°K shown in figure 31 the minimum value of susceptibility occurs at 10(2)°

Figure 34. Angular dependence of the magnetic susceptibility of $Co_2P_2O_7$ in the ac* plane at 77°K. The solid curve is the calculated susceptibility with antiferromagnetic exchange, $J = 2\ cm^{-1}$ along the b-axis and $4\ cm^{-1}$ in the ac* plane.

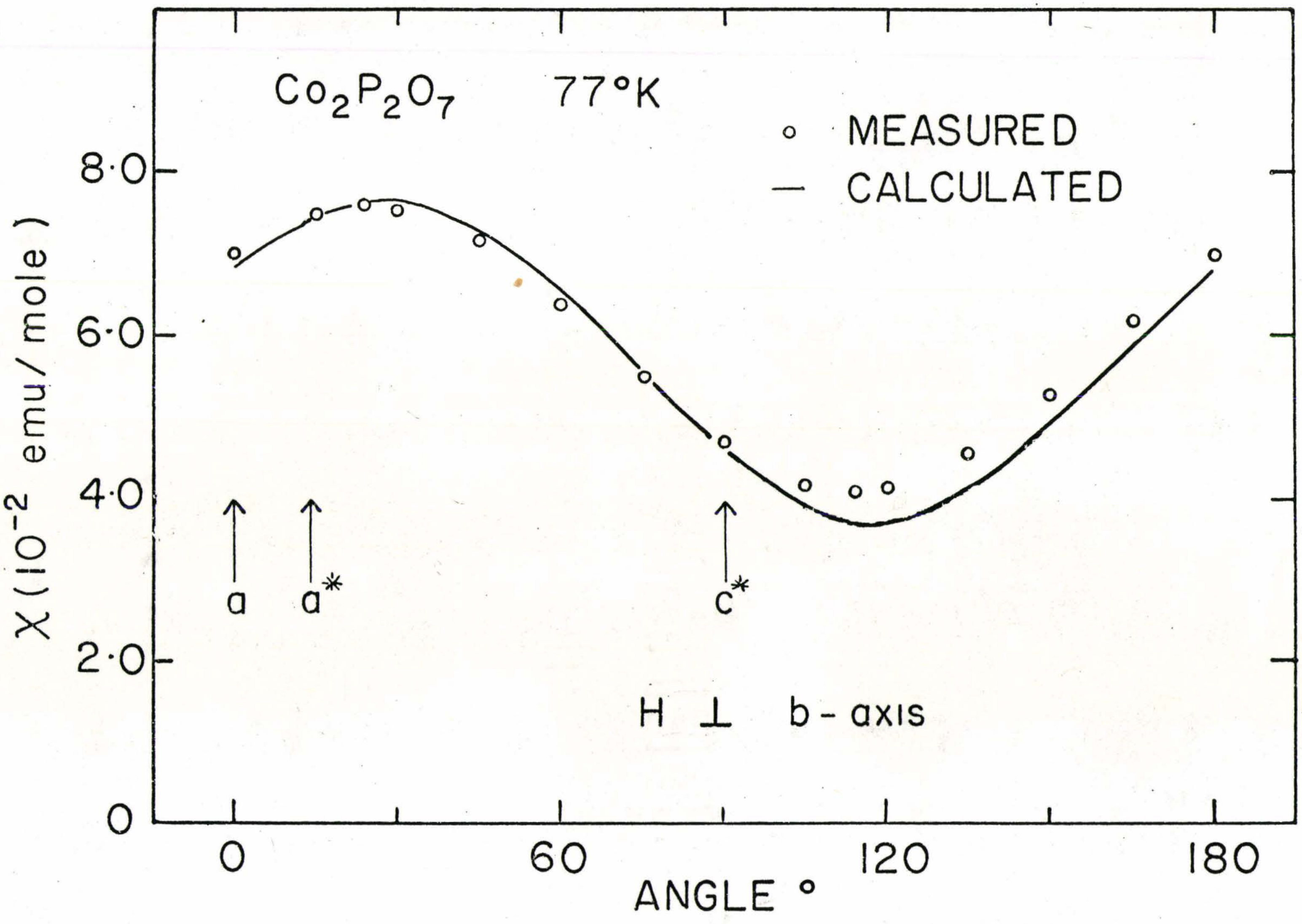
$Co_2P_2O_7$ 77°K
○ MEASURED
— CALCULATED
8·0
6·0
4·0
2·0
0
χ (10^{-2} emu/ mole)
a
a*
c*
H ⊥ b - axis
0
60
120
180
ANGLE °

Figure 35. Angular dependence of the magnetic susceptibility in the bc* plane of $Co_2P_2O_7$ at 295°K. The solid curve is the calculated susceptibility with antiferromagnetic exchange J = 2 cm^{-1} along the b axis and J = 4 cm^{-1} in the ac* plane.

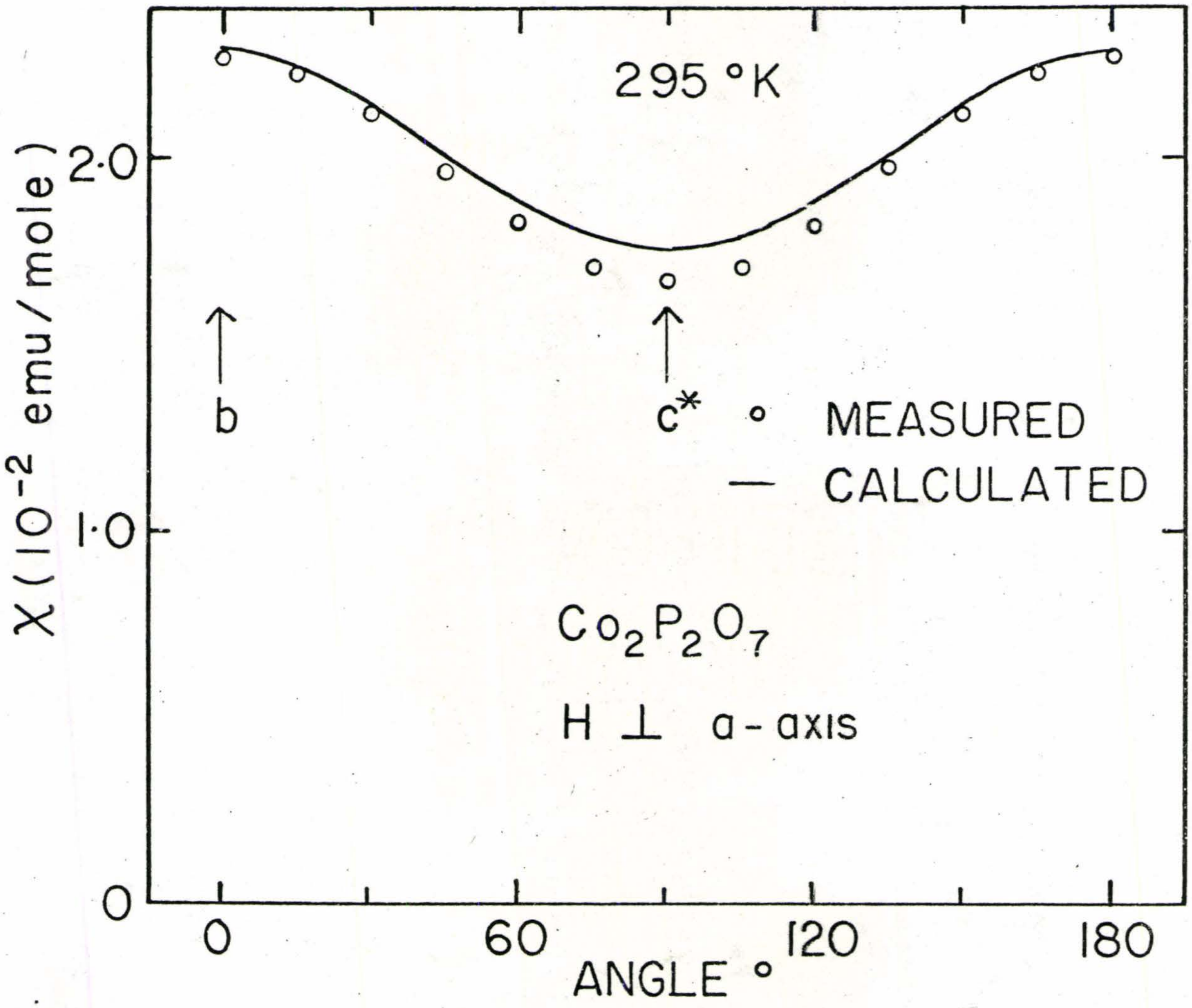
295 °K
X (10⁻² emu / mole)
2·0
1·0
0
0
60
120
180
ANGLE °
b
c*
○ MEASURED
— CALCULATED
Co₂P₂O₇
H ⊥ a - axis

from the a axis, the direction labelled || in the figure. This direction we assign as the antiferromagnetic spin direction. Since this direction is not the susceptibility minimum at all temperatures below the transition temperature, see figure 32, and since no other measurements are available to corroborate this result, the assignment must be regarded as tentative. The principal perpendicular directions are the b-axis and the direction 90 degrees from the spin direction in the ac plane.

Atkinson et al (1970) estimated the transition temperature to be 13(1)°K from the disappearance of the ^{31}P N.M.R. in $Co_2P_2O_7$. From the susceptibility data we determine the Neél temperature to be 11.0(3)°K where the susceptibility maxima has been used as the criteria for determining the transition temperature.

A.F.M.R. was not observed in $Co_2P_2O_7$ at 4.2°K. Using comparable sensitivity as was used for $Cu_2P_2O_7$ and $Mn_2P_2O_7$ no AFMR was observed at 35 GHz and 72 GHz with applied magnetic fields up to 20 kOe. An attempt was made to roughly determine the AFMR frequency in $Co_2P_2O_7$ using the known AFMR frequencies of MnF_2 (Johnson and Nethercot 1959) and CoF_2 (Richards 1963) as a basis, and from the measured value of $Mn_2P_2O_7$. The AFMR frequency of $Co_2P_2O_7$ is estimated to occur in the range 10 cm^{-1} to 20 cm^{-1}.

(iv) $Ni_2P_2O_7$

Experimental Results

The magnetic susceptibility of $Ni_2P_2O_7$ powder has been measured from 4.2°K to 300°K. The result is shown in figure 36. The low temperature susceptibility for two applied magnetic fields, 5.6 kOe and 12.6 kOe, is shown in figure 37. Also shown in figure 37 is the reduced susceptibility χ_R defined by the following relationship

$$\chi_R = \frac{M(H)-M(O)}{H}$$

where M(H) is the magnetization with applied field H and M(O) is the magnetization in zero applied field. The field dependence of the magnetization and the reduced magnetization, M(H)-M(O), at 4.2°K are shown in figure 38. Figure 39 gives the temperature dependence of the zero field magnetization.

Analysis and Discussion

Above 19°K $Ni_2P_2O_7$ is paramagnetic. The susceptibility obeys a Curie Weiss Law

$$\chi_{mole} = C_M/(T + \Theta)$$

where $C_M = \frac{2N\beta^2 S(S+1)}{3k} g_{eff}^2$. Using S = 1 for a Ni^{++} ion, the best fit to the high temperature results give $C_M = 2.56$, $\Theta = 6(1)$°K, and thus $g_{eff} = 2.26(1)$. It can be seen that since Θ is positive that the predominant exchange interaction is antiferromagnetic. There have been no electron spin resonance

Figure 36. The temperature dependence of the magnetic susceptibility of $Ni_2P_2O_7$ powder with an applied magnetic field H of 12.6 kOe. The dotted curve is the reduced susceptibility $\chi_R = \frac{M(H)-M(O)}{H}$ where M(H) and M(O) are the measured magnetizations at H = 12.6 kOe and H = 0.0 kOe respectively.

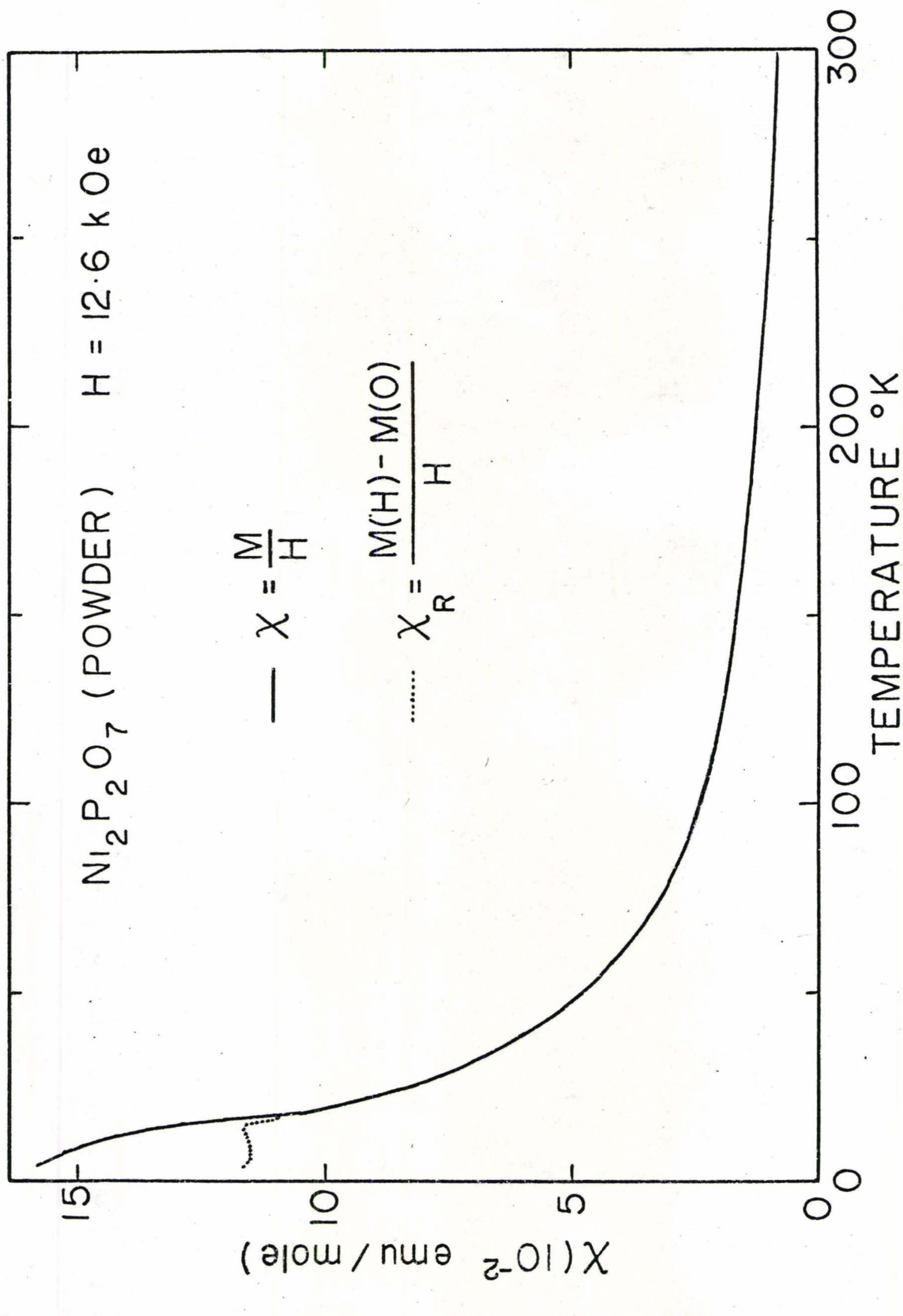
Ni$_2$P$_2$O$_7$ (POWDER)
H = 12.6 k Oe
— $\chi = \frac{M}{H}$
...... $\chi_R = \frac{M(H) - M(O)}{H}$
χ (10^{-2} emu / mole)
15
10
5
0
0
100
200
300
TEMPERATURE °K

Figure 37. The low temperature dependence of the susceptibility χ and the reduced susceptibility χ_R of $Ni_2P_2O_7$ powder for applied fields of 12.6 kOe and 5.6 kOe.

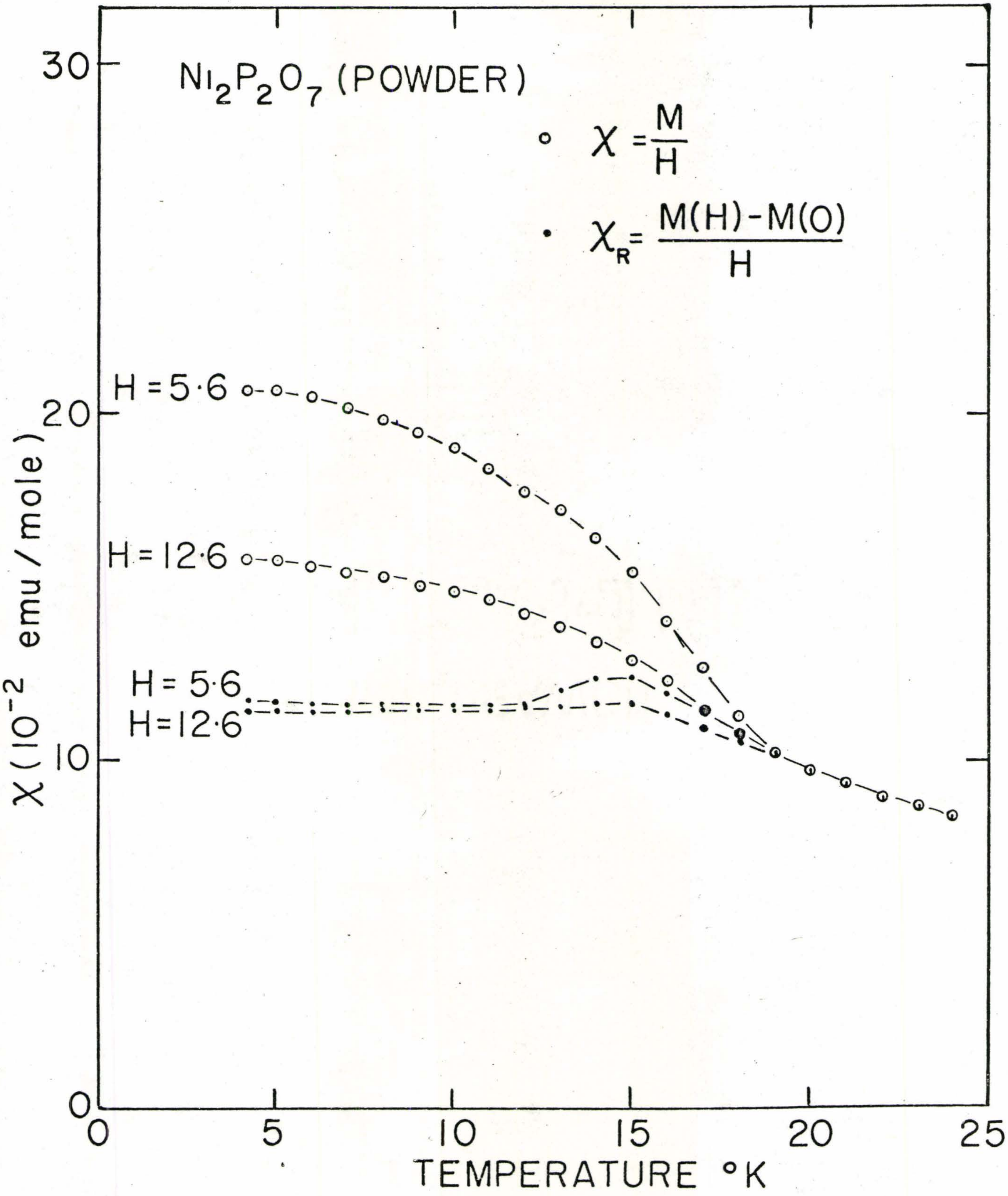
Ni$_2$P$_2$O$_7$ (POWDER)
○ $\chi = \frac{M}{H}$
• $\chi_R = \frac{M(H)-M(0)}{H}$
H = 5·6
H = 12·6
H = 5·6
H = 12·6
χ (10^{-2} emu / mole)
30
20
10
0
0
5
10
15
20
25
TEMPERATURE °K

Figure 38. Field dependence of the magnetization and reduced magnetization of $Ni_2P_2O_7$ at 4.2°K. The reduced magnetization is M(H)-M(O) where H is the applied field.

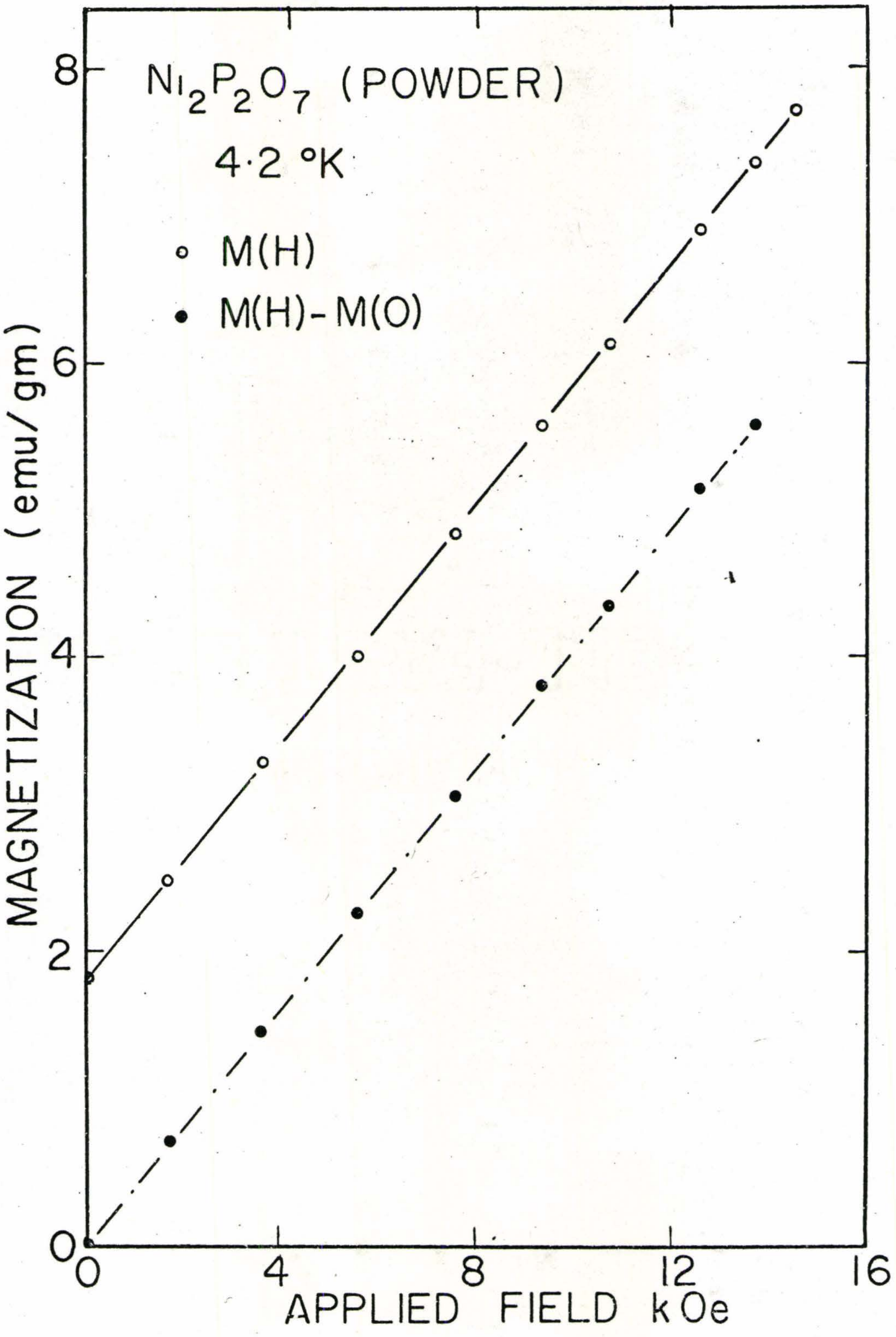
$Ni_2P_2O_7$ (POWDER)
4·2 °K
○ M(H)
● M(H) - M(O)
MAGNETIZATION (emu/gm)
0
2
4
6
8
0
4
8
12
16
APPLIED FIELD kOe

Figure 39. The temperature dependence of the zero field magnetization of $Ni_2P_2O_7$ powder. The solid and dashed lines are Brillouin function for spin S = 1 which have been normalized to the value of the magnetization at low temperatures. The transition temperature for the solid curve is 15°K and for the dashed curve 19°K.

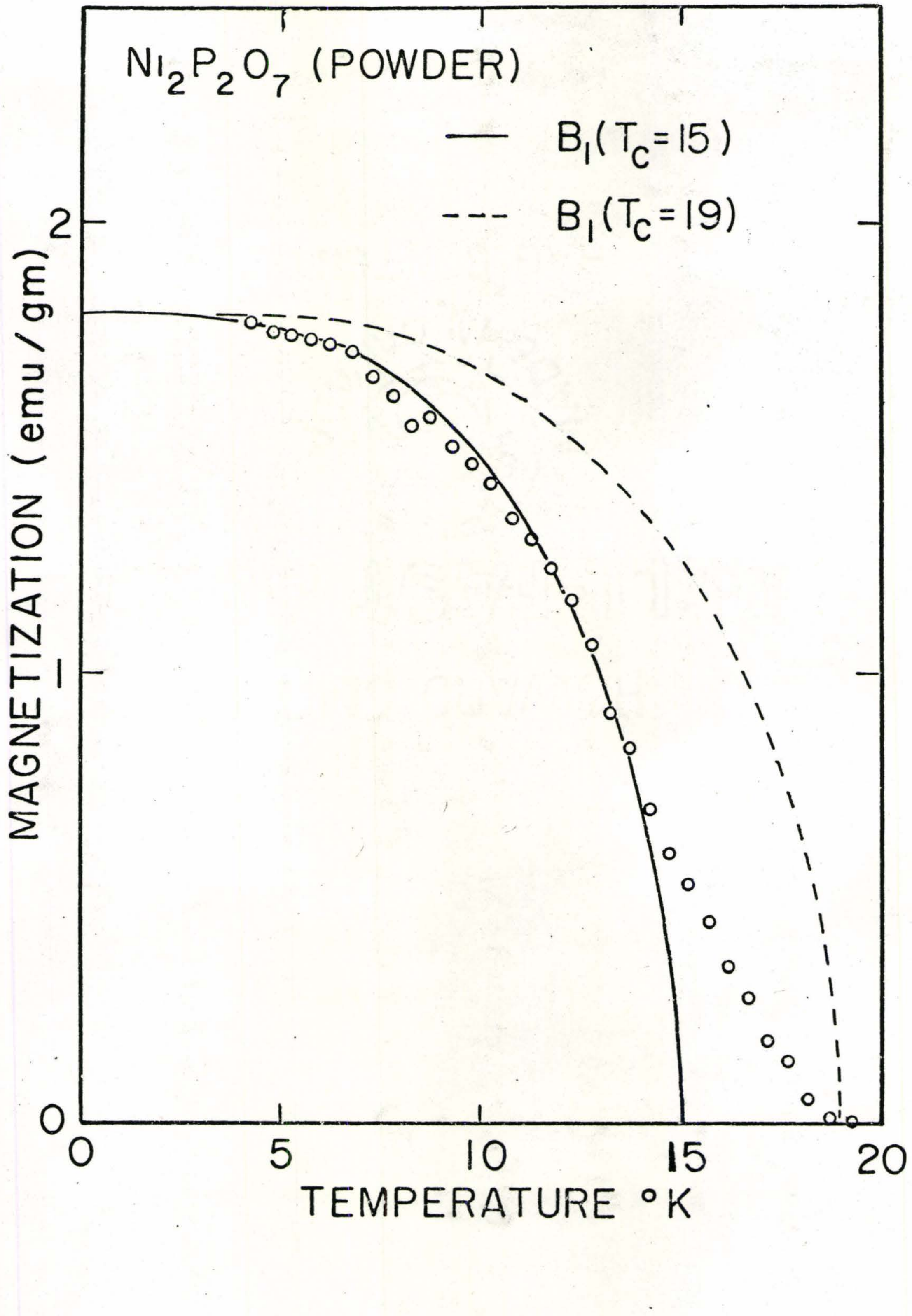
$Ni_2P_2O_7$ (POWDER)
$B_1(T_C=15)$
$B_1(T_C=19)$
MAGNETIZATION (emu/gm)
TEMPERATURE °K
0
1
2
0
5
10
15
20

measurements of Ni^{++} in the pyrophosphates but the g value is quite reasonable for nickel salts. Pake (1962) gives values in the range 2.20 to 2.30 for different nickel compounds.

Below 19°K $Ni_2P_2O_7$ becomes magnetically ordered and possesses a permanent magnetization. The observed permanent magnetic moment per Ni^{++} ion in $Ni_2P_2O_7$ at 4.2°K was 4.28×10^{-22} emu. The magnetic moment of a Ni^{++} ion when $S = 1$ and $g = 2.26$ is 2.10×10^{-20} emu. Thus the measured permanent magnetic moment is 2.04×10^{-2} times the nominal magnetic moment of the Ni^{++} ion. No saturation of the magnetization was observed with applied magnetic fields up to 14.5 kOe. It is concluded that $Ni_2P_2O_7$, below 19°K, is a weak ferromagnet probably arising from the canting of an antiferromagnetic structure.

Similar behaviour has been observed in other systems (Borovik-Romanov et al 1957), (Hirakawa et al 1960). Dzialoshinski (1958) has examined, using symmetry arguments, the conditions under which weak ferromagnetism can exist. Moriya (1960a, 1960b) has developed a theory for weak ferromagnetism on a microscopic basis. The two important mechanisms for weak ferromagnetism are, the Dzialoshinski interaction which is an antisymmetric exchange interaction having the form $\vec{d}\cdot\vec{S}_i\times\vec{S}_j$ between the spins S_i and S_j, and inequivalent magnetic sites which produce different anisotropy energies. It would appear that either of these mechanisms could cause weak ferromagnetism in $Ni_2P_2O_7$.

It would require single crystal measurements to clarify which mechanism is responsible for the observed weak ferromagnetism in $Ni_2P_2O_7$.

It was noted that the zero field magnetization did not have the same temperature dependence as a Brillouin function for S=1. In figure 39 the magnetization is compared to a Brillouin function for S = 1 and for transition temperatures of 15°K and 19°K. It was also noted that the magnetization at 4.2°K depended on how the sample was cooled through its transition temperature. This was observed only when the sample was cooled in an applied field of less than 1.8 kOe. This was thought to be due to magnetic domains.

CHAPTER VI

COMPARISON OF THE MAGNETIC PROPERTIES OF THE PYROPHOSPHATES

The paramagnetic susceptibility of the four compounds studied has been presented. That of $Mn_2P_2O_7$ was found to obey a Curie Weiss law. This is what one might expect since the energy of the first excited state is very much higher than that of the ground state. The $Co_2P_2O_7$ paramagnetic susceptibility was well explained from the measured g values of Co^{++} in $Mg_2P_2O_7$ when due account was taken of the low energy excited states and anisotropic exchange. The paramagnetic susceptibility of $Ni_2P_2O_7$ followed a Curie Weiss law while that of $Cu_2P_2O_7$ was found to deviate from the Curie Weiss law. The first excited state of the Cu^{++} ion in $Cu_2P_2O_7$ is approximately 2000 cm^{-1} above the ground state, so that at temperatures at which the measurements were made the population of the excited state is negligible. The Van Vleck temperature independent contribution to the susceptibility was also unable to account for the deviation. It was found that by using a better approximation for the exchange than the molecular field, that the experimental results could be explained in a semi-quantitative way. This was the High Temperature Series Expansion for a quadratic layer antiferromagnet. The exchange paths between the magnetic ions in $Cu_2P_2O_7$ are not clear so that the quadratic layer is just a first approximation.

The four pyrophosphates all show magnetic ordering at low temperatures. In all cases the predominant exchange interaction is antiferromagnetic. The Néel temperatures are determined to be 11.0(3)°K for $Co_2P_2O_7$, 13.8(2)°K for $Mn_2P_2O_7$, 19(1)°K for $Ni_2P_2O_7$ and 26(1)°K for $Cu_2P_2O_7$. In the case of $Co_2P_2O_7$ the Néel temperature was taken as the temperature at which the susceptibility had its maximum value. Since $Ni_2P_2O_7$ showed a resultant moment in zero field at low temperatures the Néel temperature has been taken as the highest temperature at which the resultant moment could be observed. The Néel temperature of $Mn_2P_2O_7$ and $Cu_2P_2O_7$ were taken as the temperature at which electron spin resonance of the respective magnetic ion could no longer be observed. For $Mn_2P_2O_7$ the susceptibility maximum occurred at 14.0(2)°K and in $Cu_2P_2O_7$ the susceptibility showed a definite change in behaviour at 25(1)°K.

Only $Ni_2P_2O_7$ showed a permanent moment in the ordered state which has led to the conclusion that it is a weak ferromagnet. The other three are antiferromagnets. The spin directions of the three antiferromagnets are in the ac plane. One would expect from symmetry arguments that the spin directions are either in the ac plane or along the b-axis, ie the 2-fold axis of the crystal. Nothing can be said at this time about the spin direction in $Ni_2P_2O_7$ since only powder susceptibility measurements have been made. The spin direction in $Mn_2P_2O_7$ is 22° from the a-axis and in $Co_2P_2O_7$ 10° from the a-axis, whereas in $Cu_2P_2O_7$ the spin direction is 75° from the a axis (15° from the c* axis).

The exchange fields for the three antiferromagnets are $Mn_2P_2O_7$ 77.5(8) kOe, $Cu_2P_2O_7$ 900(80) kOe and $Co_2P_2O_7$ of the order of 100 kOe. It can be seen that, although the exchange field in $Co_2P_2O_7$ is not well known, the exchange field in $Cu_2P_2O_7$ is very much larger than in the other two.

From the AFMR measurements in $Mn_2P_2O_7$ and $Cu_2P_2O_7$ it is found that both have an anisotropy energy of the orthorhombic form. In $Mn_2P_2O_7$ the intermediate direction is in the ac plane and the hard direction is along the b axis, whereas in $Cu_2P_2O_7$ the b-axis is the intermediate direction and the hard direction is in the ac plane. The zero field AFMR frequency was found to be 68.0 GHz in $Mn_2P_2O_7$ and 42.0 GHz in $Cu_2P_2O_7$. Their respective 'spin flop' fields are 26.7 kOe and 14.2 kOe.

The antiferromagnetic resonance and susceptibility results of $Mn_2P_2O_7$ could be well explained using the anisotropy energy for a two sublattice antiferromagnet in the form given by Date (1961). The antiferromagnetic resonance measurements on $Cu_2P_2O_7$ were found to deviate quite markedly from the Nagamiya Yosida theory for AFMR. To obtain a reasonable fit to this theory the ratio of anisotropy energies had to be 100 to 1. This would appear to be too large a ratio for the anisotropy energies. The equivalent anisotropy ratio in $Mn_2P_2O_7$ is 2.5 to 1. The $Cu_2P_2O_7$ results were compared to the extension of Nagamiya Yosida theory due to Date but it was found that this did not improve the fit.

In $Mn_2P_2O_7$ the crystal field term needed to give agreement between the measured spin direction and anisotropy energies, and the calculated ones were found to have the opposite sign from that measured from the E.S.R. of Mn^{++} as a dilute substitutional impurity in $Mg_2P_2O_7$. However the calculation of the susceptibility of $Co_2P_2O_7$ based on the measured g values of Co^{++} as a dilute substitutional impurity in $Mg_2P_2O_7$ gave good agreement with the experimentally measured susceptibility.

The spin configuration in $Mn_2P_2O_7$ has its dipole field energy minimum when the spin direction is along the a axis, however if the spin configuration consists of antiferromagnetic layers in the ab plane then the dipole field energy has its minimum approximately along the c* axis which is close to the experimentally determined spin direction in $Cu_2P_2O_7$. Such an antiferromagnetic layer structure is consistent with the high temperature susceptibility of $Cu_2P_2O_7$, however it would not account for the large anisotropy ratio. Stiles (1970), from the ^{31}P N.M.R. in $Cu_2P_2O_7$, suspects that $Cu_2P_2O_7$ may not be a two sublattice antiferromagnet.

BIBLIOGRAPHY

Atkinson, R. J. 1969. Ph.D. Thesis, McMaster Univ. unpublished.

Atkinson, R. J. and Stager, C. V. 1969. Can. J. Phys. 47, 1557.

Atkinson, R. J. Fowlis, D. C. and Stager, C.V. 1970. Can. J. Phys. 48, 543.

Birgeneau, R. J., Guggenheim, H. and Shirane, G. 1969. Phys. Rev. Lett. 22, 720.

Birgeneau, R. J., DeRosa, F. and Guggenheim, H. J. 1970. Solid State Comm. 8, 13.

Borovik-Romanov, A.S. and Orlova, M. P. 1957.J.E.T.P. 4, 531.

Calvo, C. 1965. Can. J. Chem. 41, 1139.

Calvo, C. 1965a. Can. J. Chem. 41, 1147.

Calvo, C. 1967. Acta. Cryst. 23, 289.

Calvo, C. 1968. Private Communication.

Calvo, C., Leung, J. S. and Datars, W. R. 1967. J. Chem. Phys. 41, 796.

Calvo, C. and Krishnamachari, N. 1970. Private Communication.

Chambers, J. G., Datars, W. R. and Calvo, C. 1964. J. Chem. Phys. 41, 806.

Choh, S. H. and Stager, C.V. 1970. Can. J. Phys. 48, 521.

Daman, H., Herr, A. and Meyer, A.J.P. 1968. J. Appl. Phys. 39, 669.

Date, M. 1961. J. Phys. Soc. Japan 16, 1337.

Date, M. and Motokawa, M. 1967. J. Phys. Soc. Japan 22, 165.

Dzialoshinski, I. 1958. Phys. and Chem. Solids 4, 241.

Fisher, M.E. 1962. Physica 28, 919.

Foner, S. 1959. Rev. Sci. Instr. 30, 548.

Foner, S. 1963. Phys. Rev. 130, 183.

Gill, G. S., Collins, M.F. and Stager, C.V. 1970. To be published.

Hirakawa, K., Hirakawa, K. and Hashimoto, T. 1960. J. Phys. Soc. Japan 15, 2063.

Johnson, J. M. and Nethercot Jr., A. H. 1959. Phys. Rev. 114, 705.

Kanamori, J. 1963. Magnetism, Vol. 1, edited by G. T. Rado and H. Suhl (Academic Press, Inc., New York) Chap. 4.

Keffer, F. 1952. Phys. Rev. 87, 608.

Keffer, F. and Kittel, C. 1952. Phys. Rev. 85, 329.

Kittel, C. 1952. Phys. Rev. 82, 565.

Lallemand, A. 1935. Ann. Phys. 3, 97.

Lines, M. E. 1967. Phys. Rev. 164, 736.

Łukaszewicz, K. 1967. Bull. Acad. Polon. Sci., Ser. Sci. Chim. 15, 47.

Łukaszewicz, K. 1968. Bull. Acad. Polon. Sci., Ser. Sci. Chim. 16, 183.

Moriya, T. 1960a. Phys. Rev. 117, 635.

Moriya, T. 1960b. Phys. Rev. 120, 91.

Moriya, T. 1963. Magnetism, Vol. 1, edited by G. T. Rado and H. Suhl (Academic Press, Inc.. New York), Chap. 3.

Nagamiya, T., Yosida, K. and Kubo, R. 1955. Advances in Phys. 4, 1.

Nye, J. F. 1957. Physical Properties of Crystals, (Oxford Univ. Press, London).

Pake, G. E., 1962. Paramagnetic Resonance, (W. A. Benjamin Inc., New York).

Richards, P. L. 1963. J. Appl. Phys. Suppl. 34, 1237.

Robertson, B.E. and Calvo, C. 1967. Acta Cryst. 22, 665.

Robertson, B. E. and Calvo, C. 1968. Can. J. Chem. 46, 605.

Robertson, B. E. and Calvo, C. 1970. J. Solid State Chem. 1, 120.

Rushbrooke, G.S. and Wood, P. J. 1958. J. Mol. Phys. 1, 257.

Stiles, J. 1970. Private Communication.

Strivastava, K. G. 1963. Phys. Lets. 4, 55.

Sykes, M.F. and Fisher, M.E. 1962. Phil. Mag. 7, 1731

Tondon, V. K. 1971. M.Sc. Thesis, McMaster Univ. unpublished.

Uryu, N. Skalyo Jr. J., and Friedberg, S. A. 1966. Phys. Rev. 144, 689.

Van Vleck, J. H. 1932. Theory of Electric and Magnetic Susceptibilities, (Oxford Univ. Press, London).